On the Role of TLR2 and SIRT1 in the Development of Diabetes Mellitus

---

Dissertation

Zur

Erlangung der naturwissenschaftlichen Doktorwürde

(Dr. sc. nat)

vorgelegt der

Mathematisch-naturwissenschaftlichen Fakultät

der

Universität Zürich

von

Daniel Meier

von

Schafisheim (AG)

Promotionskomitee

Prof. Dr. François Verrey (Vorsitz)

Prof. Dr. Marc Y. Donath (Leitung der Dissertation)

Prof. Dr. Philippe Halban

Zürich, 2011

ERKLÄRUNG

Diese Dissertation wurde von Dr. Marianne Böni-Schnetzler, Prof. Dr. Jan Ehses und Prof. Dr. Marc Donath betreut. Sie wurde selbständig und ohne unerlaubte Hilfsmittel angefertigt. Bei der Abfassung der Dissertation wurden im Sinne der Promotionsordnung der Mathematisch-naturwissenschaftlichen Fakultät der Universität Zürich vom 8. Juli 2002 keine anderen als die angegebenen Hilfsmittel verwendet.

Zürich, Februar 2011

Daniel Meier

TABLE OF CONTENTS

I TITLE PAGE

II ERKLÄRUNG

III TABLE OF CONTENTS

IV ZUSAMMENFASSUNG

V SUMMARY

VI ABBREVIATIONS

1 INTRODUCTION

1.1 Glycaemic control ……..1

1.2 The history of diabetes mellitus and the discovery of insulin…… 1

1.3 The pancreas and its hormones…….. 2

1.3.1 The endocrine pancreas……... 3

1.3.2 The exocrine pancreas……. 4

1.4 Insulin gene, synthesis and secretion in β-cells…….. 4

1.5 Insulin function and target tissues……...6

1.6 Glucagon and its function……7

1.7 Somatostatin, pancreatic polypeptide and ghrelin…….. 7

1.8 Diabetes mellitus ……8

1.8.1 Type 1 diabetes mellitus…… 9

1.8.2 Type 2 diabetes mellitus…….. 10

2 TLR2-DEFICIENT MICE ARE PROTECTED FROM INSULIN RESISTANCE AND β−CELL DYSFUNCTION INDUCED BY A HFD

2.1 Introduction ……12

2.1.1 TLRs…… 12

2.1.2 TLR2……12

2.1.3 TLR2, obesity and inflammatory diseases…….. 13

2.1.4 Aim of the thesis, TLR2 part……... 13

2.2 Methodology…….. 14

2.2.1 Animals……... 14

2.2.2 Tissue expression of TLR2..…….. 14

2.2.3 Metabolic studies……15

2.2.4 Isolated adipocyte experiments……15

2.2.5 Indirect calorimetry and physical activity……15

2.2.6 Plasma analysis…… 16

2.2.7 Glucose clamp studies…… 16
2.2.8 Total liver lipid extraction …….. 16
2.2.9 RNA extraction and real-time PCR…… 16
2.2.10 Immunohistochemistry…… 17
2.2.11 Pancreatic islet isolation and BMDM/BMDC preparation…. 17
2.2.12 TLR2 antibody treatment…… 18
2.2.13 Western blot analysis…… 18
2.2.14 Tissue triacylglycerols and glycogen…… 18
2.2.15 NEFA preparation……18
2.2.16 Statistics…….. 18
2.3 Results…… 20
2.3.1 *Tlr2* tissue expression and regulation by HFD feeding…….. 20
2.3.2 *Tlr2* $^{-/-}$ mice are resistant to the adverse effects of HFD feeding…… 21
2.3.3 *Tlr2* $^{-/-}$ mice are protected from liver insulin resistance, hepatosteatosis and liver inflammation on HFD…… 26
2.3.4 *Tlr2* $^{-/-}$ mice are protected from impaired β−cell insulin secretion and islet inflammation on HFD……28
2.3.5 Impaired inflammatory response of BMDCs and islets to NEFAs in *Tlr2* $^{-/-}$ mice……..……29
2.3.6 *Tlr2* deficiency does not protected db/db mice from hyperglycemia…… 31
2.3.6 Treatment with an anti *Tlr2* antibody fails to show beneficial effects in mice on HFD……... 32
2.4 Supplementary Results…….. 34
2.4.1 Pam2CSK4 does not induce SAA in *Tlr2* $^{-/-}$ mice…… 34
2.4.2 Glucose homeostasis in chow fed *Tlr2* $^{+/+}$ and *Tlr2* $^{-/-}$ mice…… 34
2.4.3 Glucose homeostasis in male *Tlr2* $^{+/+}$ and *Tlr2* $^{-/-}$ mice fed HFD…….. 35
2.4.4 Glucose homeostasis in female *Tlr2* $^{+/+}$ and *Tlr2* $^{-/-}$ mice fed HFD for 12 weeks…… 36
2.4.5 Adipose tissue GLUT4 expression in female *Tlr2* $^{+/+}$ and *Tlr2* $^{-/-}$ mice fed HFD for 20 weeks…… 37
2.4.6 Skeletal muscle triacylglycerols and glycogen content in female *Tlr2* $^{+/+}$ and *Tlr2* $^{-/-}$ mice fed HFD for 20 weeks…… 37
2.4.7 Blood glucose and glucose infusion rate during

hyperinsulinaemic–euglycaemic clamp……...38
2.4.8 Pam2CSK4-induced *Il-1β* mRNA in BMDMs and BMDCs derived from *Tlr2* $^{+/+}$ and *Tlr2* $^{-/-}$ mice……38
2.4.9 Plasma analysis of age-matched chow and 20-week-old HFD-fed female *Tlr2* $^{+/+}$ and *Tlr2* $^{-/-}$ mice……...39

2.5 Discussion……...40

3 SIRT1 ACTIVATION VIA SRTs DOES NOT DELAY THE ONSET OF TYPE 1 DIABETES

3.1 Introduction……45
3.1.1 Sirtuins……45
3.1.2 SIRT1…….. 45
3.1.3 SIRT1, metabolic diseases and diabetes…… 45
3.1.4 SIRT1 L107P…….. 46
3.1.5 Small activators of SIRT1……... 46
3.1.6 Aim of the thesis, SIRT1 part…… 47
3.2 Methodology…….. 48
3.2.1 Animals……... 48
3.2.2 SIRT1 activators (SRTs)…… 48
3.2.3 NOD experiments…… 48
3.2.4 MLD-STZ experiments……48
3.2.5 Tissue workup…… 49
3.2.6 Adoptive Transfer……49
3.2.7 Statistics……...50
3.3 Results……51
3.3.1 Diabetes incidence rate…… 51
3.3.2 Insulitis score……... 52
3.3.3 Adoptive Transfer of Diabetes…… 54
3.3.4 Unexpected accumulation of cases of death in SRT1720 and SRT501 treated animals…… 55
3.3.5 MLD-STZ-SRT 1720…….. 56
3.3.6 MLD-STZ-SIRT1 $^{+/-}$…… 57
3.4 Discussion…….. 59

4 REFERENCES…….. 65

5 AMENDMENT…….. 72

5.1 Contributions…….. 72

5.2 Acknowledgement…….. 74

5.3 Curriculum Vitae……75

5.4 List of publication……...…… 76

ZUSAMMENFASSUNG (DEUTSCH)

Während Typ 1 Diabetes eine klassische Autoimmunerkrankung ist, sind sich die Fachleute uneinig, welche Rolle das Immunsystem im Typ 2 Diabetes spielt. Bisher nahm man an, dass die Hauptursache des Typ 2 Diabetes darin besteht, dass Insulin in den Zielorganen seine Funktion ungenügend ausführen kann. Es besteht eine sogenannte Insulinresistenz. Nun gibt es aber immer mehr Erkenntnisse, die dem Immunsystem auch im Typ 2 Diabetes eine bedeutende Rolle zuschreiben.

Diese Dissertation ist in zwei Kapitel unterteilt. Das erste Kapitel widmet sich der Rolle von TLR2 im Typ 2 Diabetes. Dieser Rezeptor des Immunsystems erkennt und bekämpft eindringende Bakterien. Fette aus der Nahrung können TLR2 binden und aktivieren. Typ 2 Diabetiker sind häufig übergewichtig und haben daher ein erhöhtes Fettdepot. Da Übergewicht zu chronischen Entzündungen führen kann, könnte TLR ein molekulare Link zwischen der Fettleibigkeit und dem veränderten Blutzuckerhaushalt sein. Dies wird im ersten Kapitel dieser Dissertation untersucht. Die Hypothese wurde überprüft, indem Mäuse gemästet wurden. Danach wiesen sie eine erhöhte TLR Ausprägung vor. Unter anderem auch in Zellen, die mit Insulin interagieren, sowie in der Bauchspeicheldrüse (Pankreas), dem Produktionsorgan des Insulins. Diese übergewichtigen Mäuse hatten eine schlechtere Insulinsensitivität und Mühe, mit einem Zuckerschub umzugehen. Wurde der Versuch mit Mäusen durchgeführt, denen das TLR2 Gen fehlte (sogenannte *Tlr2* $^{-/-}$ Mäuse), zeigte sich Interessantes: Das Insulin war wirkungsvoller, und sie konnten besser mit Zuckerschüben umgehen. Die gemästeten *Tlr2* $^{-/-}$ Mäuse waren etwa gleich schwer wie Kontrollmäuse, bei denen das TLR2 Gen vorhanden war, sie hatten jedoch eine gesündere Fettverteilung. Ihre Fettzellen waren kleiner und reagierten sensitiver auf Insulin. Zudem waren sie teilweise vor Leberschäden geschützt. Weiter waren ihre pankreatischen β-Zellen (Insulinproduzenten) weniger entzündet und konnten mehr Insulin sezernieren. Zusammenfassend kann man sagen, dass *Tlr2* $^{-/-}$ Mäuse teilweise von den ungesunden Folgen des Übergewichtes verschont blieben.

Das zweite Kapitel beschäftigt sich mit SIRT1, einer Proteindeacetylase, die bei der Suche nach lebensverlängernden Faktoren in Hefe entdeckt wurde. SIRT1 ist bei verschiedensten biologischen Prozessen involviert. Es vermindert zellulären Stress, fördert die Entwicklung von spezialisierten Zellen und verbessert den Zuckerhaushalt sowie die Insulinsekretion von Mäusen. Das Interesse an

SIRT1 wurde geweckt, weil Angehörige einer Familie von Diabetikern eine Mutation im SIRT1 Gen tragen. Diese Punktmutation im Erbgut führt zu einem Austausch der Aminosäure Leuzin durch Prolin im SIRT1-Protein. Betroffene Familienmitglieder sind heterozygote Träger, das heisst: Neben der mutierten Form tragen sie auch ein gesundes Allel. Könnte die durch die Mutation beeinträchtigte Funktion von SIRT1 kompensiert werden, indem man das gesunde SIRT1 Allel mit chemischen Aktivatoren anregt? Zur Überprüfung dieser Hypothese wurden SIRT1 Aktivatoren (SRTs) an zwei verschiedenen Typ 1 Diabetes Tiermodellen getestet: an der non-obese diabetes (NOD) Maus und der multiple-low doses of streptozotocin (MLD-STZ) behandelten Maus. Entgegen den Erwartungen hatten die SRTs in keinem der beiden Tiermodelle positive Einflüsse. Zwei der SRTs lösten schwere Komplikationen aus, was zu mehreren Todesfällen führte. Die heterozygote *Sirt1* $^{+/-}$ Maus wurde – im Gegensatz zu den Patienten, die auch nur ein gesundes SIRT1 Allel besitzen – nicht diabetisch. Wurden diese Mäuse mit MLD-STZ diabetisch gemacht, unterschieden sie sich nicht von Kontroll-*Sirt1* $^{+/+}$-Mäusen. Schlussfolgernd kann gesagt werden, dass die *Sirt1* $^{+/-}$-Maus kein gutes Modell für die Diabetiker-Familie ist. Des Weiteren müssen SIRT1-Aktivatoren genauer untersucht werden, bevor besagte Familienangehörige damit behandelt werden könnten.

SUMMARY (ENGLISH)

The involvement of the immune system and its mediators in the development of type 2 diabetes has been discussed controversially. While type 1 diabetes clearly is an auto-immune disease, type 2 diabetes was believed to be caused mainly by insulin resistance, the inability of peripheral organs to properly use insulin. Lately, there is increasing evidence pointing to an important role of the immune system also in type 2 diabetes.

This thesis is divided into two parts. Chapter 1 highlights the importance of TLR2, a receptor of the innate immune system, in the development of type 2 diabetes. TLR2 recognizes structural parts of intruding bacteria and helps to destroy invading pathogens. TLR2 can also be activated by dietary fatty acids and studies in humans and animal models have shown that obesity leads to chronic low grade inflammation. Therefore, this part of the thesis investigates if TLR2 is a molecular link between increased dietary lipid intake and the impaired regulation of glucose homeostasis. HFD fed mice showed increased expression of certain *Tlrs* in different cell types, including insulin-sensitive tissues and pancreatic islets. Compared to their wild-type littermates, *Tlr2* $^{-/-}$ mice on a HFD displayed improved glucose tolerance and increased insulin sensitivity. Despite similar total body weight, these mice had reduced perigonadal fat pad weight, in addition to having smaller adipocytes that displayed improved insulin-stimulated glucose uptake. *Tlr2* $^{-/-}$ mice were also protected from HFD-induced liver insulin resistance, hepatosteatosis and liver inflammation. Further, β-cell insulin secretion was improved and pancreatic islet inflammation was reduced in HFD fed *Tlr2* $^{-/-}$ mice compared to wild-type controls. Overall, *Tlr2* $^{-/-}$ mice were protected from insulin resistance and β-cell dysfunction induced by a HFD.

Chapter 2 deals with SIRT1, a protein deacetylase that was originally discoverd in a screening assay for longevity factors in yeast. It was found to be involved in manifold actions such as genomic stability, stress resistance and metabolic regulation, improvement of glucose homeostasis and insulin secretion. SIRT1 attracted attention when a family of type 1 diabetics was investigated. Affected family members heterozygously carry a point mutation in SIRT1, leading to a leucine to proline exchange in the SIRT1 protein (L107P). The aim of this study was to evaluate if activation of the SIRT1 enzyme derived from the wild-type allele could be a safe and efficient way to medicate these

patients. SIRT1 activators (SRTs) were applied to two different animal models of type 1 diabetes, the non-obese diabetes (NOD) mouse and the multiple-low doses of streptozotocin (MLD-STZ) treated mouse. In contrast to what was expected, in both models SRTs were unable to delay the onset of diabetes. The amount of pancreatic immune cell infiltration (insulitis score) was also not different between SRT treated NOD and control NOD mice. Importantly, two SRTs caused severe side effects, leading to an accumulation of cases of death in these treatment groups. Further, *Sirt1* $^{+/-}$ mice did not develop auto-immune diabetes and the development of diabetes was not different in *Sirt1* $^{+/-}$ mice compared to *Sirt1* $^{+/+}$ when treated with MLD-STZ. In summary, the *Sirt1* $^{+/-}$ mouse was not a suitable model for the L107P familial diabetes and further evaluations of SIRT1 activators are needed before they can be recommended to treat the affected family members.

ABBREVIATIONS

ACOX	peroxisomal acyl-coenzyme A oxidase
BMDC	bone-marrow-derived dentritic cell
BMDM	bone-marrow-derived macrophage
BSA	bovines serumalbumin
CD	cluster of differentiation
Cpt	carnitine palmitoyltransferase
DNA	deoxyribonucleic acid
EDTA	ethylenediaminetetraacetic acid
ELISA	enzyme-linked immunosorbent assay
FACS	fluorescence activated cell sorting
Fas	fatty acid synthase
FCS	fetal calf serum
FOXO	forkhead box class O
GLUT	glucose transporter (also called SLC2A)
GSIS	glucose-stimulated insulin secretion
GTT	glucose-tolerance test
HFD	high-fat diet
IL	interleukin
IL-1Ra	interleukin-1 receptor antagonist
i.p.	intra peritoneal
ITT	insulin-tolerace test
Lcad	long-chain acyl dehydrogenase
Mcad	medium-chain acyl dehydrogenase
MCP	monocyte chemotactic protein
MIP	macrophage inflammatory protein
NEFA	non essencial fatty acid
NF-κB	nuclear factor κ-light-chain-enhancer of activated B cells
PBS	phosphate buffered saline
PCR	polymease chain reaction
Pgc	peroxisome proliferator-activated receptor gamma coactivator
RNA	ribonucleic acid
SEM	standard error of the mean
SIRT1	sirtuin (silent mating type information regulation 2 homolog) 1
TLR	toll-like receptor
TNF	tumor necrosis factor

1 INTRODUCTION

1.1 Glycaemic control

The human body needs fuel to operate properly. The utilisation of energy is manifold: exercise moves us, anabolic and catabolic processes constantly remodel our body, organs fulfil their specific task and the brain integrates information and manages the complex coordination of actions. This performance requires a constant supply of energy which is mainly taken up by food ingestion. The body's primary source of energy is glucose. A tight glycaemic control is crucial to maintain functionality at all times. Hypoglycaemia (low glucose) may interrupt important biological processes, harm the brain and even lead to life-threatening situations while hyperglycaemia (high glucose) may cause microvascular damage (e.g. retinopathy), macrovascular damage (e.g. coronary heart disease) and other diabetes related complications. Therefore, blood glucose must always be kept between 2.5 and 5 mmol/l, independent of organ activities. This is mainly achieved by two pancreatic hormones, namely the anabolic insulin and its catabolic antagonist glucagon [1], even though steroids, catecholamines, growth hormones and others also play important roles. The main stimulant for insulin release is glucose itself. After food ingestion, blood glucose (coming from the ingested food) rises, which triggers insulin secretion from pancreatic β-cells. As a consequence plasma insulin rises, commanding organs to take up glucose, which lowers blood glucose concentration and brings it back to a normal range. Glucagon is the other major player that keeps euglycaemia. Its main stimulus is low glucose. In many ways it antagonizes the action of insulin, mainly by stimulating glucose release from the liver, resulting in increased blood glucose concentration.

1.2 The history of diabetes mellitus and the discovery of insulin

It was as early as in ancient Greece that the phenomenon of sick people that excessively urinated "sweet urine" was described. The Greeks named this sickness diabetes ("to straddle"), a reference to the fact that people suffering from diabetes often urinated. In 1675 the Latin word mellitus ("honey")

was added, owing to the sweet taste of urine from diabetics. Suffering from diabetes mellitus was an almost certain death sentence with people getting weaker and weaker and finally dying of acidosis. In 1889 Oskar Minowski and Joseph von Mering from the University of Strasbourg identified the organ that was involved in the development of diabetes mellitus. They removed the pancreas from a dog and several days later they detected sugar in the dog's urine, resembling symptoms of diabetic humans. An important step towards the treatment of diabetes mellitus was achieved in 1921, when Frederik Banting and Charles Best from the University of Toronto repeated the experiments of Minowski and von Mering, and in addition "cured" the pancreatectomized dog by reinjecting a lysate derived from the removed pancreas. Only two months later, on January 11th 1922, a young diabetic man was injected with "insulin", lowering his blood glucose significantly. Banting and Best received the Nobel Prize for the discovery of insulin in 1923. For treatment of diabetics, insulin was harvested from beef and pork and only in 1980 recombinant human insulin was produced by the U.S. biotech company Genentech. In the meantime (1953), the complete amino acid sequence of insulin was determined by Frederick Sanger [2, 3] for which he received the first of his two Nobel Prizes.

Decades of research have yielded several approaches to treat diabetes. An important effort was the development of modified insulin which allows to adjust the rate at which insulin is metabolized by the body. Several supporting substances are in clinical use. Insulin secretagogues (e.g. sulfonylureas) trigger insulin release by the β-cells, insulin sensitizers (e.g. metformin, glitazones) amplify the actions of insulin and incretin mimetics (e.g. GLP-1, GIP, DPP-4 inhibitor) use other routes to ameliorate insulin secretion. Anti-diabetic drugs became a lucrative market for pharmaceutical companies and with the expected increase in patient numbers over the next decades research will be intensified and hopefully yield new exciting ways to treat this disease.

1.3 The pancreas and its hormones

In the abdomen, between the duodenum and the stomach lies the 15-20 cm long pancreas, wedge-shaped and 70-100 g in weight. It contains two types of tissue: the endocrine part which secretes hormones into the blood, and the exocrine part which secretes digestive enzymes into the gut.

1.3.1 The endocrine pancreas

Around 2 % of the pancreas account for the endocrine glands, called the islets of Langerhans. These clusters of cells range in cell number from a few cells to thousands of cells with a diameter of up to 300-400 μm [4]. The human pancreas contains about 1 million islets of Langerhans and consists of 5 types of cells that produce hormones such as insulin (β-cells, 65-80% of total islet cells), glucagon (α-cells, 15-20%), somatostatin (δ-cells, 3-10%), pancreatic polypeptide (PP cells, 3-5%), and ghrelin (ε-cells, <1%) [5].

The pancreatic islets are highly vascularized [6] allowing them to sense endocrine signals and to fine-tune hormone release into the bloodstream. The direction of blood flow is physiologically important, because hormones secreted from one cell type could act downstream in a paracrine fashion on other cell types (e.g. glucagon secreted by α-cells is a potent insulin secretagogue, somatostatin from δ-cells inhibits insulin secretion). In rodents the blood flows in a defined order, BAD (β - α - δ), restricting β-cells to sense circulating, but not paracrine hormones [7]. Structure and composition of human and rodent islets differ [8, 9], which needs to be taken into account when comparing experimental data of humans and rodents. Early reports described a simple core-mantle architecture in human islets, similar to that of rodent islets. Other publications claim that all subtypes of cells are dispersed throughout the human islet [4, 9] and/or that they might be organized in β-cell clusters surrounded by α-cells [10, 11]. A recent paper also scanned human islets three dimensionally and proposes a three layer model, where an enriched β-cell layer is sandwiched between two α-cell enriched layers [12] (Fig. 1). However, there is a general agreement that the proportion of β-cells to α-cells is smaller in human islets compared to rodent islets [9, 13, 14].

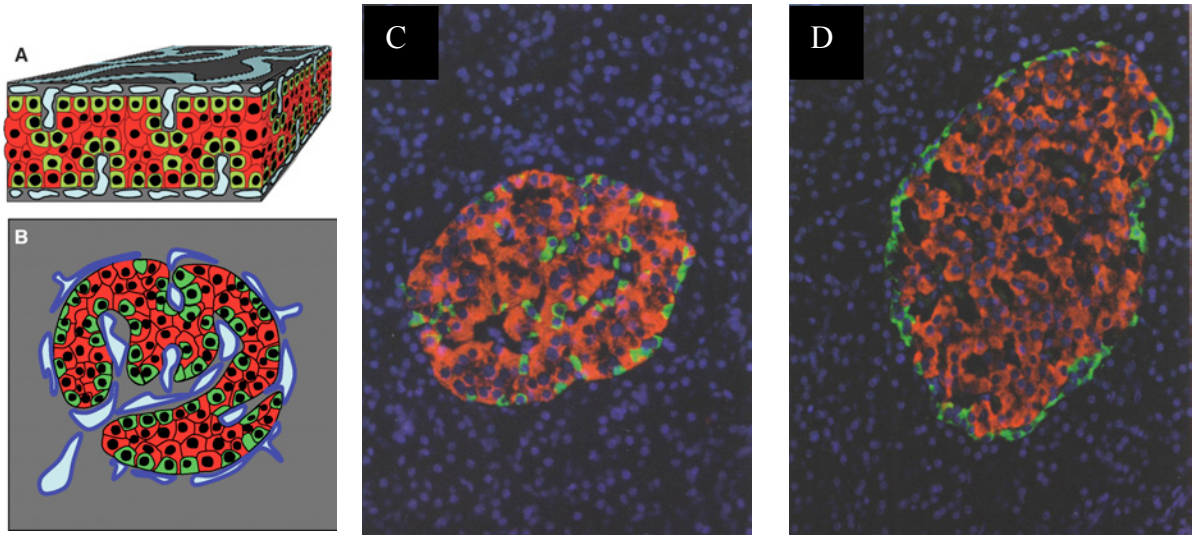

Fig. 1 Architecture of pancreatic islets. (**A**) Schematized model of human islets where a β-cell (red) layer is sandwiched by two α-cell layer (green). This thick layer is lined with vessels (blue) at both sides and is folded to form islets (**B**) **[12]**. Sections of human (**C**) and rat (**D**) adult pancreas stained for insulin (red) and glucagon (green). Graph adapted from [15].

1.3.2 The exocrine pancreas

The vast majority of the pancreas is exocrine tissue, comprised of acinar cells, ductal cells and goblet cells. Exocrine cells are specialized in the production and secretion of precursors and mature enzymes required for digestion. Each day, the human pancreas produces approximately 1.5 l of pancreatic juice containing proteases (to hydrolyze proteins), amylases (to digest carbohydrates), lipases (to breakdown lipids) and nucleases (to digest nucleic acids).

Acinar cells are epithelial cells containing digestive enzymes that are released upon neuronal or humoral stimulation. Duct cells are also epithelial cells and secrete HCO3-, which aids the micellar solubilzation of lipids. The third type of cell found in the exocrine pancreas are goblet cells. They are mainly found in the large, distal pancreatic ducts and produce mucin.

1.4 Insulin gene, synthesis and secretion in β-cells

In 1953 Frederick Sanger published the complete sequence of insulin [2, 3] for which he was awarded with the nobel prize. In humans, the insulin gene is located on the short arm of chromosome 11 [16, 17], spans three exons and two introns and is translated into a 5.8 kDa molecule containing two chains. These two chains, the 21 amino acid long A chain and the 30 amino acid long B chain, are linked by two disulfide bonds. Several tissue specific transcription factors (e.g. Pdx-1, BETA2/NeuroD, Pax-6) lead to β-cell differentiation and expression of insulin [18]. In addition, insulin is also expressed in the pituitary gland [19] which needs to be taken into consideration when the promoter of the insulin gene is used to create β-cell specific transgenic mice (e.g. rip-cre).

The mature mRNA of the insulin gene contains sequences encoding several peptide domains, called preproinsulin. This precursor is translated in the rough endoplasmatic reticulum, where the leader sequence is cleaved off, giving rise to proinsulin [20, 21]. Proteases in the trans-Golgi cleave the proinsulin at two sites, which leads to the mature insulin molecule and an equimolar amount of C peptide, which are stored in secretory granules for later exocytosis [22-24].

The main trigger for insulin release in the β-cell is glucose [22], which is transported from the blood into the β-cells via the glucose transporter (GLUT). GLUT-1 is the main glucose transporter in humans, while rodent β-cells predominantly express GLUT-2 [25]. Glucokinase phosphorylates glucose which eventually leads to NADH (and ATP, pyruvate), which is used in the TCA cycle in mitochondria to build up a H^+ gradient. This leads to production of ATP from ADP in the cytosol. ATP-sensitive K^+ channels react to this increase in ATP/ADP ratio, close and subsequently lead to a depolarization of the cell membrane. Voltage-dependent Ca^{2+} channels open and the raise in cytosolic Ca^{2+} concentration leads to fusion of the insulin-containing granules with the plasma membrane. In a first rapid reaction, stored insulin is released (first phase insulin) which is followed by a bigger release of preformed and newly synthesized insulin (second phase insulin) [26] (Fig. 2).

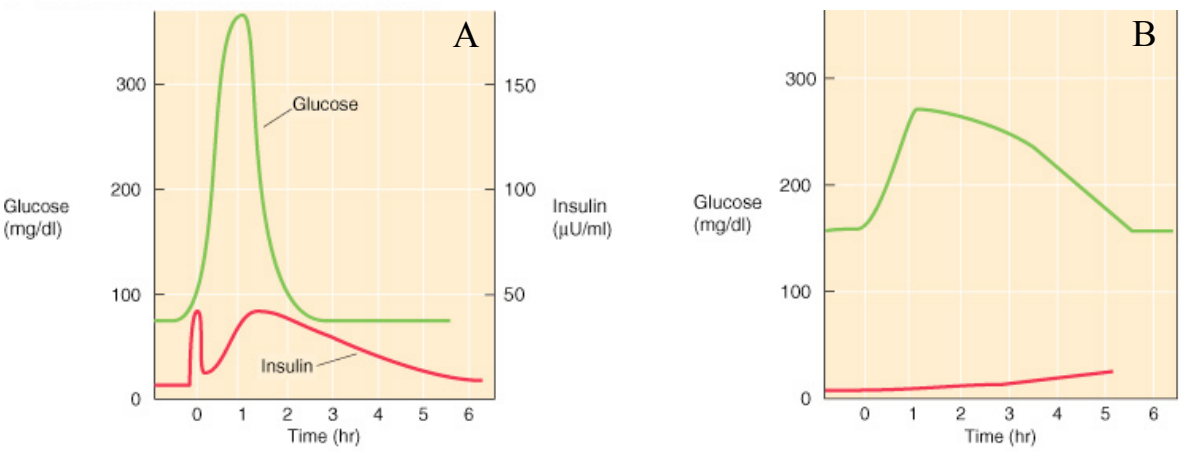

Fig. 2 First and second phase insulin. (**A**) An intravenous glucose tolerance test leads to a distinct first and second phase peak of insulin released into the circulation. (**B**) In a diabetic individual, the β-cells have lost their function and do not show any reaction to an oral glucose load. Graph adapted from [27].

1.5 Insulin function and target tissues

The primary function of insulin is to lower blood glucose by acting on enzymes in insulin sensitive tissues, namely the liver, muscle and fat.

In the liver, insulin promotes the storage of glucose as glycogen. This is achieved by regulating the enzymes that are involved in glycogenesis and glycogenolysis. First, insulin enhances the transcription of glucokinase and glycogen synthase, two key enzymes involved in the transformation of glucose to glycogen. Second, insulin suppresses the transcription of glycogenolysis enzymes, namely glucose-6-phosphatase and glycogen phosphorylase. In addition, insulin stimulates lipogenesis and protein synthesis and inhibits gluconeogenesis, all leading to lower blood glucose concentrations.

In the muscle, insulin promotes the uptake of glucose and its storage as glycogen. As in the liver, insulin activates glycogen synthase. Hexokinase, the liver specific enzyme that converts glucose to glucose-6-phosphate, is also induced by insulin. In addition, insulin stimulates protein synthesis and the recruitment of GLUT-4, which translocates from an intracellular pool to the muscle membrane where it facilitates the diffusion of glucose into muscle cells. Note that in comparison to the non-insulin sensitive GLUT-2 in liver, GLUT-4 in muscle (and fat) is positively regulated by insulin [25].

In adipocytes, insulin promotes the uptake of glucose and its storage as triglycerides. It increases glycolysis and triggers the conversion of pyruvate to free fatty acids by enhancing the transcription of pyruvate dehydrogenase and acetyl CoA carboxylase. In addition, insulin stimulates the esterification of α-glycerol-phosphate with free fatty acids to form triglycerides and inhibits the enzyme of the reverse reaction, hormone-sensitive triglyeride lipase. As in the muscle, GLUT-4 is recruited to the plasma membrane upon insulin stimulation.

1.6 Glucagon and its function

A major hormone that counteracts the blood glucose lowering effects of insulin is glucagon. It prevents hypoglycaemia by increasing hepatic glucose output [28, 29]. Glucagon acts on the liver by increasing glycogen breakdown (glycogenolysis) and de-novo synthesis of glucose (gluconeogenesis), and decreasing the rate of glucose catabolism (glycolysis). The glucagon precursor proglucagon is expressed in pancreatic α-cells, intestinal L-cells and in hindbrain neurons [30]. The prohormone convertases (PC) differentially process proglucagon.. PC2 is found in α-cells and converts proglucagon to glucagon. Contrarily, L-cells and neurons in the hindbrain express PC3/PC1 which converts proglucagon to glucagon-like-peptide (GLP)1 and GLP2 [30-32]. The major glucagon secretagogues are ingestion of protein (even though glucagon acts on carbohydrates and not protein), hypoglycaemia, circulating epinephrine, neuronal stimulation and crosstalk between α-cells and β-cells. Glucagon binds to the glucagon receptor, a G-protein coupled receptor, and signals through the second messenger adenosine 3',5'-cyclic monophosphate (cAMP) and phospholipase C (PLC) / inositol triphosphate (IP_3) pathway to exert its hyperglycaemic action.

1.7 Somatostatin, pancreatic polypeptide and ghrelin

The human endocrine pancreas comprises of 5 cell types. The two most important – insulin producing β-cells and glucagon producing α-cells – were discussed above. The three remaining cell types are δ-

cells (produce somatostatin, 3-10%), ε-cells (produce ghrelin, <1%), and PP cells (produce pancreatic polypeptide (PP), 3-5%) [5].

Somatostatin is produced in pancreatic δ-cells, intestinal D-cells and in the hypothalamus. Its main function is to inhibit the secretion of hormones like thyroid-stimulating hormone (TSH), gastrin and growth hormone (GH). In addition, it also inhibits the secretion of insulin and glucagon [33]. Ghrelin was first described in 1999 as a growth hormone-releasing peptide [34]. It is produced in pancreatic ε-cells, in the fundus of the stomach and in certain areas of the brain [35]. It seems to promote hunger by acting on the hypothalamus [36], opposing leptin. Pancreatic polypeptide is post-prandially secreted in pancreatic PP-cells [37-39] and seems to be involved in weight loss, as injection [40, 41] or β-cell specific genetic over-expression [42] of PP in ob/ob mice reduces bodyweight by decreasing food intake and increasing energy expenditure. PP infusion studies in humans have shown that food intake is reduced in patients with the Prader-Willi syndrome [43] (patients display higher levels of PP) and in healthy individuals [44, 45].

1.8 Diabetes mellitus

Diabetes mellitus is a metabolic disease characterized by high concentrations of blood glucose resulting from diminished insulin production and/or attenuated biological insulin action. Hyperglycaemia and consequently advanced glycation end-products (AGE) in endothelial cells, alterations in the microarchitecture of cells and its components, induction of inflammation and other cellular adaptations may lead to severe consequences, ranging from peripheral neuropathy (nerve damage), retinopathy (damage of the retina in the eye), nephropathy (kidney damage), to increased risk for cardio- and cerebrovascular diseases [46]. The first diabetic patient was treated in 1922 (see 1.2 The history of diabetes mellitus and insulin) and according to a survey published by the World Health Organisation (WHO) 2.8% of the earth's population had diabetes in the year 2000 and this number will almost double by 2030 [47]. This corresponds to 366 million people worldwide [48, 49]. According to data from the 2007 National Diabetes Fact Sheet, 7.8% of the population in the United States (23.6 million) have diabetes. The major risk factors that contribute to this epidemic of diabetes

are inactivity, unbalanced diets, obesity and genetic predisposition. The dramatic increase in the diabetes incident rate may be explained by the more and more sedentary lifestyle, elevated food consumption and changed age pattern in our society.

The traditional classification system distinguishes several distinct subtypes of Diabetes mellitus, although there is evidence for overlaps [50, 51] . The vast majority of diabetics belong to the type 2 diabetes mellitus group which is associated with insulin resistance and relative insulin deficiency, while less people suffer from type 1 diabetes mellitus which is characterized by autoimmune β-cell destruction and subsequent absolute insulin deficiency. Other classifications include gestational diabetes and prediabetes, a state characterised by elevated blood glucose levels that are higher than normal but not yet high enough to be diagnosed with overt diabetes.

1.8.1 Type 1 diabetes mellitus

Type 1 diabetes mellitus (T1DM) accounts for 5-10 % of all cases of diabetes. In this disease, autoimmune destruction of the insulin producing β-cells leads to absolute insulin deficiency. The absence of insulin increases the balance between produced (liver) and used (muscle) glucose and ketones. Glucose excess leads to osmotic diuresis in the kidney and the subsequent dehydration and accumulated acidosis finally leads to death from diabetic ketoacidosis.

T1DM patients display antibodies against their own β-cells, insulin, and other islet specific proteins, accompanied by immune cell infiltration into the pancreas [52-54]. Islets are smaller, islet volume and mass are decreased [55, 56], and β-cells are diminished or absent [55]. The pathology of T1DM is not completely understood, but the interaction of environmental factors (such as viral infections, stress, or toxins) and T1DM susceptibility gene variants [56] seems to trigger diabetes in genetically susceptible individuals [46, 57].

Insulin replacement therapy is used to treat T1DM. In advanced stages of the disease, organ transplantation (whole pancreas or purified islets) are also applied to increase insulin production and normalize blood glucose concentrations.

1.8.2 Type 2 diabetes mellitus

Type 2 diabetes mellitus (T2DM) accounts for 90-95 % of all cases of diabetes. T2DM patients display peripheral insulin resistance, thus higher concentrations of insulin are required to exert the same magnitude of glucose disposal in muscle and adipocytes, and to inhibit glucose output in the liver to the same extent as in healthy individuals. Only 10 % of people which are insulin resistant are diabetic [58], because the increased demand for insulin is compensated by increased insulin production. This is achieved by enlarging both islet mass and β-cell function [59]. The major cause of insulin resistance is obesity and aging [60]. Caloric excess leads to hypertrophy of adipocytes and a changed adipokine secretory profile. Nutrient overload, increased fatty acid flux and inflammation induce insulin resistance [60-62]. T2DM patients show impaired GLUT4 translocation in skeletal muscle [63], corrupted ability of insulin to phosphorylate insulin receptor substrate (IRS) in skeletal muscle [64] and adipocytes [65] and decreased expression of insulin receptors on hepatocytes [66]. The progression to T2DM develops in a biphasic pattern. First, the pancreatic β-cell mass increases in response to the increased insulin demand, which was observed in obese non-diabetic or pregnant individuals. As the need for insulin progressively increases, the β-cells not only fail to adapt further but also undergo apoptosis, which leads to insulin deficiency and diabetes [67] (Fig. 3).

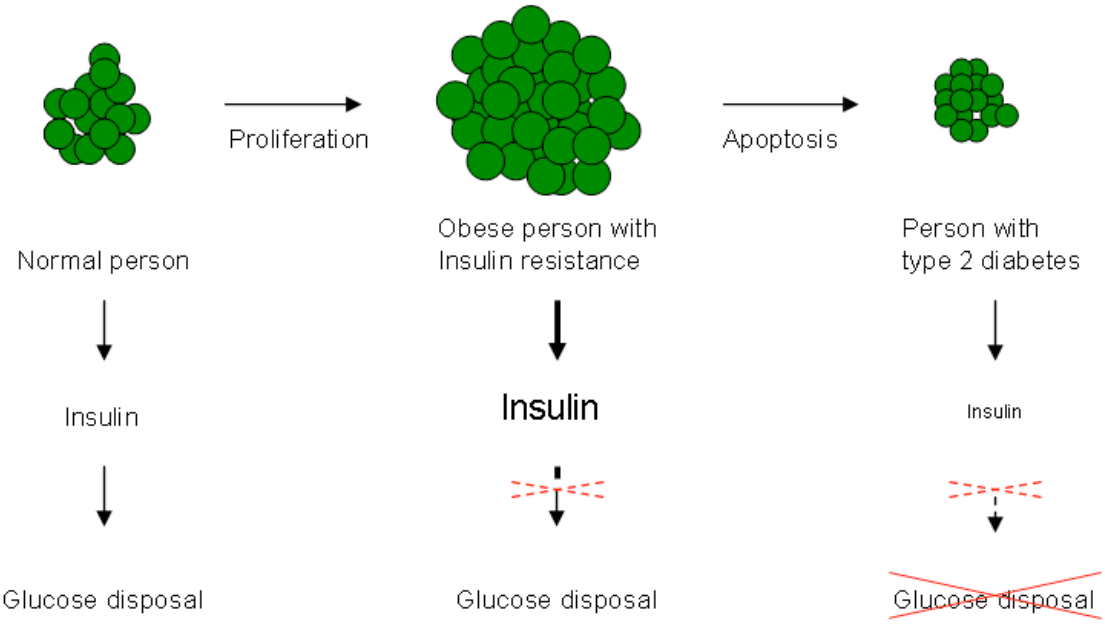

Fig. 3 Initiation of type 2 diabetes. Increased insulin demand triggers the upregulation of β-cell mass (green spheres). As insulin demand rises even more, the pancreatic β-cell mass fails to adapt, which leads to relative insulin deficiency and diabetes. Adapted from [50].

It is not quite clear why β-cells of a T2DM patient fail and undergo apoptosis. It was proposed that production of reactive oxygen species, endoplasmatic reticulum stress, dyslipidemia, accumulation of islet associated polypeptide (IAPP) and induction of Fas and IL-1β contribute to the destruction of β-cells [68-70]. Obese individuals display an increased inflammatory profile, originating from adipokines and chemokines/cytokines released by infiltrating macrophages and dendritic cells [71]. This chronic, low-grade inflammation can cause insulin resistance [72] and β-cell dysfunction [69]. T2DM patients have an increased number of islet-associated macrophages [73] which was also observed in various animal models, where HFD feeding and excessive obesity (db/db mice) display pancreatic immune cell infiltration [73, 74]. Recently, blocking inflammation in T2DM has successfully been implemented in clinical trials. Administration of the naturally occurring IL-1β receptor antagonist (IL-1Ra) or neutralizing IL-1β antibodies reduces islet inflammation and improves β-cell function *in vivo* [75-77].

2 TLR2-DEFICIENT MICE ARE PROTECTED FROM INSULIN RESISTANCE AND β-CELL DYSFUNCTION INDUCED BY A HFD

2.1 Introduction

2.1.1 TLRs

Toll-like receptors (TLRs) are widely expressed transmembrane receptors of the innate immune system, recognizing patterns of invading pathogens [78]. Eleven human TLRs and thirteen mouse TLRs have been identified so far. They are activated by lipids, carbohydrates, nucleic acids and proteins [79-81]. Upon stimulation, TLRs trigger inflammation mainly via NFκB (but also via AP1, IRF3/7 and other signalling cascades) and therefore help to destroy invading pathogens. This destructive mechanism is essential to keep cellular homeostasis, but might also lead to collateral tissue damage. Especially prolonged TLR activation may lead to a chronic low grade inflammation and may support the development of chronic diseases like alzheimer's disease, atherosclerosis, diabetes and cancer [82-85]. This is supported by the findings that TLRs and their ligands are elevated in inflammatory diseases and that blocking TLR pathways by either knocking out certain TLRs or the TLR adaptor protein myeloid differentiation primary response gene 88 (MyD88), protects against the development of inflammatory diseases in animal models [86-88]. Since TLRs are not ligand-specific and instead recognize general patterns of bacteria, fungi and viruses, they are also activated by structurally similar patterns of non-pathogens, such as dietary lipids [89, 90]. Nutritional fatty acids, such as palmitate and oleate, were shown to activate TLR4 which triggered inflammation *in vivo* and lead to insulin resistance in mice on a HFD [90]. These findings support a role for TLRs in fuel mediated chronic inflammatory diseases and link obesity with T2DM.

2.1.2 TLR2

A broad range of TLR2 receptor activators have been described, including components of bacterial cell walls, such as lipopolysaccharides (LPS), lipoproteins and glycoproteins, zymosan, peptidoglycan and other lipid based structures. TLR2 is predominantly expressed in immune cells but is also found in other tissues, including insulin sensitive adipocytes, hepatocytes and myocytes [91, 92]. TLRs signal through several adaptor molecules, but TLR2 primarily depends on the MyD88 pathway [93]. TLR2 activation via binding of ligands recruits MyD88, which in turn triggers NFκB-associated genes that encode proinflammatory cytokines such as TNFα and Il-6.

2.1.3 TLR2, obesity and inflammatory diseases

Recent studies have shown that non-essential fatty acids, including palmitate and oleate, can activate TLR2 signalling to induce proinflammatory cytokine production, leading to tissue-specific impairments and insulin resistance [89, 90, 94-96]. Chronic activation of the innate immune system is associated with type 2 diabetes, and evidence suggests that both insulin resistance and β-cell failure are promoted by low grade inflammation in humans [97-99]. Animal models of type 2 diabetes also show increased levels of cytokines, chemokines and immune cells in both insulin-responsive tissues (liver, muscle, adipose tissue) and pancreatic islets [73, 97, 100-102]. This local tissue inflammation has been causally linked to insulin resistance and β-cell function [97, 102]. Genetic ablation studies in HFD models have shown that pro-inflammatory CD11c+ cells are responsible for the induction of inflammation in insulin sensitive tissues and thereby impact on insulin sensitivity [103]. Similar results were obtained in human studies, where T2DM patients treated with salicylate (NF-κB inhibitor) displayed improved insulin sensitivity [76, 104]. In another study, T2DM patients were treated with the IL-1 receptor antagonist IL-1Ra which improved β-cell insulin secretion [75].
Several observations point to TLR2 as a important bridge between obesity, inflammation and diabetes. First, obese humans and rodents have a gram-positive bacteria enriched microbial flora [105] and therefore possibly increased TLR2 signalling. Second, TLR2 was shown to be involved in the development of palmitate-induced insulin resistance in myotubes [95]. Third, TLR2 knockout mice showed improvements in the metabolic syndrome associated with HFD-induced obesity [90, 106-108]. Fourth, inactivating TLR2 with siRNA improved insulin sensitivity in HFD-fed mice [109]. Finally, HFD-fed *Tlr2* $^{-/-}$ mice showed improvements in the metabolic syndrome relative to HFD-fed wild type mice [106], even though the underlying mechanisms are not completely understood.

2.1.4 Aim of the thesis, TLR2 part

TLR2 recognizes structural parts of intruding gram-positive bacteria [78], triggers inflammation via NFκB and helps to destroy the invading pathogen. Recently, it has been shown that TLR2 can also be activated by dietary fatty acids [89]. Given the fact that TLR2 was also shown to be involved in the induction of insulin resistance in myotubes *in vitro* [95], we decided to investigate the involvement of TLR2 in diet-induced obesity and diabetes in animal models of T2DM.

Hypothesis 1: TLR2 is expressed on pancreatic β-cells and is a molecular link between increased dietary lipid intake and the regulation of insulin.

Hypothesis 2: Blocking TLR2 *in vivo* protects from the adverse effects of HFD-induced obesity.

2.2 Methodology

2.2.1 Animals

Tlr2 $^{-/-}$ mice (strain B6.129-*Tlr2* ^{tm1Kir}/J, the Jackson Laboratory, Bar Harbor, ME, USA) backcrossed on C57BL/6J for four to five generations were bred in house with C57BL/6J mice to generate all *Tlr2* $^{+/+}$ and *Tlr2* $^{-/-}$ sex- and age-matched littermate mice used for *in vitro* and *in vivo* studies. To determine the genetic purity of *Tlr2* $^{+/+}$ and *Tlr2* $^{-/-}$ mice, we genotyped 112 microsatellite markers evenly distributed across the whole mouse genome. This confirmed that 93–95% of the genome of *Tlr2* $^{+/+}$ and *Tlr2* $^{-/-}$ littermate mice used in this study was derived from B6. *Db/wt* mice (strain B6.Cg-Dock7<m> +/+ Lepr<db>/J, the Jackson Laboratory, Bar Harbor, ME, USA) were bred in house with *Tlr2* $^{+/-}$ mice to generate all *db/db Tlr2* $^{+/+}$ and *db/db Tlr2* $^{-/-}$ sex- and age-matched littermate mice used for *in vivo* studies. Animals were housed under specific-pathogen-free conditions at the Institute of Labortierkunde, Vetsuisse faculty of the University of Zürich (Zürich, Switzerland). Experiments were performed according to Swiss veterinary law and institutional guidelines. The committee for animal welfare at the Katholieke Universiteit Leuven approved all tissue isolation protocols from mice used for TLR2 tissue expression profiling.

2.2.2 Tissue expression of TLR2

The gene array was performed in collaboration with the laboratory of Dr. Frans C. Schuit at the Department of Molecular Cell Biology, Gene Expression Unit, Katholieke University in Leuven, Belgium. RNA from whole tissues were extracted using TRIzol (Invitrogen, Basel, Switzerland), followed by a cleanup with RNeasy columns (Qiagen, Hombrechtikon, Switzerland). RNA was reverse transcribed into cDNA (SuperScript Choice System, Invitrogen, Basel, Switzerland) using oligo-dT primers and a T7 RNA polymerase promoter site. cDNA was *in vitro* transcribed and biotin-labelled (Affymetrix IVT labeling kit, Santa Clara, CA, USA). Quantity and quality of total RNA and cRNA profiles of all RNA preparations were analyzed using a NanoDrop ND-1000 spectrophotometer (NanoDrop Technologies, Wilmington, DE, USA) and 2100 Bioanalyzer (Agilent, Santa Clara, CA, USA). Quantification of mRNA was performed using Affymetrix mouse 430A 2.0 expression microarrays. The overnight biotin-labelled cRNA was fragmented during 35 min at 94°C and hybridized during 16 hours at 45°C, followed by washing/staining in a Fluidics Station and scanning using a GeneScanner 3000 (both Affymetrix, Santa Clara, CA, USA). Raw data were analyzed using GCOS software (Affymetrix, Santa Clara, CA, USA). Signal intensities were scaled using the global scaling method taking 150 as target intensity value.

2.2.3 Metabolic studies

Animals were fed a HFD containing 58, 26 and 16 cal/cal from fat, carbohydrate and protein, respectively, and a total of 23.2 kJ/g (Diet D12331, Research Diets, New Brunswick, NJ, USA) whereas the control diet contained 29, 39 and 32 cal/cal from fat, carbohydrate and protein, respectively, and a total of 11.7 kJ/g (Provimi Kliba AG, Kaiseraugst, Switzerland). For GTT, mice fasted for 12h (19:00 – 7:00) were injected i.p. with 2 mg/g body weight glucose and insulin was measured by ELISA (Mercodia, Uppsala, Sweden). ITT was performed by injecting female mice starved for 3h (8:00 – 11:00) i.p. with 0.85 U/kg human insulin (Novo Nordisk, Denmark), and male mice i.p. with 1.0 U/kg insulin. Pam2CSK4 (5 µg/mouse) dissolved in saline or saline was injected i.p. into *Tlr2* $^{+/+}$ and *Tlr2* $^{-/-}$ mice, and after 24 h plasma was analysed for serum amyloid A by ELISA (Invitrogen, Basel, Switzerland).

2.2.4 Isolated adipocyte experiments

White adipocytes were isolated by collagenase digestion, filtered through a 250 µm nylon mesh and washed twice in Krebs buffer. To determine glucose incorporation, adipocytes were incubated with D-[U-^{14}C]glucose (final glucose concentration, 0.89 mmol/l) for 60 minutes in the presence or absence of 100 nM insulin. Glucose incorporation was stopped by centrifuging the mixture in a phthalic acid dinonyl ester gradient, which allows to separate the adipocytes from the medium due to their different specific weight. The adipocyte layer was then subjected to liquid scintillation counting. Aliquots of adipocyte fractions were used to determine mean cell diameters. Photographs of isolated adipocytes in the hemocytometer were taken, and images were analyzed using ImageJ software (National Institue of Health, Bethesda, MD, USA) for quantification (http://rsbweb.nih.gov/ij/). At least 120 adipocytes per mouse were analyzed.

2.2.5 Indirect calorimetry and physical activity

Mice were placed in airtight respiratory cages that were continuously ventilated with a flow rate of 0.5 l/min to measure oxygen consumption (VO_2) and carbon dioxide production (VCO_2). For each cage, air was sampled for 30 s at 5 min intervals. Energy expenditure was calculated according to [110] using the following equation: total energy expenditure (kcal/h/kg) = 3.9 x VO_2 l/h + 1.1 x V.O_2 l/h. RQ was defined as VCO_2 (l)/ VO_2 (l). Data were analysed with AccuScan Integra ME software (AccuScan Inc., Columbus, OH, USA). After allowing animals to adapt to metabolism cages for 5 days, mice were i.p. implanted with a telemetry sensor (TA-F20) (Data Science International, St Paul MN, USA) under brief anaesthesia. The mice were allowed to recover for at least 1 week. Physical activity was measured every 5 min using Dataquest A.R.T. 3.1 software (Data Science International).

2.2.6 Plasma analysis

Plasma samples were assayed using mouse Luminex kits (Millipore, Billerica, MA, USA) according to the manufacturer's instruction. NEFAs, cholesterol and ketone bodies in plasma was analysed using colorimetric assays following the manufacturer's instructions (Wako, Richmond, VA, USA). Triacylglycerols were determined using a GPO-Trinder-based serum triacylglycerol kit from Sigma (St Louis, MO, USA).

2.2.7 Glucose clamp studies

Mice were anesthetized with isoflurane, and a catheter (MRE 025, Braintree Scientific, Braintree, MA, USA) was inserted into the left jugular vein and exteriorized at the back of the neck. After 7 days of recovery, only mice that had regained greater than 95% of their preoperative weight were studied. After a fasting period of 5 hours, 3-[^{3}H]glucose (0.1 μCi/min; PerkinElmer, Waltham, MA, USA) was infused for 80 minutes, and blood was collected from tail tip for basal turnover calculation. After basal sampling, insulin (18 mU/kg/min) was infused for 2 hours. Euglycaemia was maintained by periodically adjusting a variable infusion of 20% glucose with a syringe pump (TSE Systems, Chesterfield, MO, USA). The glucose infusion rate was calculated as the mean of the steady-state infusion (60–90 minutes) after 1 hour of insulin infusion. A blood sample was collected from tail tip after steady-state infusion. The glucose turnover rate was calculated by dividing the rate of 3-[^{3}H]glucose infusion by the plasma 3-[^{3}H]glucose–specific activity. Hepatic glucose production was calculated by subtracting the glucose infusion rate from the glucose turnover rate.

2.2.8 Total liver lipid extraction

Liver tissue (30 mg) was homogenized in PBS, and lipids were extracted in a chloroform/methanol (2:1) mixture. Total liver lipids were determined by a sulfo-phospho-vanillin reaction.

2.2.9 RNA extraction and real-time PCR

Total tissue RNA from adipose tissue, liver, muscle, isolated islets, bone-marrow-derived macrophages (BMDMs), and bone-marrow-derived dendritic cells (BMDCs) were isolated according to the manufacturer's instructions (Qiagen, Hombrechtikon, Switzerland). Commercially available mouse primers (Applied Biosystems, CA, USA) were used for real-time PCR. For *ex vivo* detection of islet inflammatory genes after HFD feeding, islets were initially allowed to recover for 4 h in suspension before extraction of total RNA.

2.2.10 Immunohistochemistry

Mouse liver and pancreatic cryosections were incubated with an anti-F4/80 primary antibody (clone CI:A3-1, BMA Biomedicals, Switzerland), or isotype control rat IgG2b (AbD Serotec, Düsseldorf, Germany) and counterstained with haematoxylin and eosin. F4/80 was visualised using goat anti-rat antibody (112-005-167) (Jackson ImmunoResearch, Newmarket, UK) and a donkey anti-goat antibody conjugated to HRP (Jackson 705-035-147). Images were captured on an Axioplan 2 imaging system (Zeiss, Feldbach, Switzerland) and F4/80 positive area/islet positive area was quantified using Image J software. For liver sections, three random fields of view were analysed in two sections per animal separated by 200 μm (an average of 3,600 ± 100 cells per animal). For the pancreas, all islets in four sections separated by 200 μm were analysed per animal (an average of 47 ± 7 islets per animal).

2.2.11 Pancreatic islet isolation and BMDM/BMDC preparation

Mouse islets were isolated by collagenase digestion, followed by Histopaque gradient centrifugation. For *in vitro* islet experiments, islets were plated on extracellular matrix (Novamed, Jerusalem, Israel). Islets were allowed to adhere and spread on the extracellular matrix dishes for 48 h before initiation of experiments.

Bone marrow was isolated from femurs and tibias of female mice and cultured in macrophage medium consisting of 50% Dulbecco's Modified Eagle Medium supplemented with 20% horse serum and 30% L929 conditioned medium (a source of macrophage colony-stimulating factor). After 7 days, cells were plated into 24-well plates (5×10^6 cells/well) for experiments and extraction of RNA. To generate BMDCs, bone marrow prepared from femurs and tibias was cultured in non-tissue-culture-treated Petri dishes with RPMI (Roswell Park Memorial Institute) medium supplemented with 2-mercaptoethanol (50 μM), 10% FCS and 200 U/ml granulocyte macrophage colony-stimulating factor. After 7 days, non-adherent cells were plated into 24-well plates (5×10^6 cells/well) for experiments and extraction of RNA. The specificity of the two differentiation protocols to generate BMDMs (CD45+F4/80+CD11b+Cd11c−) and BMDCs (CD45+CD11b+CD11c+) was verified by FACS analysis. BMDM and BMDC were resuspended in FACS buffer (2% FCS, 10 mmol/l EDTA in PBS) and incubated with anti-mouse CD16/32 (Fc-block, BD Biosciences, Heidelberg, Germany) for 5 min, then stained with anti-mouse CD45-biotin/SAV-APC/Cy7 (BD Biosciences, Heidelberg, Germany), F4/80-FITC (BD Biosciences, Heidelberg, Germany), CD11c-PE (Invitrogen, Basel, Switzerland) and CD11b-APC (BD Biosciences, Heidelberg, Germany) for 20 min. The cells were analysed with a Partec FloMax flow cytometer (Münster, Germany). 7-AAD (7-amino-actinomycin D, Invitrogen) was used to exclude nonviable cells in flow cytometric analysis. Cells were treated for 6 h with BSA or a 0.5 mmol/l palmitate:oleate (2:1 molar ratio) preparation before RNA extraction.

2.2.12 TLR2 antibody treatment

Mice were given a weekly dose of 10 mg/kg bodyweight of OPN301, a monoclonal anti mouse TLR2 antibody, isotype control antibody or saline, respectively. OPN301 and isotype control were manufactured by Opsona Therapeuticals, Ireland.

2.2.13 Western blot analysis

Total protein was prepared from perigonadal adipose tissue and blotted for GLUT4 as previously published [111].

2.2.14 Tissue triacylglycerols and glycogen

To measure triacylglycerol content in muscles, lipids were extracted from approximately 30 mg of tissue by homogenisation in 500 µl of acetone. Homogenates were centrifuged twice for 5 min at full speed to remove cell debris. Triacylglycerol concentrations were measured using TRIG kit (Diatools, Villmergen, Switzerland) according to the manufacturer's instructions. To measure glycogen content in muscles, glycogen was extracted by digesting approximately 20 mg of tissue in 2 mol/l HCl in duplicate. Glycogen was measured using the glucose HK kit (Sigma, St Louis, MO, USA).

2.2.15 NEFA preparation

Oleate or palmitate (Sigma, St Louis, MO, USA) were dissolved at 10 mmol/l concentration in RPMI medium containing 11% BSA (NEFA- and endotoxin-free) (Sigma) under an N_2 atmosphere. Eleven % BSA without NEFA served as a control, and effective NEFA concentrations were determined with a commercially available kit (Wako chemicals, Neuss, Germany). Dissolved fatty acids were tested for endotoxin contamination using the standard Limulus Ameobodyte Lysate assay (Cambrex, Charles City, IA, USA), and found to contain minimal levels in the range of 6–58 pg/ml as described [112]. Endotoxin levels were similar between BSA controls and NEFA preparations, and these endotoxin levels are unable to activate either pancreatic islets [112] or BMDCs [96].

2.2.16 Statistics

Data are expressed as means ± SEM with the number of individual experiments presented in the figure legends. All data were analysed using the nonlinear regression analysis programme PRISM (GraphPad, CA, USA), and significance was tested using Student's *t* test and analysis of variance

(ANOVA) with Dunnett's or Bonferroni's post-hoc test for multiple comparison analysis. Significance was set at $p < 0.05$.

2.3 Results

2.3.1 *Tlr2* tissue expression and regulation by HFD feeding

We initially profiled mouse tissue expression of *Tlr2* mRNA (Fig. 1A). These data indicated that *Tlr2* has a broad tissue expression profile, which includes not only organs classically described as being heavily populated by immune cells (spleen), but also insulin-sensitive tissues and the pancreatic islet. Based on this information, we analysed mRNA expression of *Tlr1, -2, -4* and *-6* in response to 20 weeks of HFD feeding in female black 6 mice in perigonadal adipose tissue, skeletal quadriceps muscle, liver tissue, pancreatic islets and circulating leucocytes (Fig. 1B). Indeed, HFD feeding resulted in increased mRNA expression of some of *Tlr1, -2, -4* and *-6* in all these tissues.

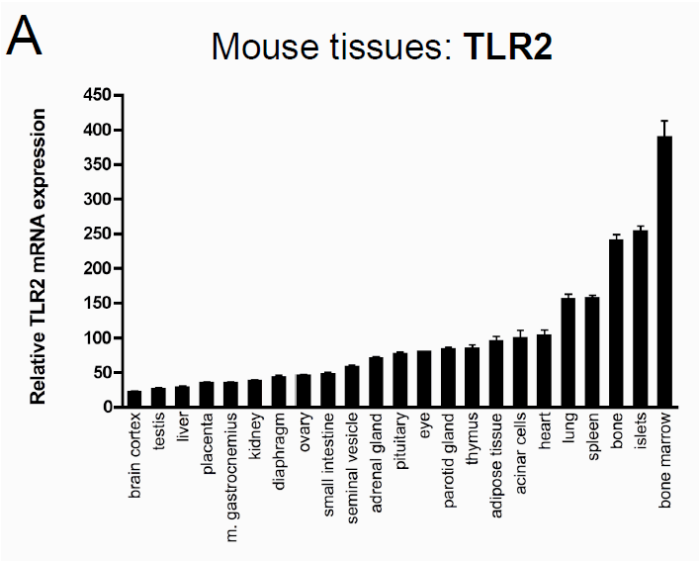

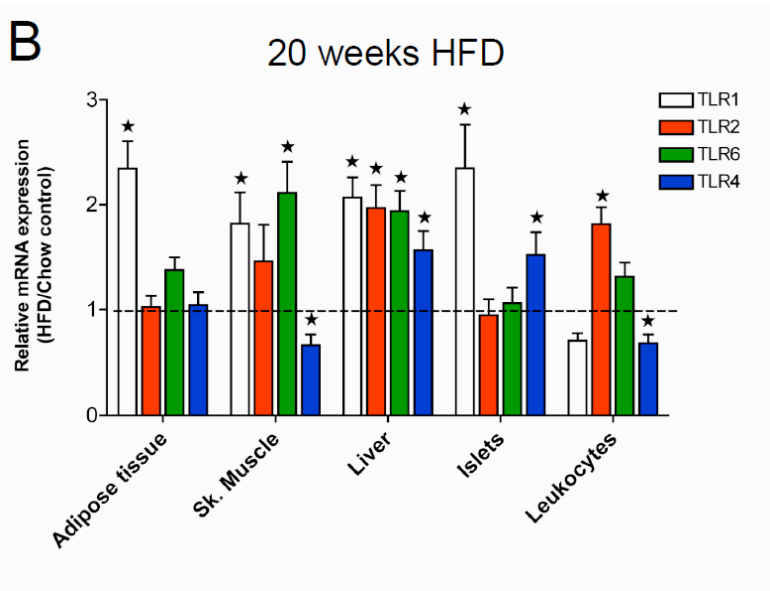

Fig. 1 HFD regulation of tissue *Tlr1, -2, -4* and *-6* mRNA expression. (**A**) Relative tissue expression profile of mouse *Tlr2* mRNA based on gene arrays (n = 3 for all tissues except islet, bone marrow and pituitary, where n = 4). (**B**) Female C57BL/6J littermate mice were fed a HFD for 20 weeks starting at 10–12 weeks of age. Perigonadal adipose tissue, quadriceps skeletal muscle, liver tissue, isolated pancreatic islets and circulating leucocytes were isolated and analysed for *Tlr* expression by quantitative PCR (chow n = 7, HFD n = 8). White bars, *Tlr1*; red bars, *Tlr2*; green bars, *Tlr6*; blue bars, *Tlr4*. *$p<0.05$, as tested by Student's t test compared with chow-fed age-matched control (1.0±SEM)

2.3.2 *Tlr2* $^{-/-}$ mice are resistant to the adverse effects of HFD feeding

Based on published data [95, 96, 113] and the upregulation of TLR expression by HFD, we reasoned that mice lacking *Tlr2* (which are unable to signal via TLR1/2, or TLR2/6 heterodimers) might show differences in susceptibility to HFD-induced glucose intolerance. *Tlr2* $^{-/-}$ mice were confirmed to be unresponsive to the synthetic TLR2 ligand, Pam2CSK4, *in vivo* (Fig. S1). Further, neither female nor male *Tlr2* $^{-/-}$ mice on a chow diet showed any difference in glucose tolerance or insulin sensitivity at 10–12 weeks of age when compared with littermate controls (*Tlr2* $^{+/+}$) (Fig. S2A-D). Thereafter, female and male *Tlr2* $^{+/+}$ and *Tlr2* $^{-/-}$ mice were put on HFD for 20 weeks, until 32 weeks of age. HFD-induced weight gain was not different between genotypes in both female (Fig. 2A) and male mice (Fig. S3A). After 12 weeks of HFD, female *Tlr2* $^{-/-}$ mice already showed improved glucose tolerance, insulin sensitivity and β-cell insulin secretion in response to a glucose challenge (Fig. S4). At this age male *Tlr2* $^{-/-}$ mice were also more insulin sensitive compared with *Tlr2* $^{+/+}$ littermates, while showing no differences in glucose tolerance or insulin secretion (Fig. S3B-D). After 20 weeks of HFD, female *Tlr2* $^{-/-}$ mice (aged 32 weeks) showed markedly improved glucose tolerance, insulin sensitivity and β-cell insulin secretion in response to a glucose challenge (Fig. 2B-D). Supporting improved peripheral insulin sensitivity, fasting circulating insulin levels were reduced both at 12 and 20 weeks of HFD feeding in female *Tlr2* $^{-/-}$ mice compared with *Tlr2* $^{+/+}$ controls (Fig. 2D and Fig. S4C). Age-matched 32-week-old chow-fed female *Tlr2* $^{+/+}$ and *Tlr2* $^{-/-}$ mice showed no differences in glucose homeostasis (Fig. S2E-F). Based on these data, we focused on female *Tlr2* $^{-/-}$ mice for the remainder of the study.

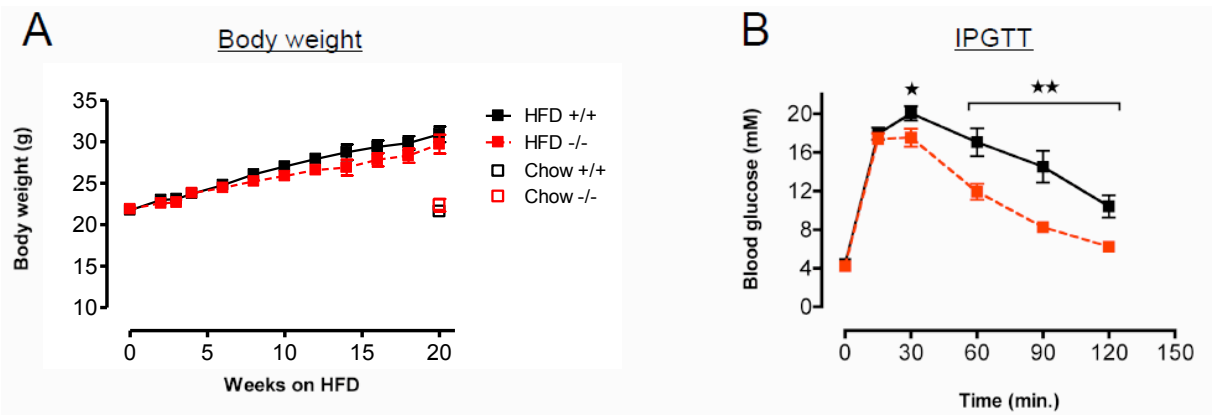

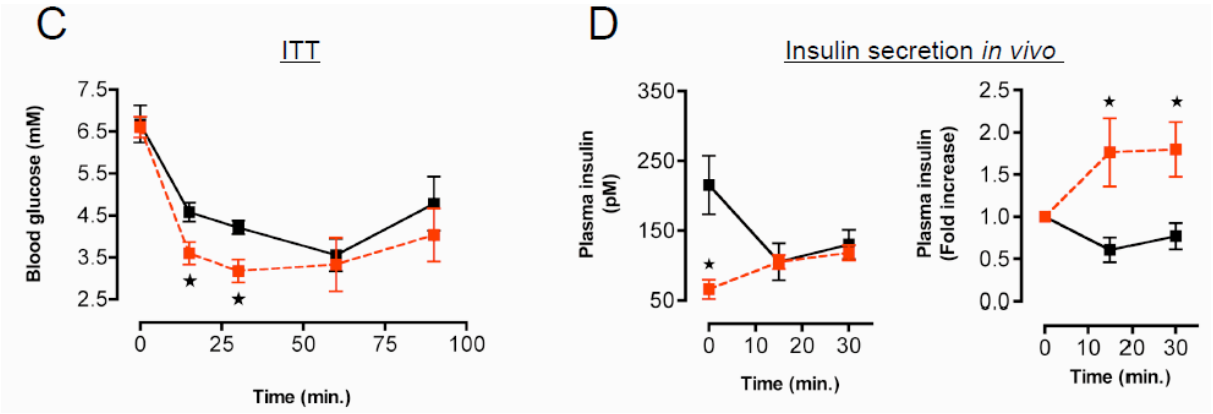

Fig. 2 *Tlr2* $^{-/-}$ mice are resistant to the adverse effects of HFD feeding. (**A**) Female *Tlr2* $^{+/+}$ and *Tlr2* $^{-/-}$ littermate mice were fed an HFD starting at 10–12 weeks of age, and body weight was monitored (n = 7 for chow groups, n = 31 for HFD *Tlr2* $^{+/+}$ and n = 32 for HFD *Tlr2* $^{-/-}$). (**B**) An IPGTT (2 g/kg glucose) was performed after 20 weeks of HFD feeding (32-week-old mice; n = 21 for HFD *Tlr2* $^{+/+}$ and n = 22 for HFD *Tlr2* $^{-/-}$). (**C**) An ITT (0.85 U/kg insulin) was performed after 20 weeks of HFD feeding (32-week-old mice; n = 8 for HFD *Tlr2* $^{+/+}$ and n = 7 for HFD *Tlr2* $^{-/-}$). (**D**) Insulin secretion during an IPGTT performed after 20 weeks of HFD feeding (32-week-old mice; n = 8 for HFD *Tlr2* $^{+/+}$ and n = 7 for HFD *Tlr2* $^{-/-}$). Black open square, chow *Tlr2* $^{+/+}$; red open square, chow *Tlr2* $^{-/-}$; black filled squares and unbroken line, HFD *Tlr2* $^{+/+}$; red filled squares and broken line, HFD *Tlr2* $^{-/-}$.*$p < 0.05$ and **$p < 0.01$, as tested by Student's t test compared with *Tlr2* $^{+/+}$ control

We went on to investigate insulin target tissue inflammation and insulin sensitivity in addition to examining islet inflammation and islet insulin secretion. HFD-fed female *Tlr2* $^{-/-}$ mice had reduced perigonadal fat pad weight compared with wild-type animals, in addition to having smaller adipocytes that displayed improved insulin-stimulated glucose uptake (Fig. 3A-D). This was consistent with increased GLUT4 protein levels in whole adipose tissue of *Tlr2* $^{-/-}$ mice (Fig. S5). Interestingly, HFD-induced adipose tissue cytokine mRNA expression was similar between genotypes, with only the chemokine *Mcp-1*, and the macrophage marker *Cd68*, showing reductions in mRNA in *Tlr2* $^{-/-}$ mice on HFD (Fig. 3E). Further, mRNA expression of *Cd36*, the fatty acid translocase known to associate with TLR2 [114], was unchanged in adipose tissue (Fig. 3F).

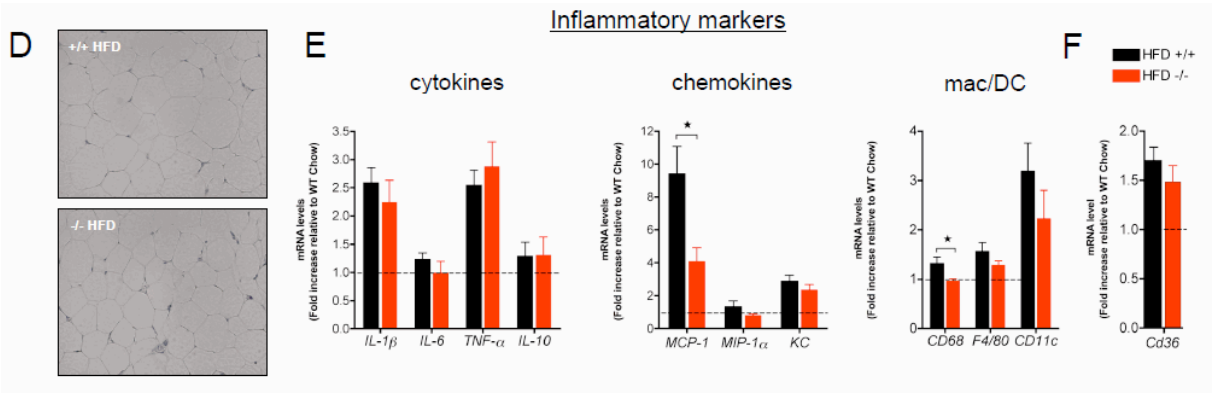

Fig. 3 Adipose tissue in female *Tlr2* $^{+/+}$ and *Tlr2* $^{-/-}$ mice after 20 weeks of HFD feeding. (**A**) Perigonadal fat pad weight as % body weight in chow- and HFD-fed female *Tlr2* $^{+/+}$ and *Tlr2* $^{-/-}$ mice (n = 13 chow *Tlr2* $^{+/+}$, n = 15 chow *Tlr2* $^{-/-}$, n = 21 HFD *Tlr2* $^{+/+}$, n = 23 HFD *Tlr2* $^{-/-}$).*$p < 0.05$ relative to *Tlr2* $^{+/+}$ chow control and #p < 0.05 relative to *Tlr2* $^{+/+}$ HFD, as tested by ANOVA with Newman–Keuls post hoc test. (**B**) Insulin (INS)-stimulated glucose incorporation in isolated perigonadal adipocytes (n = 4 per group). (**C**) Perigonadal adipocyte size distribution (n = 4 per group). (**D**) Representative image of perigonadal adipose tissue. (**E**) Relative cytokine, chemokine and macrophage/dendritic cell marker mRNA expression in perigonadal adipose tissue compared with chow-fed *Tlr2* $^{+/+}$ animals (n = 8 for HFD *Tlr2* $^{+/+}$ and n = 7 for HFD *Tlr2* $^{-/-}$). (**F**) *Cd36* mRNA expression compared with chow-fed *Tlr2* $^{+/+}$ animals (n = 8 for HFD *Tlr2* $^{+/+}$ and n = 7 for HFD *Tlr2* $^{-/-}$). Black open bars, chow *Tlr2* $^{+/+}$; red open bars, chow *Tlr2* $^{-/-}$; black filled bars, HFD *Tlr2* $^{+/+}$; red filled bars, HFD *Tlr2* $^{-/-}$. All but (**A**) *$p < 0.05$ as tested by Student's t test

In agreement with reduced adiposity, circulating leptin, MCP-1 and TNF-α levels were significantly reduced in female *Tlr2* $^{-/-}$ animals after 20 weeks of HFD feeding. However, we did not detect differences in circulating resistin, IL-6, cholesterol, NEFAs or ketones. In support of improved insulin sensitivity, circulating triacylglycerol levels were significantly reduced in *Tlr2* $^{-/-}$ mice on HFD (Table S1). Given the reduced adiposity of female *Tlr2* $^{-/-}$ mice on HFD, we investigated energy homeostasis in these animals during HFD feeding. Despite reduced adiposity, *Tlr2* $^{-/-}$ mice tended to consume more calories (10% more) (Fig. 4A). At the same time, we observed a parallel 10% increase in total energy expenditure, an effect that was more pronounced during dark phases (Fig. 4B). Increased total energy expenditure was not due to increased physical activity (Fig. 4C). Interestingly, *Tlr2* $^{-/-}$ mice preferentially used lipids as an energy source as indicated by a significantly reduced respiratory quotient (RQ), especially during the light phases (Fig. 4D). This was consistent with increased skeletal muscle *Acox1* and *Mcad* mRNA expression (enzymes involved in β-oxidation) in *Tlr2* $^{-/-}$ mice, while other genes involved in fatty acid uptake (*Cd36*) and inflammation were unchanged (Fig. 4E-F). However, at this time point we did not detect differences in skeletal muscle triacylglycerols or glycogen content between genotypes (Fig. S6). In summary, female *Tlr2* $^{-/-}$ mice show reduced adiposity on HFD compared with *Tlr2* $^{+/+}$ littermates. This was consistent with a reduced

RQ, and increased mRNA expression of some genes involved in β-oxidation in skeletal muscle. Overall energy intake and expenditure were balanced, possibly explaining why body weight did not differ between groups. Finally, adipose tissue and skeletal muscle inflammation due to HFD feeding was not strongly impacted by lack of TLR2 signalling.

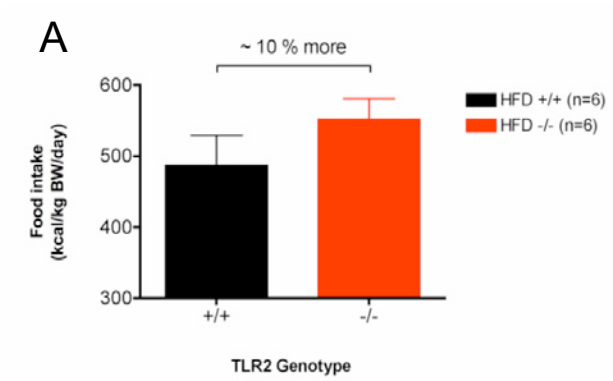

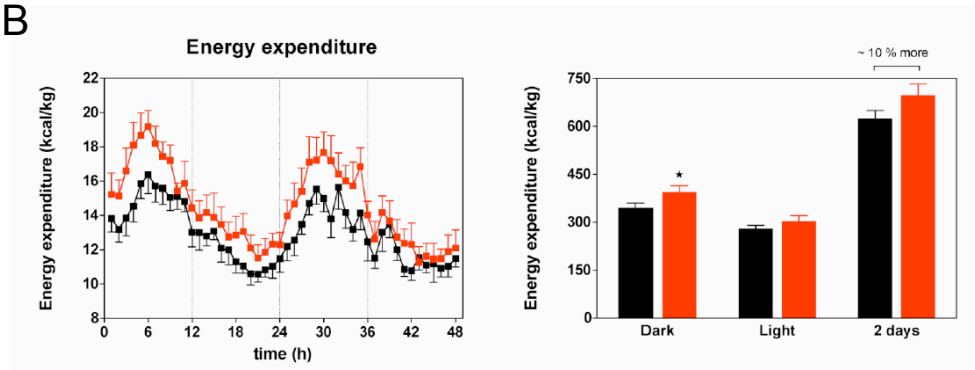

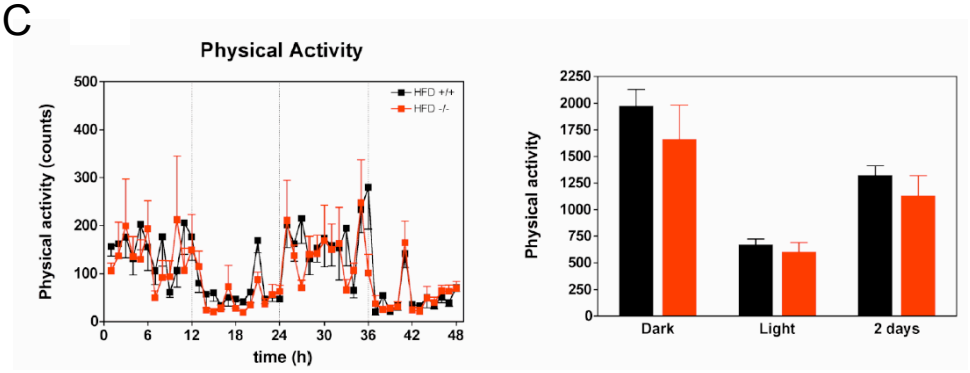

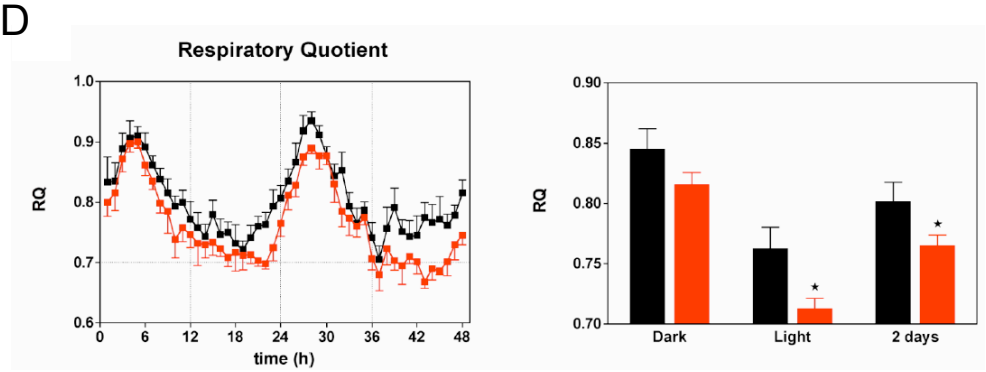

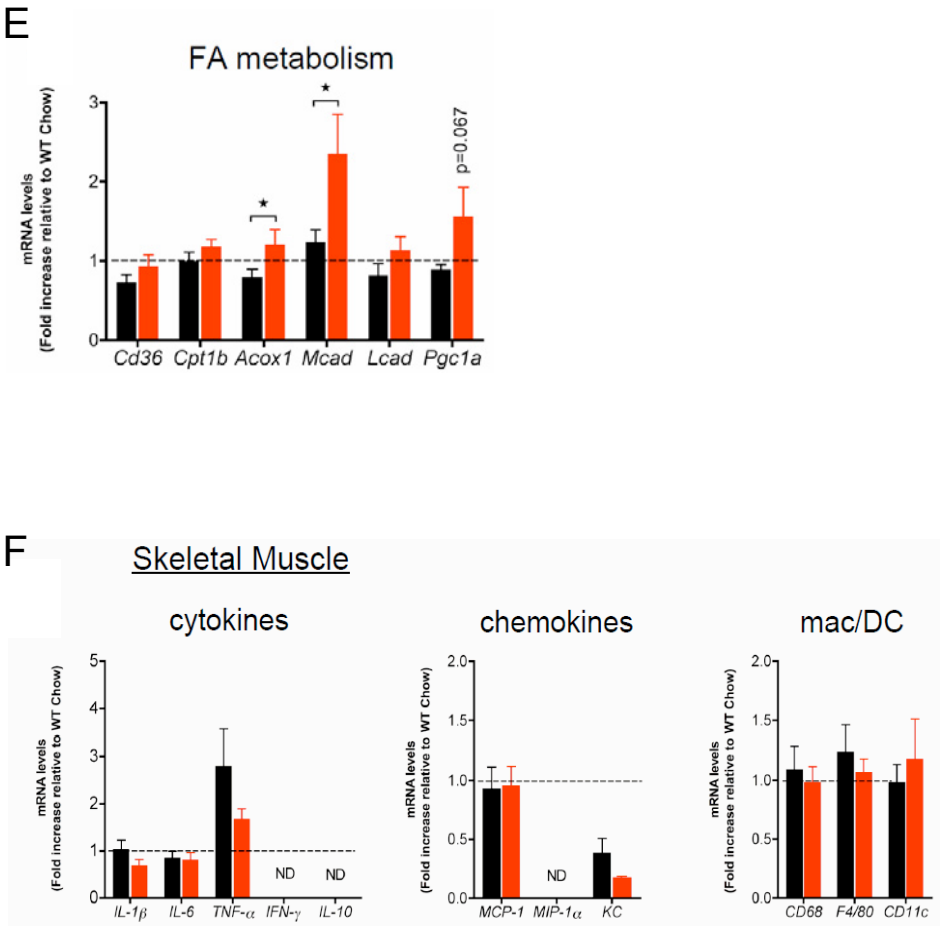

Fig. 4 Indirect calorimetry and muscle in female *Tlr2* $^{+/+}$ and *Tlr2* $^{-/-}$ mice after 20 weeks of HFD feeding. (**A**) Food intake monitored over four consecutive days as normalised to body weight ($p = 0.24$). (**B**) Energy expenditure calculated continuously over 48 h and total summed energy expenditure during dark and light phases. Time: 0 h = 18:00 h, and represents lights off; 12 h dark and light phases are separated by vertical lines. (**C**) Physical activity monitored by telemetry continuously over 48 h and averaged during dark and light phases. (**D**) RQ calculated continuously over 48 h and averaged during dark and light phases. $n = 6$ per group for all measurements. *$p < 0.05$ between genotypes as tested by Student's *t* test. (**E**) Relative mRNA expression of genes involved in fatty acid metabolism in quadriceps muscle in female *Tlr2* $^{+/+}$ and *Tlr2* $^{-/-}$ mice after 20 weeks of HFD feeding ($n = 8$ for HFD *Tlr2* $^{+/+}$ and $n = 7$ for HFD *Tlr2* $^{-/-}$). *$p < 0.05$ between genotypes as tested by Student's *t* test. (**F**) Relative cytokine, chemokine and macrophage/dendritic cell marker mRNA expression ($n = 8$ for HFD *Tlr2* $^{+/+}$ and $n = 7$ for HFD *Tlr2* $^{-/-}$). Black bars, or black squares with line, *Tlr2* $^{+/+}$; red bars, or red squares with line, *Tlr2* $^{-/-}$. BW, body weight; ND, not detectable

2.3.3 *Tlr2* $^{-/-}$ mice are protected from liver insulin resistance, hepatosteatosis and liver inflammation on HFD

We performed hyperinsulinaemic–euglycaemic clamps to assess peripheral insulin sensitivity in female *Tlr2* $^{-/-}$ and *Tlr2* $^{+/+}$ mice after HFD feeding for 20 weeks. In agreement with enhanced whole body insulin sensitivity observed during the ITT (Fig. 2C), glucose infusion rates were increased in *Tlr2* $^{-/-}$ mice concomitant with insulin-stimulated glucose turnover (Fig. 5A-B and Fig. S7). Further, liver insulin sensitivity was preserved in *Tlr2* $^{-/-}$ mice, as demonstrated by a significant reduction in hepatic glucose production during the hyperinsulinaemic clamp (Fig. 5C). Lipid content was reduced in livers of *Tlr2* $^{-/-}$ mice, suggesting protection against the development of hepatosteatosis under HFD (Fig. 5D). Consistent with this, mRNA of the fatty acid translocase, *Cd36*, was strongly reduced in *Tlr2* $^{-/-}$ mice, whereas genes involved in β-oxidation (*Acox1*, *Cpt1a*), oxidative metabolism (*Pgc1α* [also known as *Ppargc1a*]) or lipogenesis (*Fas*) were unchanged relative to controls (Fig. 5E). Indeed, *Tlr2* $^{-/-}$ mice were protected from HFD-induced liver *Il-1β*, *MCP-1* and *Cd68* mRNA expression compared with *Tlr2* $^{+/+}$ controls (Fig. 5F). However, other HFD-induced cytokines (*IL-6*, *Tnf-α*, *IL-10*) and chemokines (*MIP-1α* [also known as *Clcl3*], *Kc* [also known as *Cxcl1*]) were unchanged between genotypes. Consistent with mRNA data, numbers of liver F4/80+ cells (a macrophage marker) were unchanged between genotypes on HFD (13.7 ± 1.1 % in *Tlr2* $^{+/+}$ [n = 8] vs 13.5 ± 1.3 % F4/80+ cells/total cells in *Tlr2* $^{-/-}$ [n = 7]). Thus, female *Tlr2* $^{-/-}$ mice are protected from liver insulin resistance, hepatosteatosis and some markers of inflammation on HFD.

Hyperinsulinemic-euglycemic clamp

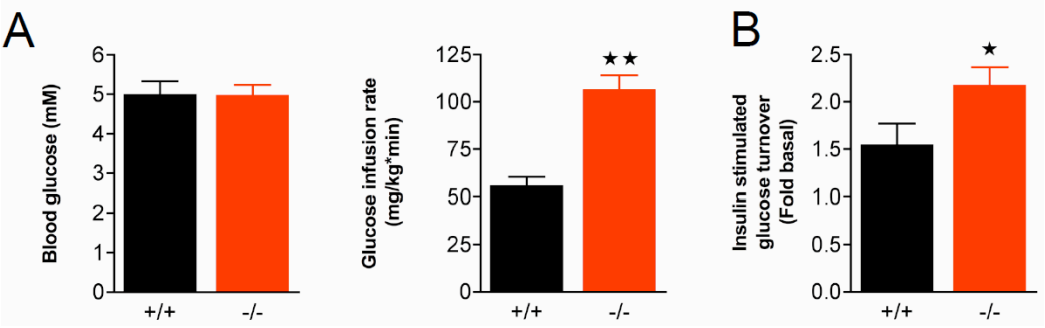

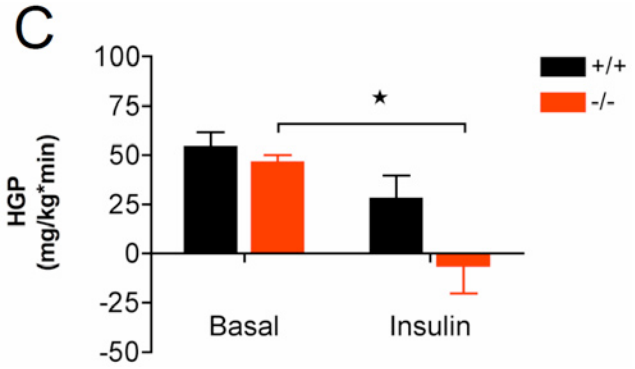
C
100
75
50
25
0
-25
-50
HGP
(mg/kg*min)
+/+
-/-
★
Basal
Insulin

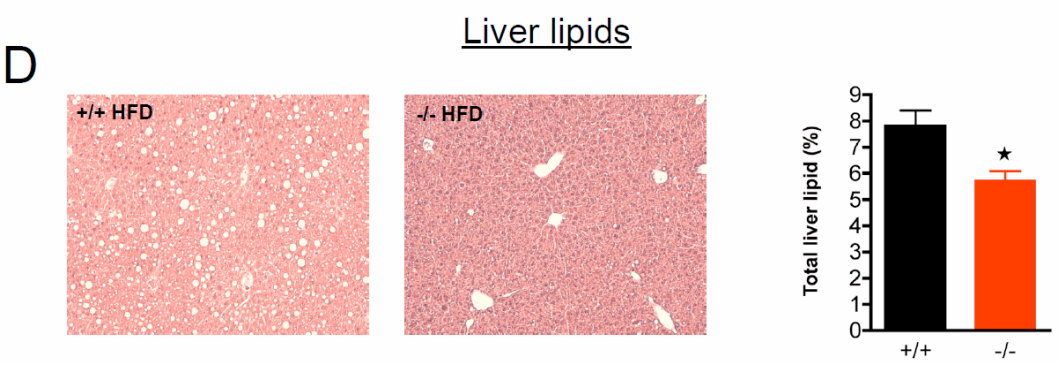
D
Liver lipids
+/+ HFD
-/- HFD
Total liver lipid (%)
9
8
7
6
5
4
3
2
1
0
★
+/+
-/-

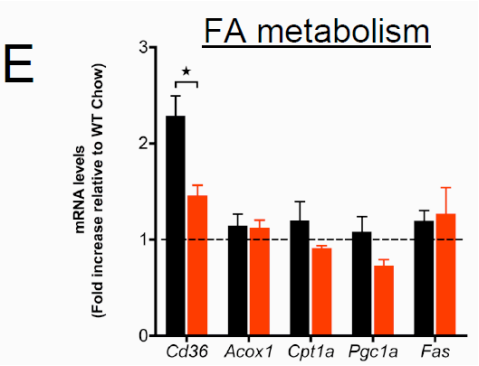
E
FA metabolism
mRNA levels
(Fold increase relative to WT Chow)
3
2
1
0
★
Cd36
Acox1
Cpt1a
Pgc1a
Fas

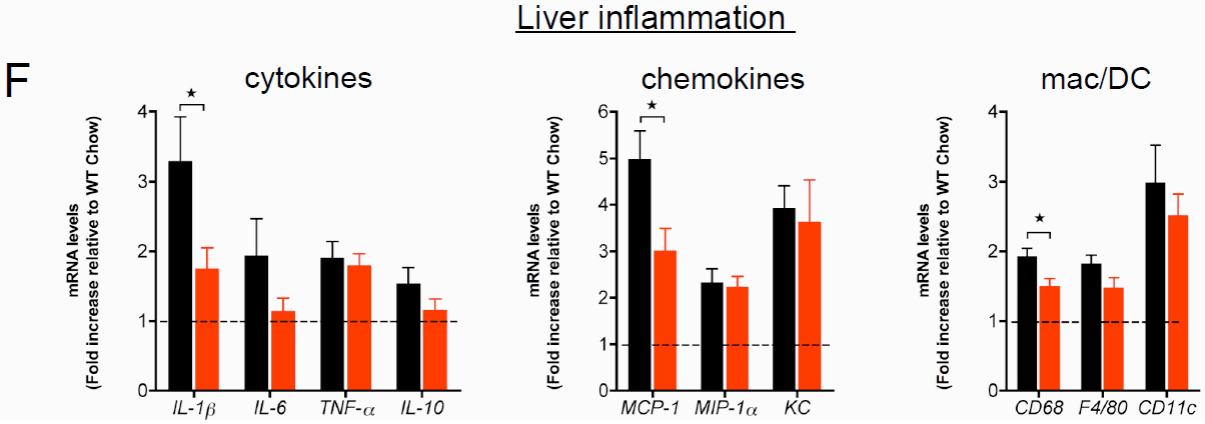
F
Liver inflammation
cytokines
chemokines
mac/DC
mRNA levels
(Fold increase relative to WT Chow)
★
IL-1β
IL-6
TNF-α
IL-10
MCP-1
MIP-1α
KC
CD68
F4/80
CD11c

Fig. 5 Liver in female *Tlr2* $^{+/+}$ and *Tlr2* $^{-/-}$ mice after 20 weeks of HFD feeding. Hyperinsulinaemic–euglycaemic clamps were performed after 20 weeks of HFD feeding in female *Tlr2* $^{+/+}$ and *Tlr2* $^{-/-}$ littermates. (**A**) Blood glucose during clamping and glucose infusion rate ($n = 4$). (**B**) Insulin-stimulated glucose turnover in female *Tlr2* $^{+/+}$ and *Tlr2* $^{-/-}$ littermates ($n = 4$). (**C**) Suppression of hepatic glucose production (HGP) during clamp ($n = 4$). (**D**) Representative liver stained with haematoxylin and eosin and total liver lipids ($n = 7$ for HFD *Tlr2* $^{+/+}$ and $n = 8$ for HFD *Tlr2* $^{-/-}$). (**E**) Relative mRNA expression of genes involved in fatty acid transport (*Cd36*), β-oxidation (*Acox1, Cpt1a, Pgc1α*) and lipogenesis (*Fas*). (**F**) Relative cytokine, chemokine and macrophage/dendritic cell marker mRNA expression in liver isolated from female HFD *Tlr2* $^{+/+}$ and *Tlr2* $^{-/-}$ littermates compared with chow *Tlr2* $^{+/+}$ controls ($n = 8$ for HFD *Tlr2* $^{+/+}$ and $n = 7$ for HFD *Tlr2* $^{-/-}$). Black bars, *Tlr2* $^{+/+}$; red bars, *Tlr2* $^{-/-}$. $*p < 0.05$ and $**p < 0.01$ as tested by Student's *t* test compared with *Tlr2* $^{+/+}$ control

2.3.4 *Tlr2* $^{-/-}$ mice are protected from impaired β−cell insulin secretion and islet inflammation on HFD

We isolated pancreatic islets after 20 weeks of HFD feeding from female littermate *Tlr2* $^{+/+}$ and *Tlr2* $^{-/-}$ mice. Islets from *Tlr2* $^{-/-}$ mice responded to an increased glucose concentration by increasing insulin secretion while *Tlr2* $^{+/+}$ islets showed no response to glucose (Fig. 6A). There was no difference in islet insulin content between genotypes (not shown). There was also no difference in glucose-stimulated insulin secretion between age-matched 32-week-old chow-fed *Tlr2* $^{+/+}$ and *Tlr2* $^{-/-}$ mice (not shown). This supports our *in vivo* findings (Fig. 2D) that female *Tlr2* $^{-/-}$ mice on HFD show improved β-cell insulin secretion compared with littermate *Tlr2* $^{+/+}$ controls.

Next, we analysed islet inflammation due to HFD feeding in female *Tlr2* $^{+/+}$ and *Tlr2* $^{-/-}$ mice. Increases in islet *Il-1β* mRNA owing to HFD positively correlated with increased macrophage/dendritic cell marker expression: *Cd68*, *F4/80* (also known as *Emr1*) and *Cd11c* (also known as *Itgax*) (Fig. 6B) (for *Cd68* $r^2 = 0.91$, $p = 0.0003$; for *F4/80* $r^2 = 0.92$, $p = 0.0006$; for *Cd11c* $r^2 = 0.60$, $p = 0.02$; $n = 8$). By contrast, islets from *Tlr2* $^{-/-}$ mice on HFD were protected from increased *Il-1β*, *Cd68* and *F4/80* mRNA. Furthermore, *Il-6*, *Tnf-α*, *Mcp-1* and *Kc* mRNA was also significantly reduced in *Tlr2* $^{-/-}$ versus *Tlr2* $^{+/+}$ islets on HFD, with no effect on islet *Cd36* expression (Fig. 6C-D). No reductions in these inflammatory markers were observed in islets isolated from sex- and age-matched chow-fed *Tlr2* $^{-/-}$ compared with *Tlr2* $^{+/+}$ mice (not shown). In contrast to *F4/80* mRNA data, and similar to the liver, the amount of islet F4/80+ cells were unchanged in HFD *Tlr2* $^{-/-}$ mice (percentage area of F4/80+ cells of total islet area: 1.9 ± 0.4% in *Tlr2* $^{+/+}$ [$n = 4$] versus 1.8 ± 0.4% in *Tlr2* $^{-/-}$ [$n = 4$]), possibly suggesting an altered activation status of liver and islet macrophages/dendritic cells in *Tlr2* $^{-/-}$ versus *Tlr2* $^{+/+}$ mice on HFD.

Finally, analysis of total peripheral leucocytes did not show differences in cytokine mRNA (*Il-1β*, *Tnf-α*) or macrophage marker expression (*Cd68*, *F4/80*) between *Tlr2* genotypes on HFD (data not shown), supporting the tissue specificity of the inflammatory response.

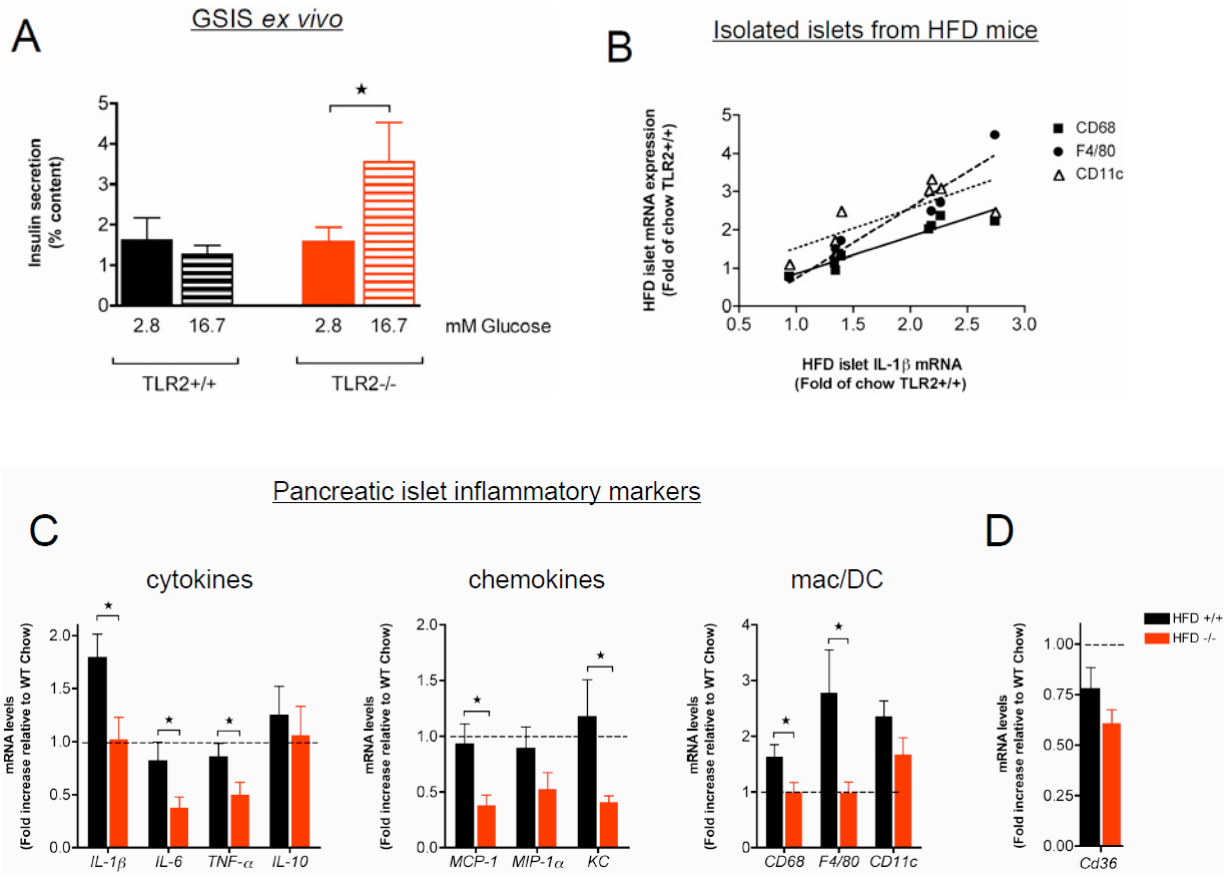

Fig. 6 Pancreatic islet in female *Tlr2* $^{+/+}$ and *Tlr2* $^{-/-}$ mice after 20 weeks of HFD feeding. (**A**) Pancreatic islets were isolated after 20 weeks of HFD feeding in *Tlr2* $^{+/+}$ and *Tlr2* $^{-/-}$ littermates and static glucose-stimulated insulin secretion was performed using 2.8 mmol/l glucose and 16.7 mmol/l glucose (1 h each, 15 islets/well) and normalised for total islet insulin content. Content was unchanged between genotypes ($n = 8$ for HFD *Tlr2* $^{+/+}$ and $n = 7$ for HFD *Tlr2* $^{-/-}$). *$p < 0.05$ as tested by Student's *t* test. (**B**) Pancreatic islets isolated from chow- and HFD-fed *Tlr2* $^{+/+}$ mice were analysed for *Il-1β*, *Cd68*, *F4/80* and *Cd11c* mRNA expression by quantitative PCR. There is a strong positive correlation between islet *Il-1β* mRNA and islet *Cd68*, *F4/80* or *Cd11c* mRNA under HFD conditions (for *Cd68* $r^2 = 0.91$, $p = 0.0003$, black squares; for *F4/80* $r^2 = 0.92$, $p = 0.0006$, black circles; for *Cd11c* $r^2 = 0.60$, $p = 0.02$, white triangles; $n = 8$). (**C**) Relative cytokine, chemokine and macrophage marker mRNA expression in pancreatic islets isolated from female HFD-fed *Tlr2* $^{+/+}$ and *Tlr2* $^{-/-}$ littermates compared with chow *Tlr2* $^{+/+}$ controls ($n = 8$ for HFD *Tlr2* $^{+/+}$ and $n = 7$ for HFD *Tlr2* $^{-/-}$). (**D**) Relative islet *Cd36* mRNA expression in HFD-fed *Tlr2* $^{+/+}$ and *Tlr2* $^{-/-}$ mice ($n = 8$ for HFD *Tlr2* $^{+/+}$ and $n = 7$ for HFD *Tlr2* $^{-/-}$). Black bars, *Tlr2* $^{+/+}$; red bars, *Tlr2* $^{-/-}$. *$p < 0.05$ as tested by Student's *t* test compared with *Tlr2* $^{+/+}$ control

2.3.5 Impaired inflammatory response of BMDCs and islets to NEFAs in *Tlr2* $^{-/-}$ mice

Numbers of F4/80+ cells in the liver and islets were unchanged, despite reductions in *Il-1β* mRNA in these tissues in *Tlr2* $^{-/-}$ mice. Thus, we hypothesized that tissue immune cells (macrophages and/or dendritic cells) from *Tlr2* $^{-/-}$ mice and/or parenchymal tissue itself may display a reduced ability to mount an inflammatory response to certain ligands present during HFD feeding. BMDMs and BMDCs from *Tlr2* $^{+/+}$ and *Tlr2* $^{-/-}$ mice were cultured for 6 h in the presence of endotoxin-free BSA control or a mix of 0.5 mM palmitate:oleate (2:1). Indeed, BMDCs from *Tlr2* $^{-/-}$ mice displayed an attenuated *Il-1β* mRNA response to the NEFAs, whereas BMDMs did not (Fig. 7A-B). Both BMDMs and BMDCs from *Tlr2* $^{-/-}$ mice were unable to respond to the *Tlr2* ligand Pam2CSK4 (Fig. S8). As a representative tissue, we also investigated the response of pancreatic islets from *Tlr2* $^{+/+}$ and *Tlr2* $^{-/-}$ mice to NEFAs. Palmitate (0.1 mmol/l) induced *Il-1β* mRNA 2.5-fold in *Tlr2* $^{+/+}$ islets, whereas this effect was absent in islets from mice lacking *Tlr2* (Fig. 7C). This effect was specific for the NEFA palmitate, as oleate (18:1) alone was unable to increase islet *Il-1β* mRNA expression (not shown). The IL-1β-induced *Il-1β* auto-amplification system [115] was unchanged in *Tlr2* $^{-/-}$ islets vs *Tlr2* $^{+/+}$ controls, indicating no developmental defect in *Tlr2* $^{-/-}$ islets with respect to the induction of *Il-1β* mRNA expression (Fig. 7D).

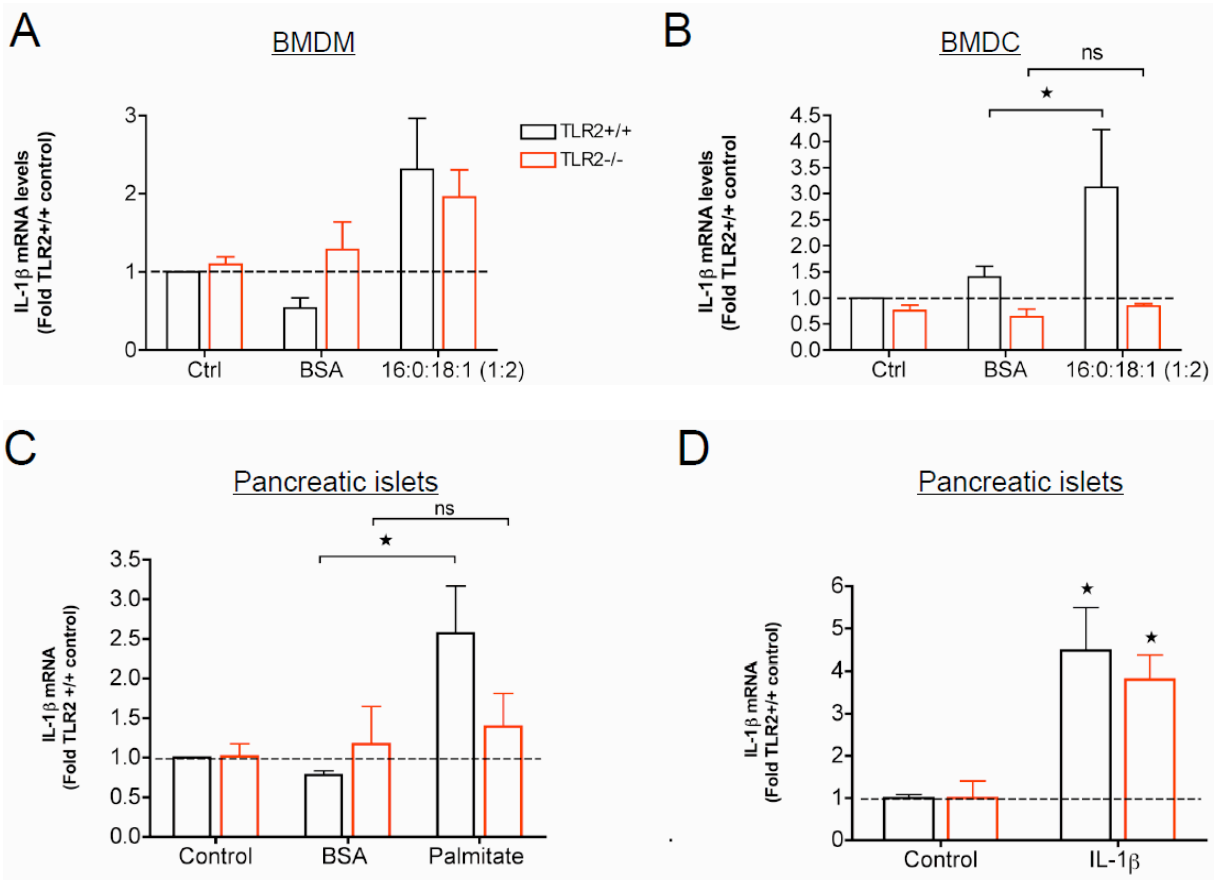

Fig. 7 Impaired inflammatory response to NEFAs in BMDCs and islets of *Tlr2* $^{-/-}$ mice. BMDMs (**A**) and BMDCs (**B**) were prepared from *Tlr2* $^{+/+}$ and *Tlr2* $^{-/-}$ mice as described and treated for 6 h with BSA control or palmitate:oleate (16:0:18:1, 2:1 molar ratio, 0.5 mmol/l). RNA was extracted and *IL-1β* mRNA is shown relative to 18S (n = 3 for *Tlr2* $^{+/+}$, n = 4 for *Tlr2* $^{-/-}$). (**C**) Regulation of islet *IL-1β* mRNA by 48 h treatment with 0.1 mmol/l palmitate in *Tlr2* $^{+/+}$ and *Tlr2* $^{-/-}$ islets (n = 3–7). (**D**) Regulation of islet *IL-1β* mRNA by 48 h treatment with 0.2 ng/ml IL-1β in *Tlr2* $^{+/+}$ and *Tlr2* $^{-/-}$ islets (n = 3–7). Black open bars, *Tlr2* $^{+/+}$; red open bars, *Tlr2* $^{-/-}$.*$p < 0.05$ as tested by Student's t test compared with BSA genotype control

2.3.6 *Tlr2* deficiency does not protect db/db mice from hyperglycemia

To confirm the beneficial effects of *Tlr2* deficiency in obesity associated hyperglycemia, *Tlr2* $^{-/-}$ mice were cross bred with *db/db* mice [116]. These mice have non functional leptin receptors and subsequently impaired leptin signalling due to a deleterious point mutation in the diabetic (*db*) gene. Hyperphagy that originates from lack of leptin signalling in the hypothalamus leads to increased fat deposition, hyperinsulinaemia and hyperglycemia [117]. *Db/db Tlr2* $^{-/-}$ mice were confirmed to be unresponsive to the synthetic TLR2 ligand, Pam2CSK4, *in vivo* (not shown). Weight gain was similar in *db/db Tlr2* $^{+/+}$ and *db/db Tlr2* $^{-/-}$ mice (Fig. 8A) and also glucose tolerance did not differ, as assessed by an IPGTT at 7 weeks of age (Fig. 8B) and 10 weeks of age (not shown). Blood glucose values (Fig. 8C) and plasma insulin (Fig. 8D) were not significantly different in *db/db Tlr2* $^{+/+}$ and *db/db Tlr2* $^{-/-}$ mice, although plasma insulin was markantly increased in the latter.

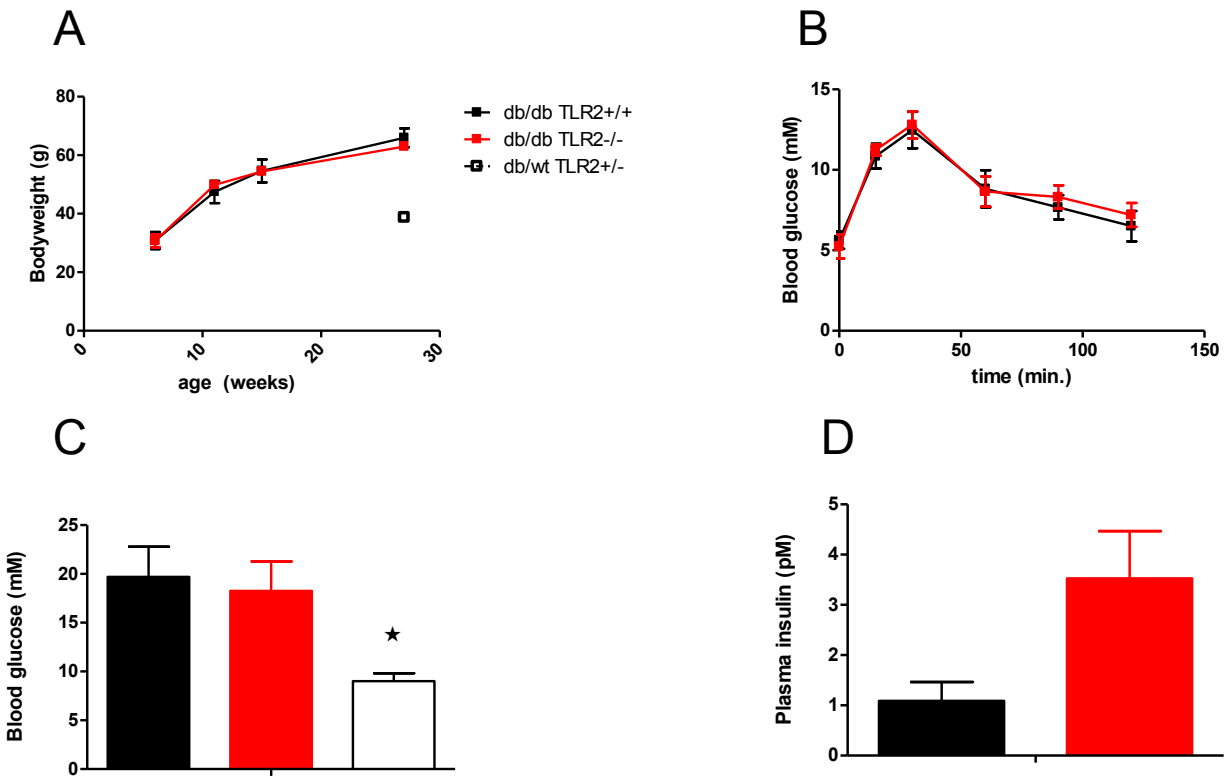

Fig. 8 *Tlr2* deficiency does not protect db/db mice from hyperglycemia. (**A**) Weight gain of *db/db Tlr2* $^{+/+}$, *db/db Tlr2* $^{-/-}$ and *db/wt Tlr2* $^{+/-}$ mice (n = 4 for *db/db Tlr2* $^{+/+}$, n = 6 for *db/db Tlr2* $^{-/-}$, n = 6 for *db/wt Tlr2* $^{+/-}$). (**B**) An IPGTT (0.2 g/kg bodyweight) was performed at 7 weeks of age (n = 4 for *db/db Tlr2* $^{+/+}$, n = 4 for *db/db Tlr2* $^{-/-}$). Mice were fasted for for 3h (8:00 - 11:00) and blood glucose (**C**) and plasma insulin (**D**) were assessed (n = 4 for *db/db Tlr2* $^{+/+}$, n = 6 for *db/db Tlr2* $^{-/-}$, n = 5 for *db/wt Tlr2* $^{+/-}$). White open square or bar, *db/wt Tlr2* $^{+/-}$; black square or bar, *db/db Tlr2* $^{+/+}$; red square or bar, *db/db Tlr2* $^{-/-}$. *p < 0.05 as tested by ANOVA with Dunnett post-hoc test or by Student's t test compared with *db/db Tlr2* $^{+/+}$

2.3.7 Treatment with an anti *Tlr2* antibody fails to show beneficial effects in mice on a HFD

Finally, we took a pharmacological approach and investigated the potentially beneficial effect of OPN301, a monoclonal anti mouse TLR2 antibody in an intervention study. 10 week old C57bl/6 wildtype mice were put on HFD for 15 weeks and thereafter evenly distributed into treatment groups according to bodyweight and fed blood glucose values. Mice were injected weekly with 10 mg/kg bodyweight OPN301, 10 mg/kg bodyweight isotype control (IgG) or saline and 10 weeks later metabolic parameters were analyzed.

HFD-induced weight gain was not different between treatment groups (Fig. 9A). Mice receiving OPN301 tended to have lower fed and fasted blood glucose levels compared to saline injected mice, similar to the effects seen in istoype control treated littermates (Fig. 9B-C). While insulin sensitivity was not different between groups (Fig. 9D), glucose tolerance tended to be improved in OPN301 treated animals (Fig. 9E), again to a similar level as the isotype control group. Insulin secretion following a glucose challenge was improved in OPN301 mice and even more in isotype controlled mice (Fig. 9F).

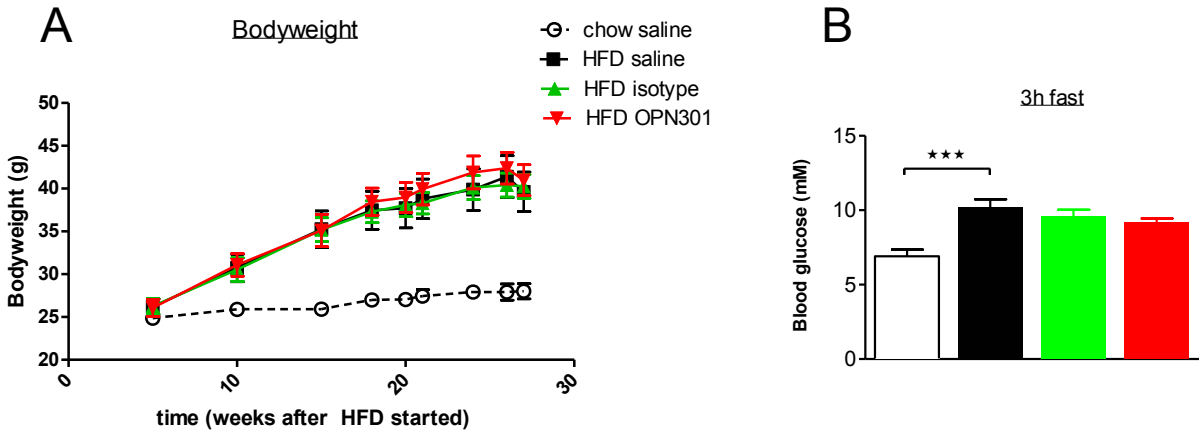

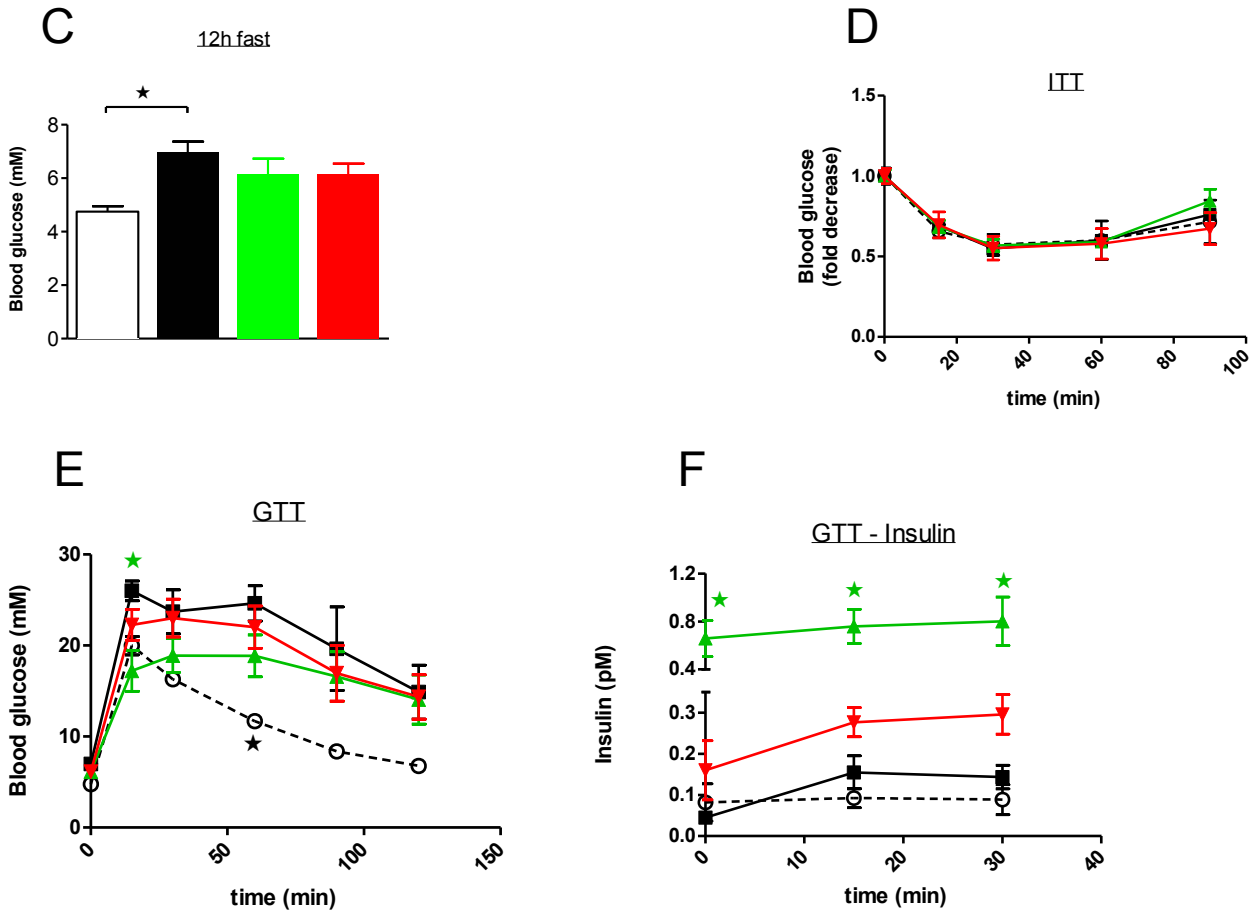

Fig. 8 Tendency towards lower blood glucose and improved insulin secretion in OPN301 and isotype treated mice on HFD. (**A**) Bodyweight of wild type littermate mice that were fed an HFD for 15 weeks prior to weekly anti TLR2 antibody, isotype or saline injections (n = 11-13 for chow group, n = 12 for HFD OPN301, isotype and saline group). After 10 weeks of treatment, animals were fasted for 3h (**B**) (n = 6 for chow group, n = 8 for HFD OPN301, isotype and saline group) or 12h (**C**) (n = 4 for chow group, n = 4 for HFD saline, n = 8 for HFD OPN301 and isotype group) and blood glucose was determined. (**D**) An ITT (1.20 U/kg insulin) was performed (n = 6 for chow group, n = 8 for HFD OPN301, isotype and saline group). (**E**) An IPGTT (2g/kg glucose) was performed (n = 4 for chow group, n = 4 for HFD saline, n = 8 for HFD OPN301 and isotype group). (**F**) Insulin secretion during an IPGTT (n = 4 for chow group, n = 4 for HFD saline, n = 8 for HFD OPN301 and isotype group). White open circle or bar, chow saline; black square or bar, HFD saline; red triangle or bar, HFD OPN301; green triangle or bar, HFD isotype. *p < 0.05 and ***p < 0.001, as tested by ANOVA with Dunnett post-hoc test compared with HFD saline

2.4 Supplementary Results

2.4.1 Pam2CSK4 does not induce SAA in *Tlr2* $^{-/-}$ mice

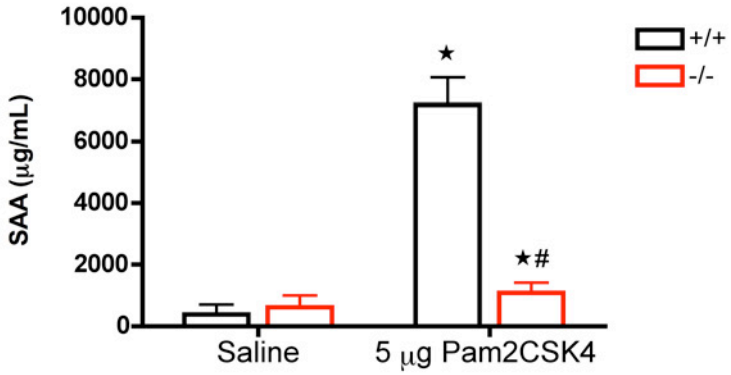

Fig. S1 Pam2CSK4 does not induce SAA in *Tlr2* $^{-/-}$ mice. 5 μg Pam2CSK4 or saline was injected intraperioneally into *Tlr2* $^{+/+}$ (n = 7-8) and *Tlr2* $^{-/-}$ mice (n = 3-7) and plasma serum amyloid A (SAA) was analyzed by ELISA after 24 h. Black open bars, *Tlr2* $^{+/+}$; red open bars, *Tlr2* $^{-/-}$. *p<0.05 compared to saline control and # p<0.05 compared to +/+ Pam2CSK4 as tested by ANOVA with Newman Keuls post hoc test

2.4.2 Glucose homeostasis in chow fed *Tlr2* $^{+/+}$ and *Tlr2* $^{-/-}$ mice

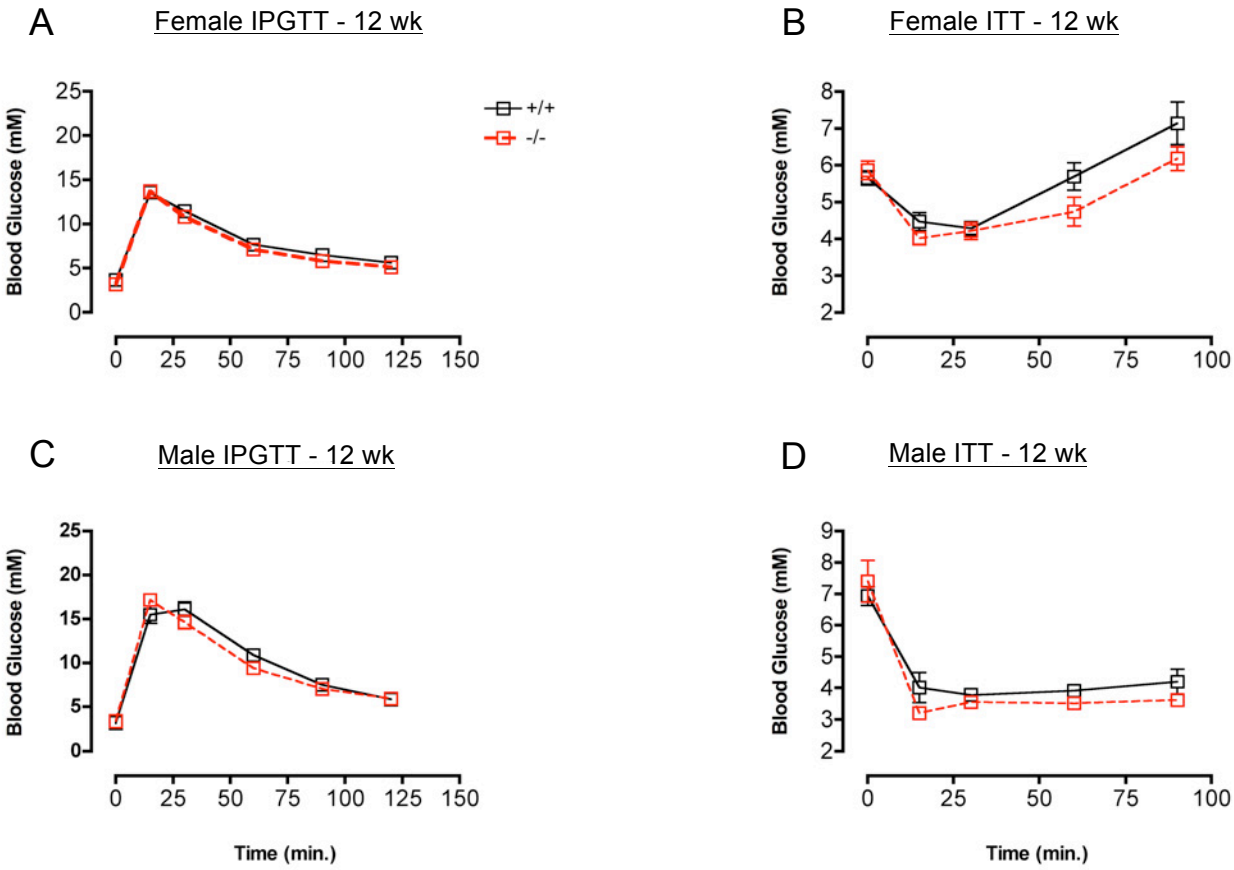

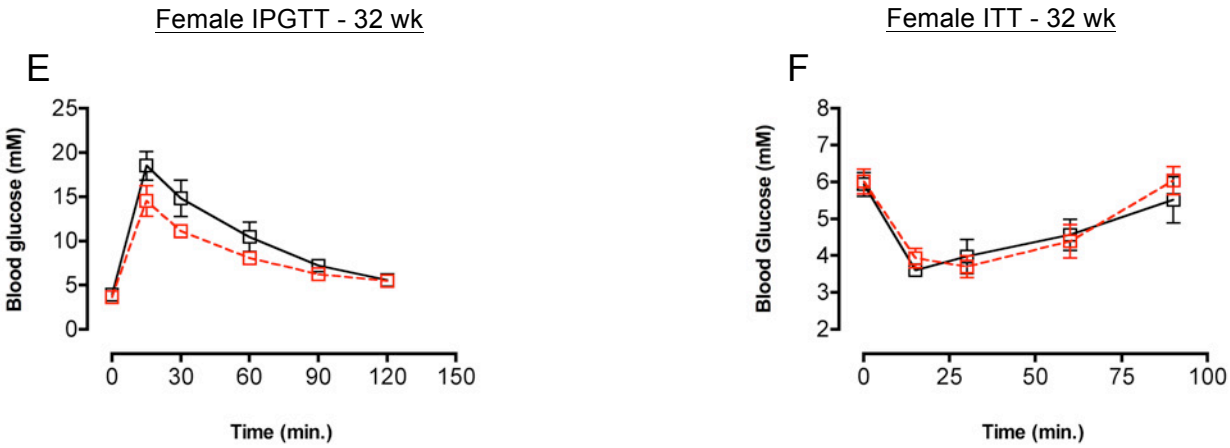

Fig. S2 Glucose homeostasis in chow fed *Tlr2* $^{+/+}$ and *Tlr2* $^{-/-}$ mice. (**A**) IPGTT (2 g/kg glucose) and (**B**) ITT (0.85 U/kg insulin) in female mice at 12 weeks of age (n = 12 for *Tlr2* $^{+/+}$, n = 10 for *Tlr2* $^{-/-}$). (**C**) IPGTT (2 g/kg glucose) and (**D**) ITT (1.0 U/kg insulin) in male mice at 12 weeks of age (n = 6 for *Tlr2* $^{+/+}$, n = 4 for *Tlr2* $^{-/-}$). (**E**) IPGTT (2 g/kg glucose) and (**F**) ITT (0.85 U/kg insulin) in female mice at 32 weeks of age (IPGTT: n = 4 for *Tlr2* $^{+/+}$, n = 4 for *Tlr2* $^{-/-}$; ITT: n = 10 for *Tlr2* $^{+/+}$, n = 7 for *Tlr2* $^{-/-}$). Black unbroken line, *Tlr2* $^{+/+}$; red broken line, *Tlr2* $^{-/-}$.

2.4.3 Glucose homeostasis in male *Tlr2* $^{+/+}$ and *Tlr2* $^{-/-}$ mice fed HFD

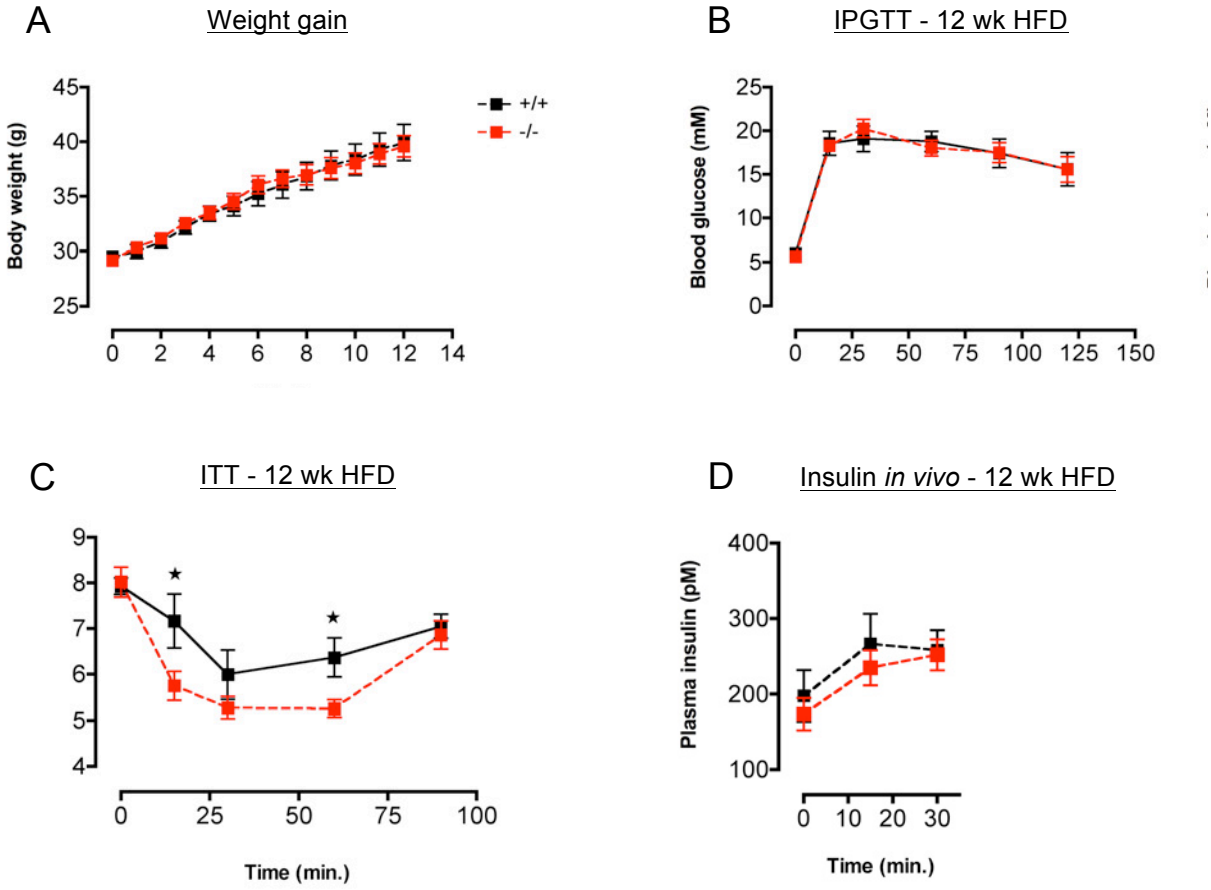

Fig. S3 Glucose homeostasis in male *Tlr2* $^{+/+}$ and *Tlr2* $^{-/-}$ mice fed HFD. (**A**) Male *Tlr2* $^{+/+}$ and *Tlr2* $^{-/-}$ littermate controls were fed a HFD starting at 10-12 weeks of age and body weight was monitored. (**B**) IPGTT (2 g/kg glucose) was performed after 12 weeks of HFD feeding. (**C**) ITT (1.0 U/kg insulin) was performed after 12 weeks of HFD feeding. (**D**) Insulin secretion during an IPGTT performed after 12 weeks of HFD feeding (n = 10 for *Tlr2* $^{+/+}$, n = 12 for *Tlr2* $^{-/-}$ for all data). Black unbroken line, *Tlr2* $^{+/+}$; red broken line, *Tlr2* $^{-/-}$. *p<0.05 as tested by Student's t-test compared to *Tlr2* $^{+/+}$ control

2.4.4 Glucose homeostasis in female *Tlr2* $^{+/+}$ and *Tlr2* $^{-/-}$ mice fed HFD for 12 weeks

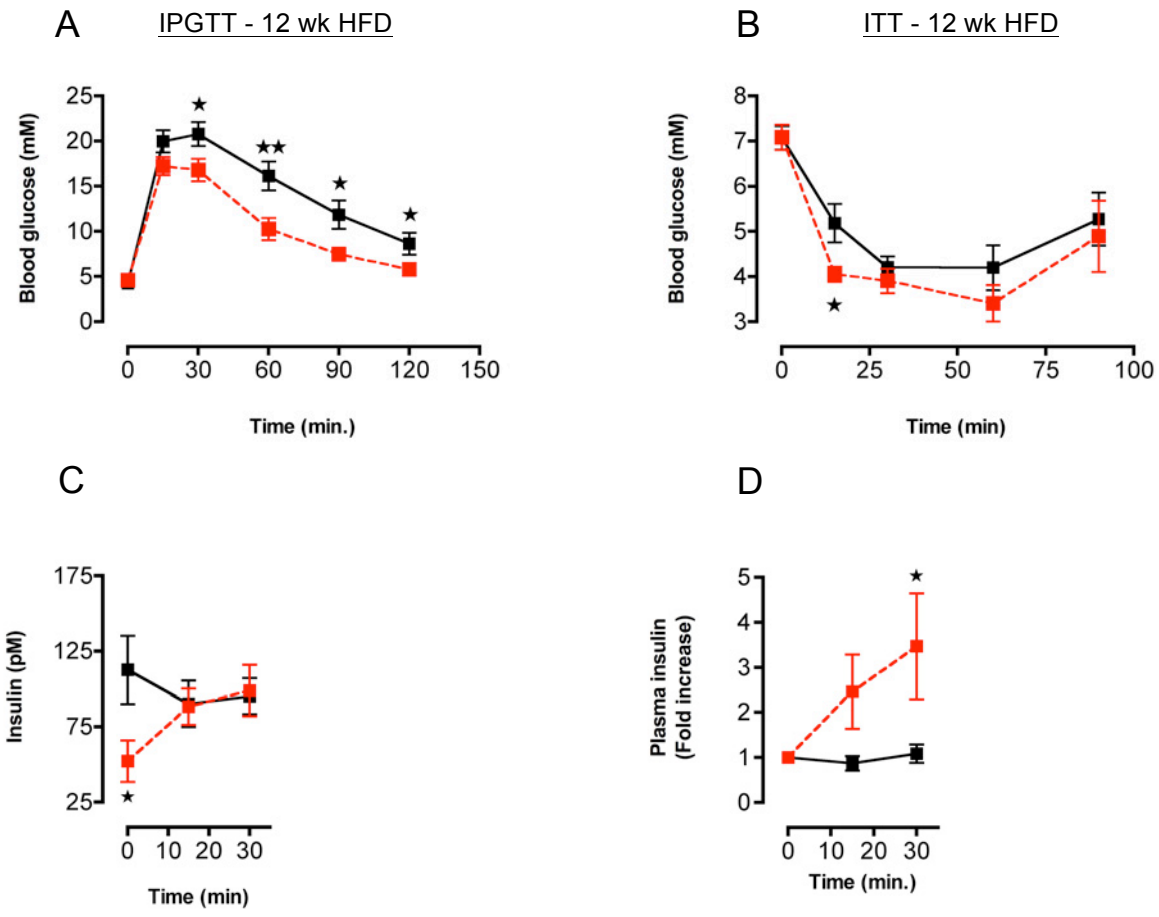

Fig. S4. Glucose homeostasis in female *Tlr2* $^{+/+}$ and *Tlr2* $^{-/-}$ fed HFD for 12 weeks. (**A**) An IPGTT (2 g/kg glucose) was performed after 12 weeks of HFD feeding (n = 13 for *Tlr2* $^{+/+}$, n = 15 for *Tlr2* $^{-/-}$). (**B**) An ITT (0.85 U/kg insulin) was performed after 12 weeks of HFD feeding (n = 12 for *Tlr2* $^{+/+}$, n = 11 for *Tlr2* $^{-/-}$). (**C**) Insulin secretion during the IPGTT (n = 8 for *Tlr2* $^{+/+}$, n = 7 for *Tlr2* $^{-/-}$). Black unbroken line, *Tlr2* $^{+/+}$; red broken line, *Tlr2* $^{-/-}$. *p<0.05 and **p<0.01 as tested by Student's t-test compared to +/+ control

2.4.5 Adipose tissue GLUT4 expression in female *Tlr2* $^{+/+}$ and *Tlr2* $^{-/-}$ mice fed HFD for 20 weeks

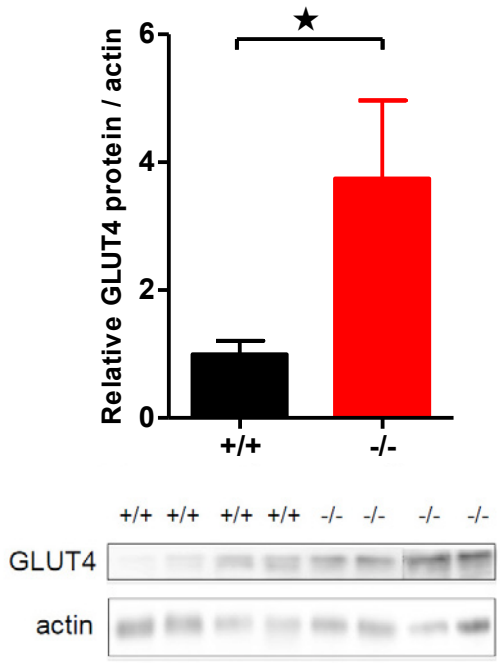

Fig. S5 Adipose tissue GLUT4 expression in female *Tlr2* $^{+/+}$ and *Tlr2* $^{-/-}$ mice fed HFD for 20 weeks. Protein was extracted from whole perigonadal adipose tissue and analysed using anti-GLUT4 and anti-actin antibodies as shown. Four representative samples are shown from each genotype, and quantification was performed on $n = 9$ for *Tlr2* $^{+/+}$ and $n = 9$ for *Tlr2* $^{-/-}$. Black bars, *Tlr2* $^{+/+}$; red bars, *Tlr2* $^{-/-}$. *$p < 0.05$ as tested by Student's *t* test compared with *Tlr2* $^{+/+}$ control

2.4.6 Skeletal muscle triacylglycerols and glycogen content in female *Tlr2* $^{+/+}$ and *Tlr2* $^{-/-}$ mice fed HFD for 20 weeks

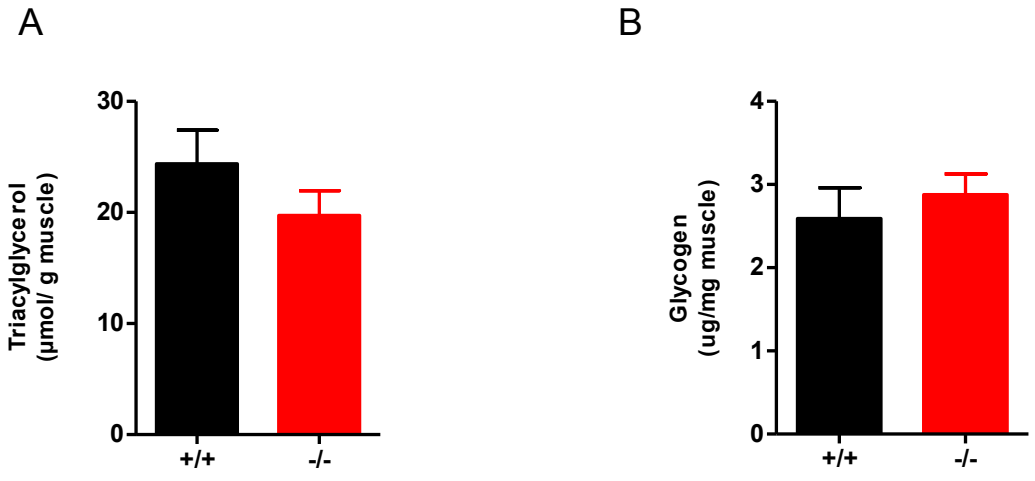

Fig. S6 Skeletal muscle triacylglycerols and glycogen content in female *Tlr2* $^{+/+}$ and *Tlr2* $^{-/-}$ mice fed HFD for 20 weeks. (**A**) Skeletal muscle triacylglycerols were quantified as described (n = 9 for *Tlr2* $^{+/+}$, n = 10 for *Tlr2* $^{-/-}$). (**B**) Skeletal muscle glycogen content was quantified as described (n = 9 for *Tlr2* $^{+/+}$, n = 10 for *Tlr2* $^{-/-}$). Black bars, *Tlr2* $^{+/+}$; red bars, *Tlr2* $^{-/-}$

2.4.7 Blood glucose and glucose infusion rate during hyperinsulinaemic–euglycaemic clamp

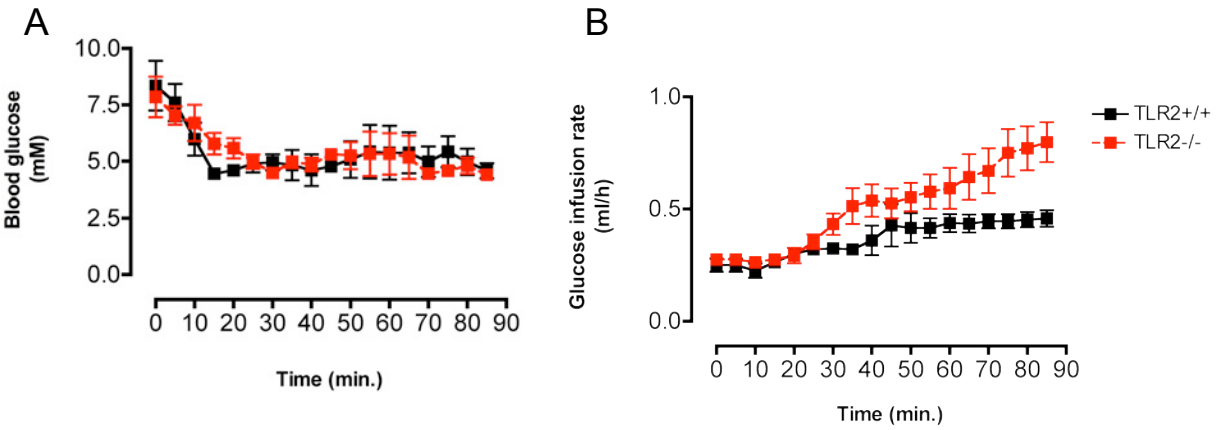

Fig. S7 Blood glucose and glucose infusion rate during hyperinsulinaemic–euglycaemic clamp. Hyperinsulinaemic–euglycaemic clamps were performed after 20 weeks of HFD feeding in female *Tlr2* $^{+/+}$ and *Tlr2* $^{-/-}$ littermates. (**A**) Blood glucose levels were clamped between 5 and 6 mmol/l in both *Tlr2* $^{+/+}$ and *Tlr2* $^{-/-}$ mice. (**B**) To maintain euglycaemia, glucose infusion rate was adjusted over time (n = 4). Black squares, unbroken line, *Tlr2* $^{+/+}$; red squares, broken line, *Tlr2* $^{-/-}$

2.4.8 Pam2CSK4-induced *Il-1β* mRNA in BMDMs and BMDCs derived from *Tlr2* $^{+/+}$ and *Tlr2* $^{-/-}$ mice

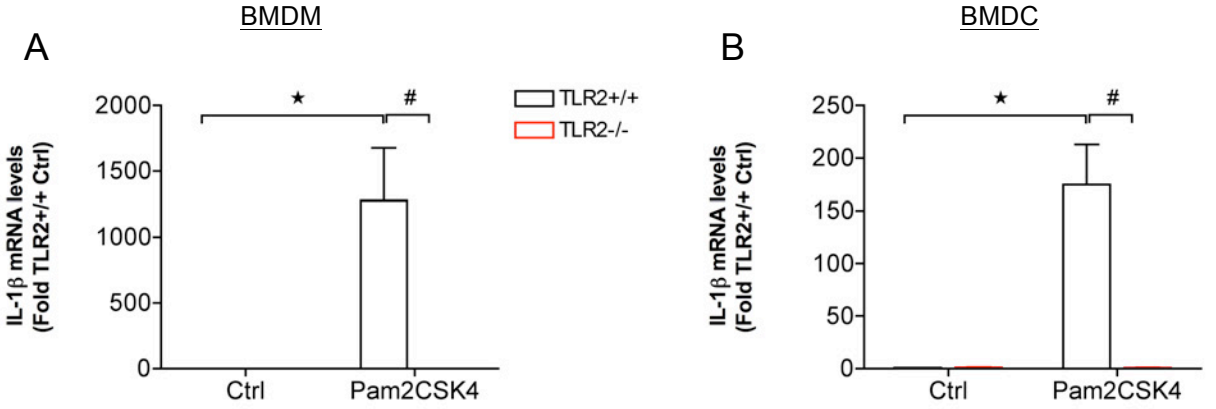

Fig S8 Pam2CSK4-induced *Il-1β* mRNA in BMDMs and BMDCs derived from *Tlr2* $^{+/+}$ and *Tlr2* $^{-/-}$ mice. (**A**) BMDMs and (**B**) BMDCs were prepared from *Tlr2* $^{+/+}$ and *Tlr2* $^{-/-}$ mice as described and treated for 6 h with

100 ng/ml Pam2CSK4. RNA was extracted and *Il-1β* mRNA is shown relative to 18S ($n = 3$ for *Tlr2* $^{+/+}$, $n = 4$ for *Tlr2* $^{-/-}$). Black open bars, *Tlr2* $^{+/+}$; red open bars, *Tlr2* $^{-/-}$. *$p < 0.05$ compared with control and #$p < 0.05$ compared with *Tlr2* $^{+/+}$ Pam2CSK4 as tested by ANOVA with Newman–Keuls post hoc test

2.4.9 Plasma analysis of age-matched chow and 20-week-old HFD-fed female *Tlr2* $^{+/+}$ and *Tlr2* $^{-/-}$ mice

	Chow		HFD	
	+/+ (n=7)	**–/– (n=7)**	**+/+ (n=8)**	**–/– (n=7)**
Leptin (pg/ml)	710±174	926±288	4611±978	1700±593*
Resistin (pg/ml)	1304±142	1528±101	3940±673	2988±438
Cholesterol (mmol/l)	2.1±0.2	2.5±0.5	1.7±0.3	1.50±0.3
NEFA (mmol/l)	0.84±0.12	0.71±0.03	0.64±0.7	0.7±0.06
Triacylglycerols (mmol/l)	0.88±0.08	0.78±0.11	1.2±0.1	0.96±0.04*
Ketones (mmol/l)	0.26±0.03	0.31±0.03	0.31±0.04	0.26±0.05
IL-6 (pg/ml)	2.7±0.6	4.7±1.3	3.6±0.4	5.0±0.9
TNF- (pg/ml)	3.3±0.5	3.5±0.7	4.3±0.4	3.2±0.1*
MCP-1 (pg/ml)	11.5±1.3	25.8±8.3	22.8±4.2	14.1±0.3*

Table S1 Plasma analysis of age-matched chow and 20-week-old HFD-fed female *Tlr2* $^{+/+}$ and *Tlr2* $^{-/-}$ mice. All data are representative of fasting values and littermate mice at 30–32 weeks of age. *p<0.05 compared with *Tlr2* $^{+/+}$ HFD

2.5 Discussion

According to the World Health Organization (WHO), the global incidence of diabetes in the year 2000 was 2.8%, corresponding to 171 million people worldwide [118]. Due to changing life habits, urbanisation and aging the global incidence rate is estimated to increase to 4.4% in 2030, corresponding to 366 million people worldwide [47]. The major risk factor that contributes to this diabetic epidemic is obesity. The current (2009) prevalence of obese individuals (BMI ≥ 30) in the USA is 27.2 % [119] with some European countries (especially Southern and Eastern Europe) catching up fast [120, 121]. The molecular mechanisms by which metabolic stress induces islet inflammation and therefore β-cell damage *in vitro* and *in vivo* remain elusive. This thesis identifies *Tlr2* as a major player in inducing the adverse effects of HFD feeding in mice.

It has been known for a long time that obesity and Type 2 diabetes are associated with chronic activation of the innate immune system [122]. The impact of inflammation on insulin resistance and β-cell dysfunction has been confirmed clinically in patients with type 2 diabetes [97] [75]. A clinical trial in which Type 2 diabetic patients received the naturally occurring Il-1β antagonist Il-1Ra, showed that β-cell secretory function was enhanced after injection of the *Il-1β* blocker. Nevertheless, the triggering mechanism responsible for induction of the inflammatory response in obesity and type 2 diabetes is not known. Recent studies have implicated TLR4 and its associated co-receptor, CD14, in HFD- and NEFA-stimulated tissue inflammation and insulin resistance. Jeffrey Flier's group has shown that the lack of TLR4 protects against fatty acid induced inflammatory signalling in adipose tissue and macrophages [90]. This was confirmed by Poggi *et al.* who in addition showed that *Tlr4* $^{-/-}$ mice have blunted lipopolysaccharide-induced insulin resistance in differentiated adipocytes [107]. Along the same lines, D.M. Tsukumo *et al.* published a study demonstrating that *Tlr4* $^{-/-}$ mice (the same as used by Poggi *et al.*) are partially protected against the development of diet-induced obesity [108]. Additional proof of the importance of TLR4 signalling in the obesity-inflammation axis came from P.D. Cani *et al.* who showed that HFD feeding increases plasma lipopolysaccharide. Continuously subcutaneous infusion of lipopolysaccharide into mice increased glycaemia, insulinaemia, markers of inflammation in adipose tissue and liver insulin resistance. Importantly, mutant mice for CD14, TLR4's associated co-receptor, were protected against most of these lipopolysaccharide-induced effects [123].

NEFAs, including palmitate and oleate, can not only activate TLR4 but also TLR2. By signalling through TLR2, they induce proinflammatory cytokine production in various tissues, leading to tissue-specific impairments. Not all dietary fatty acids have the same effect on tissue inflammation. Saturated fatty acids activated but (poly)unsaturated fatty acids inhibited TLR2 and TLR4 signalling [89, 94], suggesting that inflammatory responses can be modulated depending on the kind of TLRs expressed and the type of dietary fatty acid present. A study by J.J. Senn identified TLR2 as indispensable for palmitate-induced insulin resistance and IL-6 production in muscle cells [95]. Furthermore, TLR2 and TLR4 mediated the proinflammatory activation of BMDC and, to a lesser extent, BMDM [96], highlighting the importance of resident and infiltrating subpopulations of macrophages for fatty acid mediated tissue inflammation.

Based on these published data and the upregulation of TLR expression by HFD, we decided to investigate TLR2 in the context of obesity, insulin resistance and diabetes. Here, we show that TLR2 signalling is detrimental for proper glucose homeostasis under HFD conditions. Overall, TLR2 deficiency protected from HFD-induced insulin resistance and β-cell dysfunction via regulation of energy substrate utilisation and tissue inflammation.

During the preparation of this thesis, another study on the role of genetic deletion of TLR2 during HFD feeding was published [106]. Overall, their data on improved whole body glucose homeostasis and liver lipid content are consistent with our data. Our study extends on these data and indicates that a lack of TLR2 positively regulates energy-substrate utilisation, hepatic and adipose tissue insulin sensitivity, β-cell insulin secretion and liver and islet tissue inflammation. Furthermore, our *in vitro* data suggest a role for TLR2 in tissue immune cells (BMDCs) or parenchymal tissue itself (islets) in regulating the inflammatory response to elevated fatty acids during HFD feeding.

Our male and female *Tlr2* $^{-/-}$ mice were less protected from HFD than the male *Tlr2* $^{-/-}$ mice used in the study of Himes and Smith [106]. This may be explained by differences in diets used, or the use of littermate controls in our study, a critical point not mentioned in the other study. Indeed, we initially also performed our experiments on non-littermate-controlled *Tlr2* $^{+/+}$ and *Tlr2* $^{-/-}$ mice, with data matching those of Himes and Smith in male mice (not shown). Repeating the study with littermate mice resulted in the sexually dimorphic phenotype shown here in response to HFD, and a milder resistance to the obesity phenotype than the one published [106]. Interestingly, our data are similar to a published report on *Tlr4* $^{-/-}$ mice [90], which also showed sexual dimorphism in their resistance to the adverse effects of HFD feeding, with males showing only a partial resistance compared to females. Currently we

cannot explain these differences, but it will be interesting to investigate the effects of sex on tissue inflammation with respect to obesity and diabetes.

After 20 weeks of HFD, *Tlr2* $^{-/-}$ mice showed lower adiposity than their *Tlr2* $^{+/+}$ littermates. Therefore, we investigated energy homeostasis in these mice. Surprisingly, the caloric intake in *Tlr2*$^{-/-}$ mice was 10% higher, despite reduced adiposity. This observation was paralleled by a 10% increase in total energy expenditure, which was more pronounced during the night when rodents are active. Therefore, we tested if this increased energy expenditure was due to altered locomotor behaviour, but we could not detect any change in physical activity. Moreover, *Tlr2* $^{-/-}$ had a reduced RQ, especially during the light phases, which means that they preferentially used lipids as an energy source. This was consistent with increased mRNA expression of enzymes involved in β-oxidation of fatty acids in skeletal muscle of *Tlr2* $^{-/-}$ (*Acox1* and *Mcad*). However, skeletal muscle triacylglycerols and glycogen content between genotypes were not different. Perigonadal fat pad weights were reduced in *Tlr2* $^{-/-}$ mice. Their adipocytes were smaller, displayed improved insulin-stimulated glucose uptake and GLUT4 protein levels in whole adipose tissue was increased in *Tlr2* $^{-/-}$ mice. This overall attenuated adiposity, together with a reduction in liver lipid content in *Tlr2* $^{-/-}$ animals, suggests that fatty acids are being shunted away from the liver to be increasingly oxidised in other tissues, such as skeletal muscle. This would be consistent with a diminished capacity of the liver to take up lipids due to suppressed *Cd36* mRNA expression. TLR2 has been shown to associate with CD36 at the plasma membrane following receptor ligand activation, suggesting that the absence of TLR2 activation in the liver may protect from fatty acid uptake [114].

Reduced adiposity and reduced hepatosteatosis were also consistent with overall improvements in whole body and hepatic insulin sensitivity as determined by the hyperinsulinaemic–euglycaemic clamp. Thus, our data show for the first time that TLR2 regulates hepatic insulin sensitivity during HFD, extending findings that reduced TLR2 expression by antisense oligonucleotides improved insulin signalling in muscle and white adipose tissue of HFD-fed mice [109].

Beyond improved insulin sensitivity, we also observed improvements in β-cell insulin secretion in response to glucose load, both *in vivo* and *in vitro*. 20 weeks of HFD feeding abolished glucose stimulated insulin secretion in isolated islets of *Tlr2* $^{+/+}$ mice. In contrast, isolated islets from littermate *Tlr2* $^{-/-}$ mice were able to secrete insulin in response to increased glucose concentrations. Since there was no difference in islet insulin content between genotypes, it can be ruled out that a developmental defect resulting in reduced insulin synthesis is responsible for the described differences, although a developmental defect in the

insulin secretion pathway cannot be excluded. In accordance with these *ex vivo* findings, compared with HFD-fed *Tlr2* $^{+/+}$ mice, littermate *Tlr2* $^{-/-}$ mice showed markedly improved glucose tolerance and β-cell insulin secretion in response to a glucose challenge *in vivo*. Furthermore, *Tlr2* $^{-/-}$ mice were more sensitive to insulin and had reduced fasting circulating insulin levels, as tested by insulin injection and subsequent blood glucose sampling. Thus, the overall improved glucose tolerance of HFD Tlr2 −/− mice was due to improved insulin sensitivity and β-cell insulin secretion, which correlated well with a partially attenuated tissue inflammatory response in the liver and islet.

We went on to investigate why tissue inflammation might be suppressed in *Tlr2* $^{-/-}$ mice on HFD. Reductions in tissue inflammation may be due to reduced immune cell content of tissues, a reduced activation status of tissue immune cells or reduced inflammation of the parenchymal tissue. Despite reductions in *Cd68*, and/or *F4/80* mRNA levels in adipose tissue, liver and in islets, we did not observe differences between genotypes in the number of F4/80+ cells by immunohistochemistry in the liver or islet. Thus, we hypothesised that the activation status of proinflammatory immune cells in *Tlr2* $^{-/-}$ mice or the parenchymal tissue itself had a reduced capacity to mount an inflammatory response under HFD conditions. Pro-inflammatory CD11c+ cells have been causally linked to tissue inflammation and the induction of insulin resistance in response to HFD in the C57bl/6 mouse [103]. Our data showing increased *Cd11c* mRNA expression during HFD feeding in adipose tissue, liver tissue and islets are consistent with the notion that CD11c+ cells are recruited to these tissues during obesity [96, 124]. Indeed, *Tlr2* $^{-/-}$ BMDCs (CD45+CD11b+Cd11c+) showed a refractory response to NEFA-induced *Il-1β* mRNA *in vitro*, whereas BMDMs (CD45+F4/80+CD11b+Cd11c−) did not. The pancreatic islet was also tested as a representative tissue with respect to NEFA induction of *Il-1β* mRNA. Consistent with the effects seen in BMDCs and our *in vivo* effects, *Tlr2* $^{-/-}$ islets were also refractory to palmitate-induced *IL-1β* mRNA. We previously found no effect of oleate on mouse islet *Il-1β* mRNA (not shown) [112]. These data suggest that *Tlr2* $^{-/-}$ CD11c+ cells are resistant to the effects of NEFAs present in HFD, possibly resulting in the reduced tissue inflammation seen in the liver and islets of HFD *Tlr2* $^{-/-}$ mice. However, given the broad tissue expression of *Tlr2* mRNA, we cannot conclude whether the observed reductions in tissue inflammation *in vivo* are due to an immune cell, or parenchymal cell, origin.

HFD diet-induced obesity only leads to mild hyperglycaemia and diabetes in animal models of type 2 diabetes [125]. To examine if similar findings can be obtained in an animal model of type 2 diabetes with a stronger diabetes phenotype, we investigated db/db mice crossed with

Tlr2 $^{-/-}$ mice [116]. Since these mice show a massive weight gain in a short period of time we expected that the beneficial effect of the absence of TLR2 seen in the HFD model would be even more pronounced. To our surprise neither female nor male (not shown) *db/db Tlr2* $^{-/-}$ were protected from the deleterious effects of obesity compared to their *db/db Tlr2* $^{+/+}$ littermates. The ability to handle a glucose challenge and also insulin sensitivity were not different between genotypes. Female *db/db Tlr2* $^{-/-}$ tended to have increased fasted plasma insulin levels, suggesting that they might be even more insulin resistant than their wildtype littermates. These experiments suggest that the lack of TLR2 has only a minor effect on the *db/db* mouse model. Obese humans have higher leptin levels than lean individuals, but they are also leptin resistant [126]. Leptin replacement therapy restored metabolic functions, development and immune repertoire in congenital leptin deficient humans (homozygous leptin gene mutation as consequence of consanguineous marriage) [127, 128], but administration of leptin as a weight-losing drug in obese individuals showed to be only mildly effective [129]. Therefore, the *db/db* mouse is probably not the ideal model for obese humans while the HFD model is a more valid representation.

To examine the pharmacological potential of the inhibition of TLR signalling, we used an anti-TLR2 antibody in a HFD intervention study. The TLR2 antibody tended to lower fed and fasted blood glucose values without affecting insulin sensitivity and glucose tolerance. In response to a glucose challenge, TLR2 antibody treated animals tended to be able to release more insulin, an effect which was even more pronounced in isotype treated control mice. In general, the isotype control antibody preparation had a similar or even better blood glucose improving effect during fasting and after a glucose challenge than the TLR2 specific antibody. Therefore, we are not able to conclude that the protective effects seen in *Tlr2* $^{-/-}$ mice can be reproduced via pharmacological means. This highlights the importance of including isotopye control conditions in antibody treatment experiments. Prevention studies usually lead to higher statistical significance than intervention studies. This might be explained be the fact that it is in general easier to protect something from destruction than rebuilding it after demolition. Our congenital *Tlr2* $^{-/-}$ model resembles the prevention study setup which also hints at using this setup in the initial experiment instead of an intervention study setup. Possibly, the lack of effect of the TLR2 antibody is due indirect effects of free fatty acids. Indeed, TLR2 activation by free fatty acids may occur independently of ligand binding to TRL2.

Recent data also suggest a role for TLR2 in human type 2 diabetes. One study has shown increased production of TLR2 protein in circulating monocytes following feeding of a high-

fat / high-carbohydrate single meal in healthy lean human participants [130]. Evidence for increased TLR2 protein levels in monocytes and increased circulating TLR2 ligands in recently diagnosed type 2 diabetes patients has also been reported [131]. Monocytes from these type 2 diabetic individuals showed increased proinflammatory cytokine secretion following TLR2 stimulation. Further, analysis of adipose tissue from individuals with obesity and type 2 diabetes revealed increased protein levels of TLR2 compared to healthy individuals [132]. Whether TLR2 activation also contributes to insulin resistance and β-cell dysfunction in humans with type 2 diabetes awaits further investigation.

In summary, these data show that deficiency in TLR2-mediated signalling has a positive impact on glucose homeostasis, insulin sensitivity, insulin secretion and energy-substrate utilisation during HFD feeding. The overall improved metabolic phenotype of *Tlr2* $^{-/-}$ mice on HFD is likely to be due to both reduced fat accumulation and reduced tissue inflammation, impacting on tissue-specific functions to improve both insulin sensitivity and secretion. It remains to be elucidated, how TLR2 activation occurs during HFD.

3 SIRT1 ACTIVATION VIA SRTs DOES NOT DELAY THE ONSET OF TYPE 1 DIABETES

3.1 Introduction

3.1.1 Sirtuins

The sir family was originally discovered as gene silencing factors in yeast [133] and it was only 16 years later when they were shown to be key regulators of lifespan [134, 135]. Especially homologues of one family member, the sirtuins (sir2), received a lot of attention because they were implicated in promoting the life-prolonging effects of caloric restriction in several species [136]. In yeast and flies, sirtuin levels rise during caloric-restriction and overexpression of sir2 extends lifespan [135, 137]. In addition, the longevity effect of caloric restriction is absent in sirtuin-deficient yeast and mice [138]. This raised the idea that sir2 activation could mimic a low caloric state resulting in improved fat utilization and eventually expansion of lifespan in higher organisms.

3.1.2 SIRT1

SIRT1, one of the 7 known human homologues of the yeast sir2 gene, is a NAD^+ dependent protein and histone deacetylase that is found both in the nucleus and in the cytoplasm. SIRT1 was shown to be involved in genomic stability, DNA repair and stress handling [139]. Sirtuins are also engaged in metabolic regulation. PGC-1α mediated gluconeogenesis and fatty acid oxidation in the liver was shown to be SIRT1 dependent [140]. SIRT1 also modulates the threshold for cell death. It does so by attenuating heat shock proteins [141], by regulating the tumor suppressor protein p53 and by binding and deacetylating FOXO3 [142] and thereby inducing stress resistance genes and promoting cell survival. Finally, SIRT1 was also shown to be able to deacetylate components of the circadian clock, probably linking food availability and sleep/wake rhythms [143].

3.1.3 SIRT1, metabolic diseases and diabetes

There are several lines of evidence implicating SIRT1 in the development of metabolic diseases and thus diabetes. First, SIRT1 modulates glucose homeostasis and insulin secretion, shown by β-cell specific SIRT1 overexpressing mice that have improved [144], and SIRT1 deficient mice that have deteriorated insulin secretion [145]. The improvement in insulin secretion is believed to be due to repressing uncoupling protein 2 [144, 145]. Pharmacological activation [146] or genetic overexpression [147, 148] of SIRT1 improves glucose tolerance and protects mice against the

deleterious effects of HFD feeding. Blocking SIRT1 genetically or pharmacologically was shown to induce insulin resistance*, in vitro* and *in vivo* [149]. SIRT1 activity is also advantageous in other age related diseases, such as cardiovascular diseases [150, 151], atherosclerosis [152], cancer [153], and neurodegeneration in a mouse model of Alzheimer's disease [154], as well as in cholesterol transport [155].

A role for SIRT1 in autoimmunity and therefore a possible involvement in the development of type 1 diabetes emerged recently, when SIRT1 was implicated in T cell tolerance. Self-reactive T cells that escape negative selection in the thymus are inactivated in the periphery by clonal anergy which results in longterm unresponsiveness to foreign and self antigens. SIRT1 is abundantly expressed in the thymus and was shown to suppress activator protein 1 (AP-1) transcriptional activity in T cells [156], an important mechanism in T cell anergy [157]. Further, resveratrol, which is believed to activate SIRT1, was shown to suppress proliferation and cytokine production in T cells [158]. Thymocytes from Sirt1 $^{-/-}$ mice display increased sensitivity to radiation-induced apoptosis [159]. These observations suggest that SIRT1 is an important modulator of immunity, acting on T cell development and tolerance.

A hallmark of diabetes is cytokine-induced impairment and destruction of pancreatic β-cells. Among TNF and IFN, IL-1β is a major contributor and signals via the NFκB pathway. NFκB acetylation of the subunit p65 of NFκB at Lys310 is required for full transcriptional activity. SIRT1 inhibits NFκB activity by deacetylating Lys310 and thereby attenuates inflammation [160]. This is also true for the β-cells, where overexpression of SIRT1 or activation by resveratrol reduced cytokine-mediated cytotoxicity via suppression of NFκB activity [161].

3.1.4 SIRT1 L107P

A novel form of monogenic diabetes with features of both type 1 diabetes (auto-immunity), and type 2 diabetes (insulin resistance) was found in a family of Ashkenazy Jews. The pattern of inheritance amongst the affected family members was indicative of an autosomal dominant mutation. A candidate gene approach was used to identify mutations which could explain a combined dysfunction in insulin secretion due to a defect in metabolism-secretion coupling, and insulin resistance. In fact, direct sequencing of the SIRT1 gene of patients revealed the presence of a T to C exchange in exon 1, leading to a leucine107 to proline (L107P) exchange in the SIRT1 protein. Every family member diagnosed with type 1 diabetes carried one mutated allele (heterozygous) and non-affected family members were healthy, except for two individuals displaying features typical of type 2 diabetes. One exception was an 18 year old woman carrying the mutation who displayed severe ulcerative colitis, a disease with a profound autoimmune component, a feature shared with type 1 diabetes (Anna Biason-Lauber *et al*., manuscript submitted).

3.1.5 Small activators of SIRT1

In 2007, novel small-molecule activators of SIRT1 (SRTs) were described [162]. They were found by high-throughput mass spectrometry screenings. SRTs seem to bind the enzyme-substrate complex and thereby lower the Michaelis constant (K_M), which is a measurement for the enzyme-substrate affinity [163]. Hence, SRTs increase SIRT1 activity by increasing the binding affinity for acetylated substrates.

The therapeutical potential of SRTs was investigated in several animal models of type 2 diabetes. In diet-induced obese and ob/ob mice, SRT1720 and SRT501 improved insulin sensitivity, normalized glucose and insulin levels, and elevated mitochondrial capacity [162]. In a metabolic study, SRT1720 administration enhanced endurance running and protected against diet-induced obesity [146]. This was mainly due to promoting fat consumption in skeletal muscle, liver and brown adipose tissue. In another animal species, the Zucker fa/fa rat, SRT1720 ameliorated the metabolic disturbances as assessed by IPGTT and clamp studies [162].

3.1.6 Aim of the thesis, SIRT1 part

Several *in vivo* SIRT1 studies were conducted in the context of type 2 diabetes [144-155], all showing that overexpression or activation of SIRT1 increases insulin sensitivity and secretion and ameliorates glucose metabolism. Although these studies point to a promising role of SIRT1 as a therapeutic target in age-associated diseases and type 2 diabetes, no research on SIRT1 activation in animal models of type 1 diabetes was done yet. The detection of a SIRT1 gene mutation in type 1 diabetic patients (see above) and reports on the involvement of SIRT1 in autoimmunity [156, 158, 159] lead to the following hypothesis.

Hypothesis 1: Administration of SIRT1 activators (SRTs) delays the onset of diabetes in animal models of type 1 diabetes, namely the NOD and the MLD-STZ mouse.

Hypothesis 2: Genetic ablation of SIRT1 will accelerate the development of MLD-STZ-induced diabetes.

Hypothesis 3: The SRT compounds are safe enough to initiate a program to treat the affected family members.

3.2 Methodology

3.2.1 Animals

NOD (NOD/Ltj) breeding pairs were bought from Charles River Italy. NOD-SCID (NOD.CB17-Prkdc<scid>/J) breeding pairs were bought from Charles River France. SIRT1$^{+/-}$ (129Sv-SirT1<tm1Mmc>) mice were a gift from Dr. Michael McBurney (OHRI, Ottawa, Canada). Bl6 (C57BL/6J) were bred in house. Experimental animals were born and bred in our SPF barrier facility. All experiments were done in a littermate controlled fashion. NOD experiments were done with females, MLD-STZ experiments with males and adoptive transfer experiments with both genders. Experiments were performed according to Swiss veterinary law and institutional guidelines.

3.2.2 SIRT1 activators (SRTs)

Compounds were synthesized at Sirtris Pharmaceuticals, MA, USA. All of them are SIRT1 activators with different potencies and specificities [162]. The following dosages were used: 1. STRT 1720 (100 mg/kg BW), 2. SRT 2379 (100 mg/kg BW), 3. SRT 2104 (200 mg/kg BW), 4. SRT 501 (1000 mg/kg BW). They were freshly dissolved in 20% PEG400, 0.5% Tween80 and 79.5% deionized water every 3 days and applied by oral gavage. The control group received the solvent alone.

3.2.3 NOD experiments

3 week old animals were SRT dosed daily by oral gavage. Drug administration was stopped after 8 weeks. For insulitis score experiments, 8 animals per group were sacrificed at 12 weeks of age. The same animals were used as donors for the adoptive transfer experiments. 20 animals per group were tested for glucosuria (Diabur-Test 5000, Roche Diagnostics, Mannheim, Germany) 3 times per week (Monday, Wednesday, Friday), starting at 10 weeks of age. Animals positively tested for glucosuria were tested for hyperglycaemia (FreeStyle, Abbott, Oxon, UK). Diabetes was defined as random blood glucose higher than 14 mM measured on two consecutive days.

3.2.4 MLD-STZ experiments

11 week old animals were distributed into groups of 11-12 animals and i.p. injected with 50 mg / kg bodyweight streptozotocin (Sigma, St Louis, MO, USA) or sodium citrate buffer on 5 consecutive days. Streptozotocin was prepared freshly by dissolving it in sodium acetate buffer adjusted to pH 4.5. In parallel to the first streptozotocin injection, animals were drug dosed with 100 mg/kg bodyweight SRT 1720 or solvent daily, according to the following scheme:

STZ \ SRT1720	-	+
-	group 1	group 2
+	group 3	group 4

Fed blood glucose was measured 3 times per week (Monday, Wednesday, Friday), starting at the day of the first STZ injection (FreeStyle, Abbott, Oxon, UK).

3.2.5 Tissue workup

Animals were euthanized by CO_2. Blood plasma was harvested by cardiac puncture. Pieces of liver, quadriceps muscle and epididimal fat were snap frozen and stored for protein analysis or incubated in RNAlater (Ambion / Applied Biosystems, Foster City, CA, USA) over night and snap frozen after RNAlater removal and stored for RNA analysis the following day. Pancreata were embedded in paraffin and 2 sections 200 µm apart were stained with haematoxylin and eosin. 8 animals and 300-400 islets per treatment group were scored blindly according to the following: 1. no visible infiltration, 2. periinsulitis, 3. Insulitis ≤ 50 % infiltation, 4. Insulitis ≥ 50 % infiltration.

3.2.6 Adoptive Transfer

Whole spleens were crushed through a 40 µm cell strainer (BD Falcon, Franklin Lakes, NJ, USA). Red blood cells were lysed with ACK (155 mM NH_4Cl, 10 mM $KHCO_3$, 1 mM EDTA). Splenocytes were resuspended in PBS and injected intra venously into the tail vein of 5 week old female and male SCID mice.

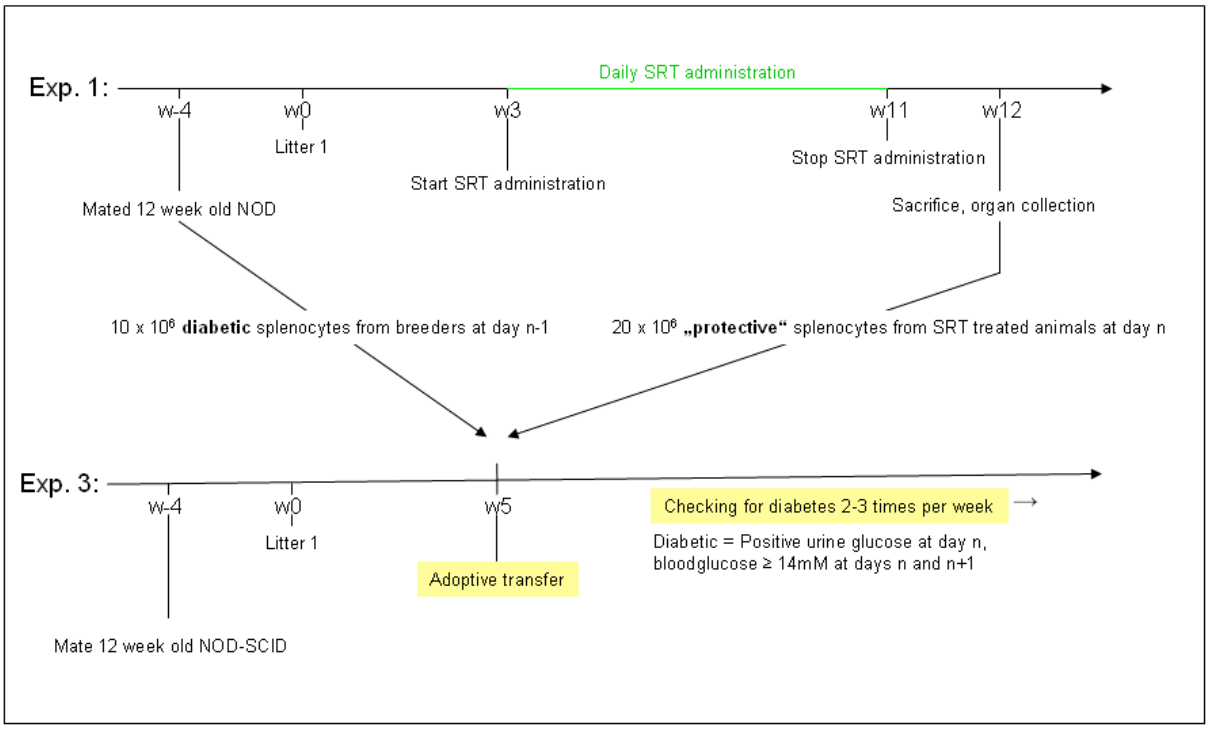

3.2.7 Statistics

Data were expressed as means ± S.E.M. All data were analyzed using the nonlinear regression analysis program PRISM (GraphPad, CA, USA), and significance was tested using analysis of variance (ANOVA) with Bonferronni's post hoc test or Log-rank (Mantel-Cox) test for survival curves. Significance was set at $p<0.05$.

3.3 Results

3.3.1 Diabetes incidence rate

The first experiment was designed to investigate a potential delay in onset of diabetes in NOD animals receiving SIRT1 activators (SRTs). Animals were distributed into 4 treatment and 1 control group upon weaning in a littermate controlled fashion. Baseline bodyweight and plasma blood glucose concentrations were identical in all 5 experimental groups (Fig. 1A-B). Bodyweight development during the experimental period was also similar (Fig. 1C)

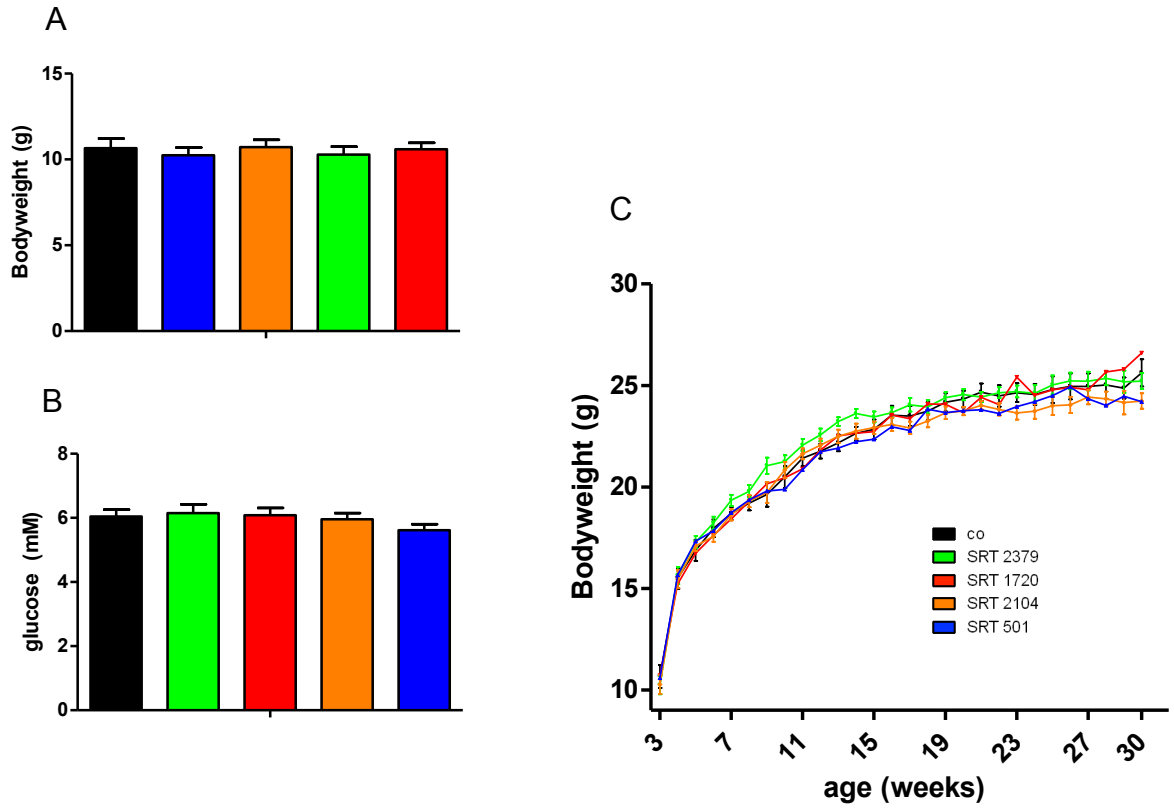

Fig. 1 Baseline measurements diabetes incidence experiment. Bodyweight (**A**) and glucose (**B**) of female NOD mice at 3 weeks of age. (**C**) Bodyweight development during 27 weeks of the experimental phase. *n* = 20 per group. Black bar or line, control; green bar or line, SRT 2379; red bar or line SRT 1720; orange bar or line, SRT 2104, blue bar or line SRT 501. *$p<0.05$, as tested by ANOVA with Bonferronni's post hoc test

Starting at 3 weeks of age animals were SRT dosed daily by oral gavage at a dose of 100 – 1000 mg/kg body weight. Drug administration was stopped after 8 weeks. Starting at 10 weeks of age animals were tested for glucosuria and hyperglycemia 3 times per week. The development of diabetes

in the 5 different groups was identical (Fig. 2), indicating that none of the SIRT1 activators is able to delay the onset of diabetes in the NOD mouse.

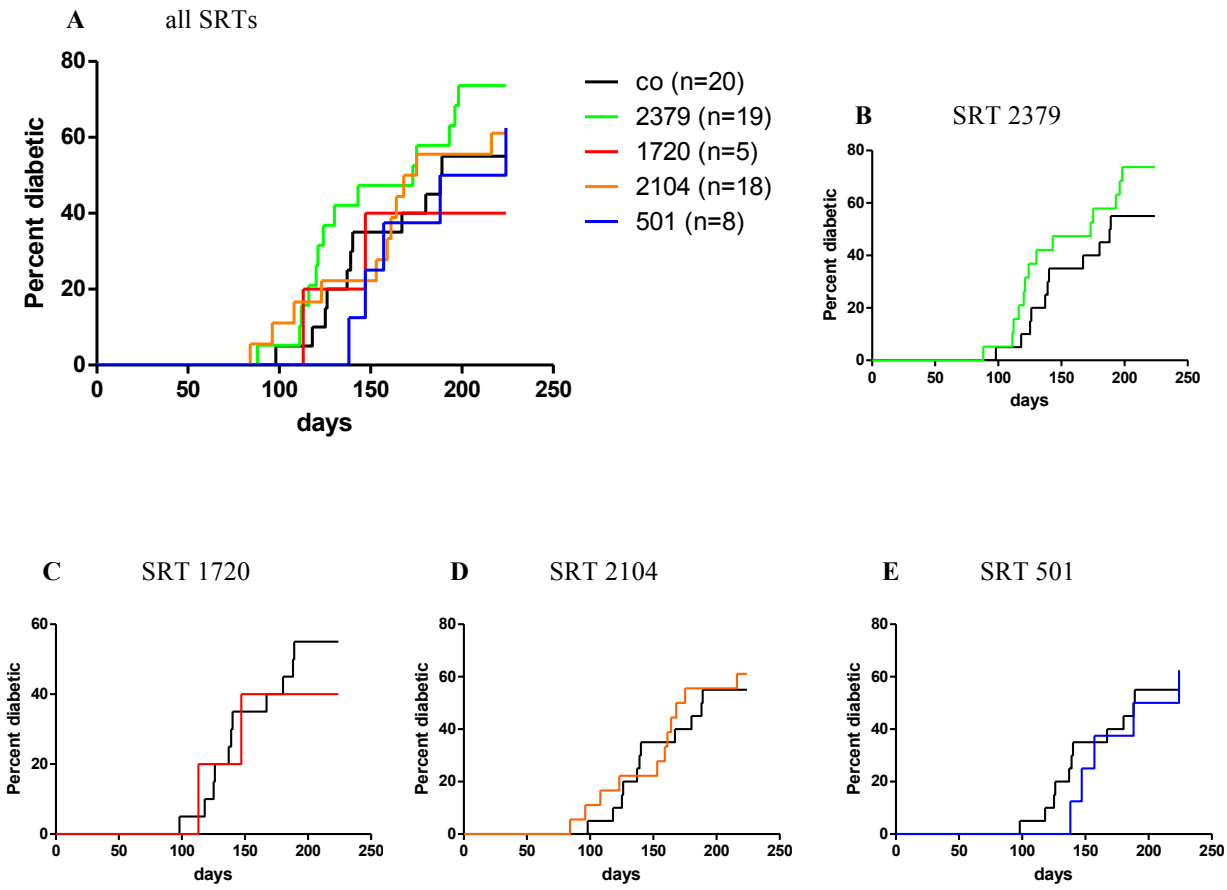

Fig. 2 Diabetes incidence rate. (**A**) Diabetes incidence rate of all treatment groups. For illustration purposes each group is also plotted against the control group, namely SRT 2379 (**B**), SRT 1720 (**C**), SRT 2104 (**D**), and SRT 501 (**E**). Experiment started with $n = 20$ per group. Black line, control; green line, SRT 2379; red line SRT 1720; orange line, SRT 2104, blue line SRT 501. *$p<0.05$, as tested by Log-rank (Mantel-Cox) test for survival curves.

3.3.2 Insulitis score

The second experiment was designed to investigate a potential decrease in immune cell infiltration into the pancreas in SRT treated NOD animals. Mice were distributed into 4 treatment and 1 control group upon weaning in a littermate controlled fashion. Baseline bodyweight (Fig. 3A) and plasma blood glucose concentrations (Fig. 3C) did not differ between experimental groups. Bodyweight and plasma blood glucose concentrations were followed during the 8 weeks of SRT administration (Fig. 3B+D). None of the treatment groups displayed an altered blood glucose or bodyweight development, compared to the control group.

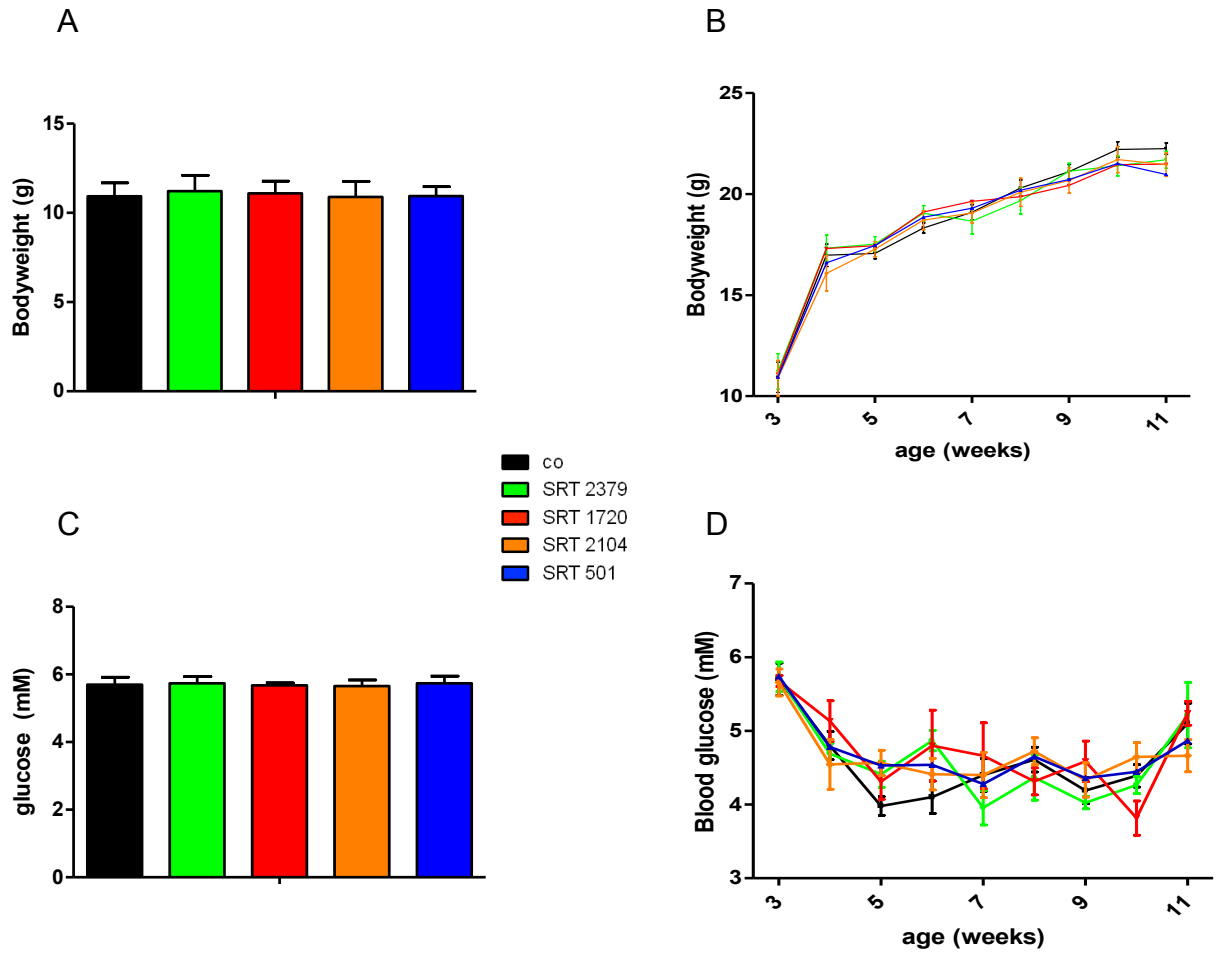

Fig. 3 Bodyweight and blood glucose concentrations in the insulitis score experimental groups. Bodyweight at 3 weeks of age (**A**) and during the 8 weeks of the experimental phase (**B**). Blood glucose at 3 week of age (**C**) and during the 8 weeks of the experimental phase (**D**). *n* = 10 per group. Black bar or line, control; green bar or line, SRT 2379; red bar or line SRT 1720; orange bar or line, SRT 2104, blue bar or line SRT 501. **p<0.05*, as tested by ANOVA with Bonferronni's post hoc test

Starting at 3 weeks of age animals were SRT dosed daily by oral gavage. Drug administration was stopped after 8 weeks. Animals were sacrificed at 12 weeks of age and pancreata were excised and analyzed for immune cell infiltration (Fig. 4). SRT treatment did not have a favourable effect on any experimental group. Periinsulitis (less than half of the area covered with infiltrates) was the only condition showing significant differences. In contrast to what was expected, SRT 2379 and SRT 501 treated animals had a higher immune cell infiltration than the control mice, while SRT 1720 and SRT 2104 treated animals did not show altered immune cell infiltration (Fig. 4B).

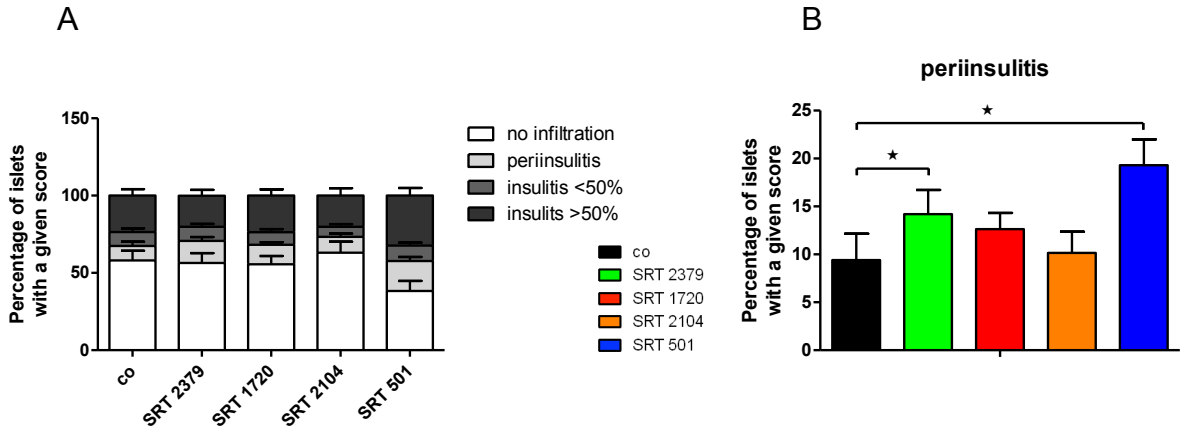

Fig. 4 Pancreatic immune cell infiltration. (**A**) Insulitis score. 300-400 islets per treatment group were scored blindly according to the following: 1. no visible infiltration (white bar), 2. periinsulitis (gray bar), 3. Insulitis ≤ 50 % (dark gray bar), 4. Insulitis ≥ 50 % (black bar). (**B**) Periinsulitis scores of all groups. All other scores did not show any significant difference relative to control group. $n = 8$ per group. Black bar, control; green bar, SRT 2379; red bar SRT 1720; orange bar, SRT 2104, blue bar SRT 501. *$p<0.05$, as tested by ANOVA with Bonferronni's post hoc test

3.3.3 Adoptive Transfer of Diabetes

The third experiment was designed to investigate the involvement of regulatory T cells (Treg) in the potentially beneficial effects of SIRT1 activation. Therefore, 3 week old female NOD mice were drug dosed daily for 8 weeks with activators of SIRT1 (the same animals as described under 3.3.2). At 12 weeks of age animals were sacrificed, splenocytes were purified and transferred into NOD-SCID recipient mice. The next day diabetes was induced by transferring splenocytes from diabetic NOD mice into the same NOD-SCID recipient mice. Progression to diabetes was checked thereafter. All of the adoptively transferred mice became diabetic, demonstrating that the method worked well. The diabetes incidence rate was similar in all groups, suggesting that treatment with the putative SIRT1 activators via did not influence Tregs (Fig. 5).

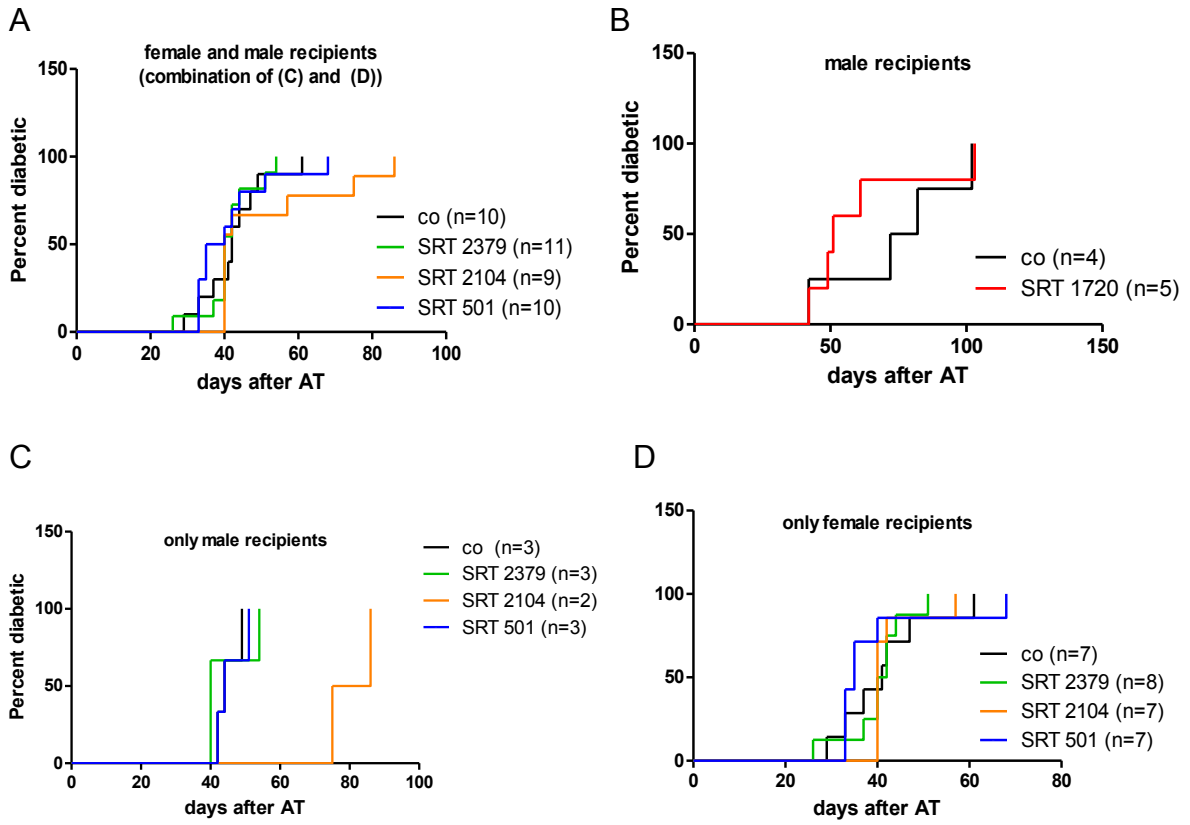

Fig. 5 Diabetes incidence rate (DIR) in NOD-SCID mice after adoptive transfer (AT) of diabetes. Since not enough NOD-SCID recipient mice of one gender were available, experiments were done with male and female mice. (**A**) DIR after AT in female and male recipient mice receiving splenocites from co, SRT 2379, SRT 2104 and SRT 501 treated animals. This figure is a combination of (C) and (D). (**B**) DIR of male recipient mice receiving splenocites from co and SRT 1720 treated mice. (**C**) DIR of male recipient mice receiving splenocites from co, SRT 2379, SRT 2104 and SRT 501 treated animals. (**D**) DIR of female recipient mice receiving splenocites from co, SRT 2379, SRT 2104 and SRT 501 treated animals. Black lines, control; green lines, SRT 2379; red lines SRT 1720; orange lines, SRT 2104, blue lines SRT 501. None of the DIR curves were found to be significantly different from the co group

3.3.4 Unexpected accumulation of cases of death in SRT1720 and SRT501 treated animals

SRT 1720 and SRT 501 treated animals of experiment 1 (see 3.3.1) showed an accumulation of cases of death. These cases occurred mainly during the first 3 weeks of the SRT application (SRT 1720), or during the whole period of SRT application (SRT 501) (Fig. 6).

Three SRT1720 treated and two SRT 501 treated animals that died were analyzed by the institute of lab animal sciences of University Zürich. Neither a pathological autopsy nor a bacteriological or histological analysis revealed any obvious cause of death. Asphyxiation due to perilous gavage handling was also ruled out by the autopsy.

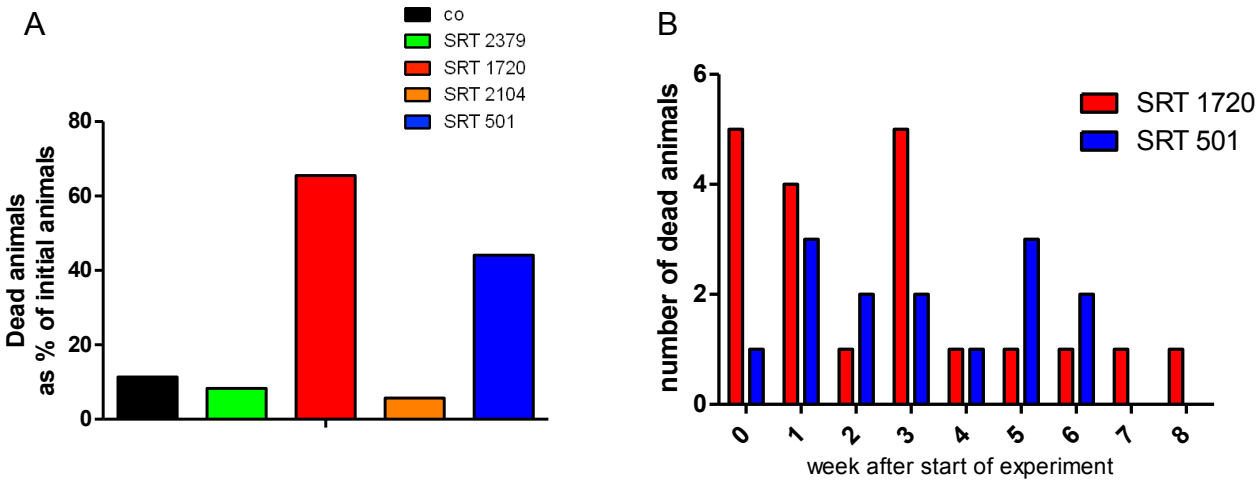

Fig. 6 Cases of death in SRT treated NOD mice. (**A**) Percentage of total animals that were found dead. (**B**) Number of dead animals per week after start of SRT application (3 weeks of age) in SRT 1720 and SRT 501 treatment groups. Black bars, control; green bars, SRT 2379; red bars SRT 1720; orange bars, SRT 2104, blue bars SRT 501

3.3.5 MLD-STZ-SRT 1720

Since there was no report of toxicity of the SRTs in any other animal model and Sirtris Pharmaceuticals never saw side effects in toxicity tests, we concluded that this intolerance could be a specific feature of the NOD mouse. After all these mice are immune-compromised and might behave different than the standard bl/6 mouse. We therefore established another model of type 1 diabetes, the multiple low doses of streptozotocin (MLD-STZ) mouse model. In a pilot study the optimal STZ dose was found to be 50 mg/kg bodyweight (Fig. 7A). Thereafter, littermate bl/6 mice were distributed into 4 groups with matched bodyweight and blood glucose concentrations. All groups received injections of either saline or 50 mg/kg bodyweight STZ on five consecutive days and a daily oral gavage of 100 mg/kg bodyweight SRT 1720 or solvent, starting at 11 weeks of age. Bodyweight and blood glucose were monitored regularly (Fig. 7B+C). SRT 1720 treated animals displayed lower blood glucose concentrations in the basal state, but only showed a trend towards improved glycaemia when challenged with STZ (Fig. 7C).

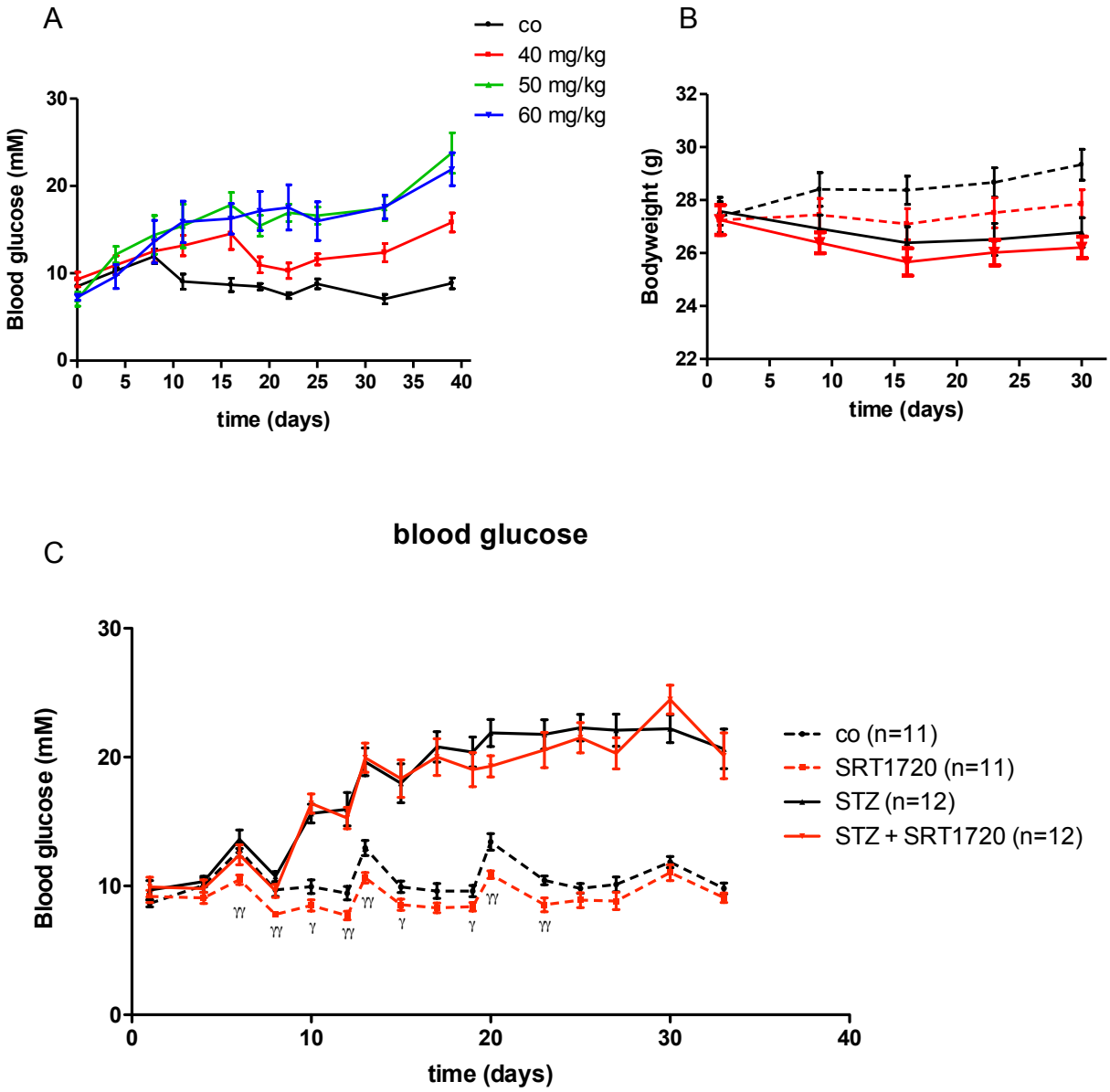

Fig. 7 MLD-STZ-SRT1720 study. (**A**) Blood glucose development in a pilot study with 5 injections of 3 doses of STZ. *n* = 4 per group. Black line, control; red line, 40 mg/kg STZ; green line, 50 mg/kg STZ; blue line, 60 mg/kg STZ. (**B**) Bodyweight and (**C**) blood glucose concentrations of STZ and/or SRT 1720 treated mice. Broken black line, co mice, *n* = 11; broken red line, SRT 1720 treated mice, *n* = 11; solid black line, STZ treated mice, *n* = 12; solid red line, STZ + SRT 1720 treated mice, *n* = 12. **Y*p*** < 0.05 and **YY***p* < 0.01, as tested by Student's *t* test compared with control

3.3.6 MLD-STZ-SIRT1 $^{+/-}$

We went on to investigate if genetic ablation of SIRT1 impairs glycaemia. Homozygous SIRT1 knockout mice are not viable and therefore we treated 11 week old male *Sirt1*$^{+/-}$ mice with STZ and investigated the resulting blood glucose concentrations in comparison to their wildtype littermates.

Identical to the SRT experiments described above, we injected 5 times 50 mg/kg bodyweight of streptozotozin. Unlike in the before described experiment, the destruction of the pancreatic β-cells was not severe enough to induce hyperglycemia in these mice. Therefore we injected 3 more doses of STZ at days 32-34. There was no overt deterioration due to the lack of one allele of *Sirt1*.

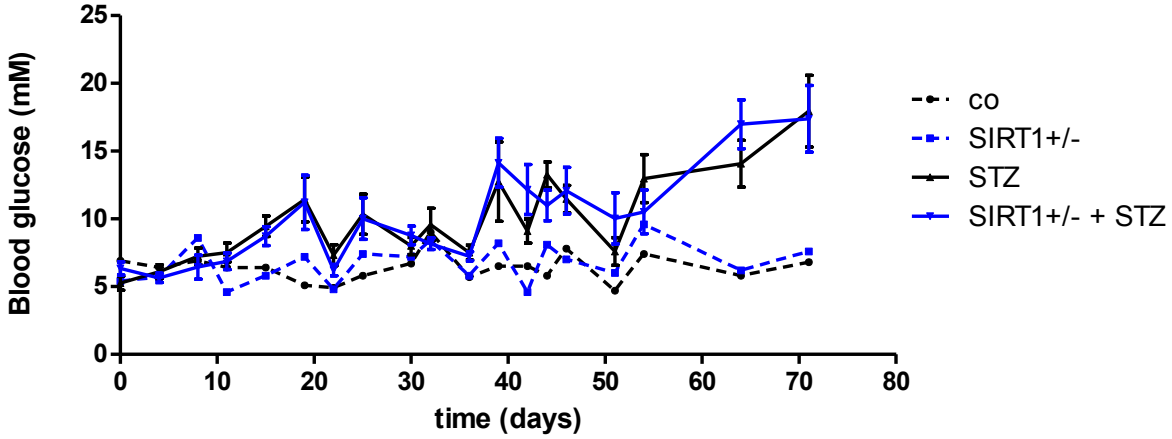

Fig. 8 MLD-STZ-SIRT1. *Sirt1* $^{+/-}$ mice and littermate *Sirt1* $^{+/+}$ were injected with 50 mg/kg STZ (days: 1-5 and 32-34) and random blood glucose concentrations were measured by tail tip bleeding. Broken black line, *Sirt1* $^{+/+}$, $n = 1$; broken blue line, *Sirt1* $^{+/-}$; $n = 1$; solid black line, *Sirt1* $^{+/+}$, STZ treated, $n = 6$; solid blue line, *Sirt1* $^{+/-}$, STZ treated, $n = 5$.

3.4 Discussion

SIRT1, the best studied member of the sirtuin family, is a NAD^+ dependent protein and histone deacetylase that has pleiotropic functions, ranging from supporting genomic stability, DNA repair and stress handling to metabolic regulation [139, 140] and even influencing the circadian clock, linking food availability and sleep/wake rhythms [143]. In animal models, SIRT1 also modulates glucose homeostasis and insulin secretion and protects from the development of diabetes. It does so by increasing insulin secretion (probably via repressing uncoupling protein 2) [144] [145] and by improving glucose tolerance as shown in several genetic *in vitro* and *in vivo* studies [147, 148] [149] as well as pharmacological SIRT1 activation experiments in mice [146].

Our interest in SIRT1 evolved from a family that carries a SIRT1 point mutation (T to C exchange at position 373 of exon 1) leading to a leucine to proline mutation in the SIRT1 protein (L107P). Non-affected family members were healthy, but the 5 carriers displayed auto-immune diseases. 4 were diagnosed with type 1 diabetes and 1 had ulcerative colitis. The index patient was diagnosed with the typical features of type 1 diabetes, including a lean body mass, auto-antibodies to islet antigens and a rapid dependence on insulin. Strikingly, the patient was also insulin resistant, which is not a typical property of type 1 diabetes, even though insulin resistance might be underestimated in patients of type 1 diabetes [164].

SIRT1 animal models support the features described in affected family members. β-cells of homozygous SIRT1 knockout mice fail to increase ATP levels after glucose stimulation and display reduced insulin secretion [145]. In contrast, targeted over-expression of SIRT1 in β-cells enhances insulin secretion [144] and SIRT1 activation by resveratrol enhances insulin sensitivity *in vitro* and protects against HFD-induced insulin resistance [149]. In line with the observed development of type 1 diabetes in the described family members, homozygous SIRT1-null mice also develop auto-immune conditions and produce antibodies that react with nuclear antigens [165]. Furthermore, SIRT1 deficient mice are predisposed to develop colitis (personal communication, Dr. Lenny Guarente, MIT, Cambridge, MA), a disease that one of the carriers of the L107P mutation developed. These findings suggest that the phenotype of affected family members could be a consequence of decreased SIRT1 activity.

To establish an animal model for the SIRT1 mutation in the patient family, we investigated *Sirt1* knockout mice [166]. As the L107P patients carry the mutation in only one allele, we investigated whether the heterozygous *Sirt1* knockout mouse (on a sv129 background) develops diabetes. Untreated *Sirt1* $^{+/-}$ mice did not develop hyperglycaemia. When treated with MLD-STZ, they became hyperclycaemic and reached similar blood glucose levels as wildtype littermate controls. Thus, they do not represent the human patients.

Homozygous *Sirt1* knockout mice are only viable on a CD1 outbred background [166]. The more inbred genes they contain the lower the survival rate becomes [159, 166, 167]. When our collaborator

Michael McBurney (University of Toronto, Canada) treated outbred homozygous *Sirt1* $^{-/-}$ mice with MLD-STZ, he noticed that *Sirt1* $^{-/-}$ displayed significantly higher blood glucose values compared to littermate *Sirt1* $^{+/+}$ and *Sirt1* $^{+/-}$ control mice (data not shown). Thus, there seems to be a difference between humans an rodents in this matter. While the heterozygous human SIRT1 L107P patients display inflammatory diseases, the heterozygous SIRT1 knockout mouse has no or only a faint phenotype [152]. This could simply be due to species differences. Another possible explanation is that L107P SIRT1 silences the wild type allele in humans or that L107P SIRT1 is an imprinted gene, meaning that only one allele is preferentially expressed. We conclude that the *Sirt1* knockout mouse (on a sv129 background) is not a model mimicking the L107P mutation of our human patients. A more suitable way to characterize the molecular consequences of SIRT1 L107P could be to create a knockin mouse carrying the mutated gene, a project that is in progress.

Since the patients carry L107P heterozygously, one could treat them by activating the healthy SIRT1 gene product. Recently, novel small-molecule activators of SIRT1 (SRTs) were described [162] and successfully used to treat animal models of type 2 diabetes, namely diet-induced obesity and ob/ob mice as well as Zucker fa/fa rats [146] [162]. In addition, some of these compounds are currently under investigation in phase II clinical trials, thus their application seemed to be reasonable. We used these compounds to treat several animal models of type 1 diabetes. We started by investigating the NOD mouse, the most commonly used animal model for type 1 diabetes. This mouse spontaneously displays massive pancreatic immune cell infiltration and we tested if SRT treatment could diminish the resulting insulitis. Therefore, NOD animals were treated with 4 different SRTs with different potencies and concentrations, starting at the day of weaning and insulitis score (degree of immune cell infiltration) was measured after 2 months of treatment. None of the SRTs were able to lower the immune cell infiltration compared to the control group. SRT2379 and SRT501 treated mice even showed significantlly more periinsulitis (immune cells around pancreatic islets) than control mice. We conclude that these SIRT1 activators are not able to diminish immune cell infiltration indicating that the development of diabetes in NOD animals cannot be retarded by SRTs.

To test this hypothesis, we initiated a diabetes prevention study in which animals were treated with the same protocol as in the insulitis score study. Glucosuria positive animals were subjected to blood glucose sampling and the development of hyperglycaemia in the different treatment groups was compared. None of the treament groups showed a significantly different onset of diabetes.

Regulatory T cells (Treg) have the potential to delay the onset of diabetes [168]. Since SIRT1 was implicated in T cell tolerance and clonal anergy (see introduction), we investigated a potentially beneficial role of Tregs of SRT treated mice. We set up adoptive transfer of diabetes experiments, where mice were rendered diabetic by transplanting splenocytes from diabetic NOD donor mice. In addition, recipient mice obtained splenocytes from SRT treated mice. If SRT treatment empowered Tregs, the recipient mice should experience a delayed onset of diabetes. In order to obtain conclusive results, an animal number of at least 8 animals of the same gender per recipient group was needed.

Due to an accident in our animal facility, we did not have enough recipient mice of the same gender. Therefore, some of the experiments were performed with animals of both genders. When considering both female and male recipient mice, there was no delay of diabetes onset in neither of the four treatment groups. When considering only male recipient mice, there was a trend towards a delay in mice receiving Tregs from SRT2104 treated mice. But since the animal number used in this experiment was very low, no trustful conclusion can be drawn. Altogether, we conclude that Tregs from SRT treated animals are not empowered to delay the onset of diabetes in recipient mice.

Notably, there was an unexpected accumulation of cases of death in SRT1720 and SRT501 treated NOD animals. This left us with too few animals to do reasonable statistics, but it also appears that these two SIRT1 activators do not influence the onset of diabetes. No serious *in vivo* side effects of SRT administration were so far reported in the literature and therefore these cases of death were unexpected but important. SRT1720 treated animals mainly died during the first 3 weeks of SRT administration while cases of death were observed with SRT501 treatment over the whole application period. 1-3 days before an individual animals was found dead in the cage, it lost weight (dorsal spine was extremely bony, no fat at all), animals seemed moony and inactive, started to shiver and had a decreased body temperature as sensed through the gloves when picked up. Rectal temperatures were decreased 2 days before animals died, but not enough animals were analyzed to do proper statistics. It is not clear if animals died because of the decreased body temperature or if the decreased body temperature is a consequence of the death struggle. A hint comes from Feige et al. [146] who reported a massive decrease in body temperature in mice dosed with SRT1720. Furthermore, they saw an overall increase in energy expenditure, improved lipolysis and decreased fat pad size, which was favourable in their obese / type 2 diabetes setting. Since the NOD mouse is a model for type 1 diabetes and per se very lean, this depletion of fat storage through SIRT1 activation might simply be deleterious because of the lack of energy or of the heat preserving fat layer. In addition, the NOD mouse is strongly insulin resistant and SRT administration increases insulin sensitivity [146]. The resulting anabolic state might further decrease availability of nutrients for energy expenditure and hence exacerbate maintenance of body temperature. We can exclude that these animals died because of mishandling. The autopsy showed no signs of incorrect gavage application. Esophagus and trachea were not injured. Over all, no clear cause of death could be pointed out by the pathological examination. Also Sirtris, the manufacturer of the SRTs, could not explain the observed cases of death. They claim that they never saw any side effects of these substances. We did not receive safety data on these SRTs, but since those substances are already in clinical trials, we have to assume that these side effects might be NOD specific, and may happen only in this immune compromised animal model. SRT titers in NOD animals were analyzed at Sirtris but they only told us that the titers were lower than expected without going into details. This could be due to an improper blood sampling timepoint (too late after SRT dosage) or due to an insufficient usage of the required inhibitor (Dichlorvos). In 2010, it reported that the commonly used “SIRT1 activators” resveratrol and the

Sirtris compounds SRT1720, SRT2183 and SRT1460 do not directly activate SIRT1. They only interact when a fluorophore modified substrate is present in the SIRT1 activity assay but not when a native substrate is present [169]. The authors were also not able to reproduce the beneficial *in vivo* effects on blood glucose and other metabolic parameters that were reported earlier with these compounds [146, 162]. Similar to our findings, they observed that 100 mg/kg SRT1720 was not well tolerated and lead to reduced food intake and death. Noteworthy, they used *ob/ob* animals on HFD and did not investigate diet-induced obese and *ob/ob* animals seperately, as Sirtris and their partners did. In addition, they reported various other interaction partners of these SRTs, including receptors, enzymes, ion channels, and transporters. However, one has to take into consideration that the authors are employees of Pfizer, which is a direct business rival of Sirtris, the manufacturer of the SRTs. Half a year later, a paper was published by Sirtris, providing evidence that these compounds can activate SIRT1 independently of the fluorophore tag [170]. They do not comment on the specificity of the SIRT1 activators, a point that was also critically discussed by the Pfizer report. We observed effects of SRT2183 in MEF SIRT$^{-/-}$ cells (data not shown) which supports the Pfizer finding, that some actions of the SRTs might be due to off-target effects. Concerning the reported positive *in vivo* effects of SRT1720, it seems unlikely that all independent researchers that published beneficial data were chasing a ghost. The likely explanation is that SRT1720 has desirable effects *in vivo*, but that these effects are, at least partly, not SIRT1 mediated.

Since the NOD mouse is a rodent model for type 1 diabetes and does not necessarily represent all aspects of human type 1 diabetes, we decided to test another *in vivo* model of type 1 diabetes, the MLD-STZ induced diabetes mouse model. SRT1720 treatment lowered blood glucose values in animals that were treated with sodium acetate-solution (the solvent for stz). This is most likely due to the insulin-sensitising effect of SRT1720 and was reported before [146]. This effect disappeared when animals were treated with STZ. Both STZ groups displayed rather high glucose values and this could have masked an expected effect of SRT1720 treatment. Therefore, we repeated this study with 20% less STZ (40 mg/kg instead of 50 mg/kg). At the same time we doubled the dose of SRT1720 (200 mg/kg instead of 100 mg/kg) because work published by Feige et al. [146] suggested that 500 mg/kg produces considerable effects while 100 mg/kg only slightly improves metabolic parameters. Unfortunately, 200 mg/kg SRT1720 in STZ treated mice had similar lethal effects as previously observed with 100 mg/kg in NOD mice. For ethical reasons, the experiment was stopped (data not shown). The reason why Feige et al. were able to use an even 2.5 fold higher dose of SRT1720 without getting lethal effects remains elusive. Maybe the STZ treatment and the resulting catabolic state made our mice more susceptible. While we drug dosed our mice by daily oral gavage, Feige et al. mixed the drug into the food. SRT application by oral gavage might have induced a strong peak of SRT action while mixing the activator into the food might have lead to a mildly attenuated but prolonged SRT action.

In 2011, Lee et al. reported that resveratrol-treated NOD mice were protected and rescued from

pancreatic insulitis and hyperglycaemia ([171]. Resveratrol is often used to activate SIRT1, even though its specificity is debated [169]. The authors concluded that resveratrol blocks inflammatory cells from migrating to the pancreas and therefore protects these animals from insulitis. As with the SRTs, it is not clear whether these effects are mediated by SIRT1 or if other targets lead to the described results.

This study aimed to investigate potential beneficial effect of small molecular activators of SIRT1 (SRTs) in animal models of type 1 diabetes. Further, it should have provided supportive data to initiate treatment of family members carrying a heterozygous mutation in SIRT1 with SRT. Results show that SIRT1 activation via the synthetic activators SRTs does not influence the development of hyperglycaemia and diabetes in the NOD and in the MLD-STZ mouse model. Further, lethal side effects of some of the SRTs were uncovered in these mice, strongly suggesting to reconsider the use of these drugs for the treatment of the family with the SIRT1 mutation. In order to investigate whether SIRT1 is important in the development of diabetes, other genetic models should be used. One possibility is to use the SIRT1-overexpresser mouse [172]. This would circumvent the problem of lacking specificity as in pharmacological SIRT1 activator studies. Another way to investigate the impact of SIRT1 on glucose metabolism is to examine tissue specific SIRT1 knockout mice. SIRT1 could be knocked out in β-cells in a constitutive or – in order to avoid developmental defects - in an inducible fashion. These and other studies will shed more light on the role of SIRT1 in the development of diabetes.

4 REFERENCES

1. Gerich, J.E., *Physiology of glucose homeostasis.* Diabetes Obes Metab, 2000. **2**(6): p. 345-50.
2. Sanger, F. and E.O. Thompson, *The amino-acid sequence in the glycyl chain of insulin. II. The investigation of peptides from enzymic hydrolysates.* Biochem J, 1953. **53**(3): p. 366-74.
3. Sanger, F. and E.O. Thompson, *The amino-acid sequence in the glycyl chain of insulin. I. The identification of lower peptides from partial hydrolysates.* Biochem J, 1953. **53**(3): p. 353-66.
4. Brissova, M., et al., *Assessment of human pancreatic islet architecture and composition by laser scanning confocal microscopy.* J Histochem Cytochem, 2005. **53**(9): p. 1087-97.
5. Prado, C.L., et al., *Ghrelin cells replace insulin-producing beta cells in two mouse models of pancreas development.* Proc Natl Acad Sci U S A, 2004. **101**(9): p. 2924-9.
6. Murakami, T., et al., *The insulo-acinar portal and insulo-venous drainage systems in the pancreas of the mouse, dog, monkey and certain other animals: a scanning electron microscopic study of corrosion casts.* Arch Histol Cytol, 1993. **56**(2): p. 127-47.
7. Bonnerweir, S., *Morphological Evidence for Pancreatic Polarity of Beta-Cell within Islets of Langerhans.* Diabetes, 1988. **37**(5): p. 616-621.
8. Brunicardi, F.C., et al., *Microcirculation of the islets of Langerhans. Long Beach Veterans Administration Regional Medical Education Center Symposium.* Diabetes, 1996. **45**(4): p. 385-92.
9. Cabrera, O., et al., *The unique cytoarchitecture of human pancreatic islets has implications for islet cell function.* Proc Natl Acad Sci U S A, 2006. **103**(7): p. 2334-9.
10. Erlandsen, S.L., et al., *Pancreatic islet cell hormones distribution of cell types in the islet and evidence for the presence of somatostatin and gastrin within the D cell.* J Histochem Cytochem, 1976. **24**(7): p. 883-97.
11. Orci, L., *The microanatomy of the islets of Langerhans.* Metabolism, 1976. **25**(11 Suppl 1): p. 1303-13.
12. Bosco, D., et al., *Unique arrangement of alpha- and beta-cells in human islets of Langerhans.* Diabetes, 2010. **59**(5): p. 1202-10.
13. Bonner-Weir, S. and T.D. O'Brien, *Islets in type 2 diabetes: in honor of Dr. Robert C. Turner.* Diabetes, 2008. **57**(11): p. 2899-904.
14. Bosco, D., et al., *Expression and secretion of alpha1-proteinase inhibitor are regulated by proinflammatory cytokines in human pancreatic islet cells.* Diabetologia, 2005. **48**(8): p. 1523-33.
15. Matthews, M., *Pancreatic β-Cell in Human Type 2 Diabetes.* 2009.
16. Harper, M.E., A. Ullrich, and G.F. Saunders, *Localization of the human insulin gene to the distal end of the short arm of chromosome 11.* Proc Natl Acad Sci U S A, 1981. **78**(7): p. 4458-60.
17. Owerbach, D., et al., *The insulin gene is located on the short arm of chromosome 11 in humans.* Diabetes, 1981. **30**(3): p. 267-70.
18. Melloul, D., S. Marshak, and E. Cerasi, *Regulation of insulin gene transcription.* Diabetologia, 2002. **45**(3): p. 309-26.
19. Hrytsenko, O., et al., *Insulin expression in the brain and pituitary cells of tilapia (Oreochromis niloticus).* Brain Res, 2007. **1135**(1): p. 31-40.
20. Chance, R.E., R.M. Ellis, and W.W. Bromer, *Porcine proinsulin: characterization and amino acid sequence.* Science, 1968. **161**(837): p. 165-7.
21. Steiner, D.F. and P.E. Oyer, *The biosynthesis of insulin and a probable precursor of insulin by a human islet cell adenoma.* Proc Natl Acad Sci U S A, 1967. **57**(2): p. 473-80.
22. Rhodes, C.J. and M.F. White, *Molecular insights into insulin action and secretion.* Eur J Clin Invest, 2002. **32 Suppl 3**: p. 3-13.
23. Steiner, D.F., et al., *Structure and evolution of the insulin gene.* Annu Rev Genet, 1985. **19**: p. 463-84.
24. Tager, H.S., D.F. Steiner, and C. Patzelt, *Biosynthesis of insulin and glucagon.* Methods Cell Biol, 1981. **23**: p. 73-88.
25. Olson, A.L. and J.E. Pessin, *Structure, function, and regulation of the mammalian facilitative glucose transporter gene family.* Annu Rev Nutr, 1996. **16**: p. 235-56.

26. MacDonald, P.E., J.W. Joseph, and P. Rorsman, *Glucose-sensing mechanisms in pancreatic beta-cells.* Philos Trans R Soc Lond B Biol Sci, 2005. **360**(1464): p. 2211-25.
27. Boulpaep, B., *Medical Physiology.* Elsevier Saunders, 2008.
28. Rosen, S.G., et al., *Epinephrine supports the postabsorptive plasma glucose concentration and prevents hypoglycemia when glucagon secretion is deficient in man.* J Clin Invest, 1984. **73**(2): p. 405-11.
29. Boyle, P.J., S.D. Shah, and P.E. Cryer, *Insulin, glucagon, and catecholamines in prevention of hypoglycemia during fasting.* Am J Physiol, 1989. **256**(5 Pt 1): p. E651-61.
30. Gromada, J., I. Franklin, and C.B. Wollheim, *Alpha-cells of the endocrine pancreas: 35 years of research but the enigma remains.* Endocr Rev, 2007. **28**(1): p. 84-116.
31. Furuta, M., et al., *Severe defect in proglucagon processing in islet A-cells of prohormone convertase 2 null mice.* J Biol Chem, 2001. **276**(29): p. 27197-202.
32. Philippe, J., et al., *Alpha-cell-specific expression of the glucagon gene is conferred to the glucagon promoter element by the interactions of DNA-binding proteins.* Mol Cell Biol, 1988. **8**(11): p. 4877-88.
33. Unger, R.H. and L. Orci, *Possible roles of the pancreatic D-cell in the normal and diabetic states.* Diabetes, 1977. **26**(3): p. 241-4.
34. Kojima, M., et al., *Ghrelin is a growth-hormone-releasing acylated peptide from stomach.* Nature, 1999. **402**(6762): p. 656-60.
35. Inui, A., et al., *Ghrelin, appetite, and gastric motility: the emerging role of the stomach as an endocrine organ.* FASEB J, 2004. **18**(3): p. 439-56.
36. Tschop, M., D.L. Smiley, and M.L. Heiman, *Ghrelin induces adiposity in rodents.* Nature, 2000. **407**(6806): p. 908-13.
37. Adrian, T.E., et al., *Distribution and release of human pancreatic polypeptide.* Gut, 1976. **17**(12): p. 940-44.
38. Larsson, L.I., F. Sundler, and R. Hakanson, *Immunohistochemical localization of human pancreatic polypeptide (HPP) to a population of islet cells.* Cell Tissue Res, 1975. **156**(2): p. 167-71.
39. Track, N.S., R.S. McLeod, and A.V. Mee, *Human pancreatic polypeptide: studies of fasting and postprandial plasma concentrations.* Can J Physiol Pharmacol, 1980. **58**(12): p. 1484-9.
40. Malaisse-Lagae, F., et al., *Pancreatic polypeptide: a possible role in the regulation of food intake in the mouse. Hypothesis.* Experientia, 1977. **33**(7): p. 915-7.
41. Gates, R.J. and N.R. Lazarus, *The ability of pancreatic polypeptides (APP and BPP) to return to normal the hyperglycaemia, hyperinsulinaemia and weight gain of New Zealand obese mice.* Horm Res, 1977. **8**(4): p. 189-202.
42. Ueno, N., et al., *Decreased food intake and body weight in pancreatic polypeptide-overexpressing mice.* Gastroenterology, 1999. **117**(6): p. 1427-32.
43. Berntson, G.G., et al., *Pancreatic-Polypeptide Infusions Reduce Food-Intake in Prader-Willi Syndrome.* Peptides, 1993. **14**(3): p. 497-503.
44. Batterham, R.L., et al., *Pancreatic polypeptide reduces appetite and food intake in humans.* Journal of Clinical Endocrinology & Metabolism, 2003. **88**(8): p. 3989-3992.
45. Jesudason, D.R., et al., *Low-dose pancreatic polypeptide inhibits food intake in man.* British Journal of Nutrition, 2007. **97**(3): p. 426-429.
46. *Diagnosis and classification of diabetes mellitus.* Diabetes Care, 2008. **31 Suppl 1**: p. S55-60.
47. Wild, S., et al., *Global prevalence of diabetes: estimates for the year 2000 and projections for 2030.* Diabetes Care, 2004. **27**(5): p. 1047-53.
48. Patlak, M., *New weapons to combat an ancient disease: treating diabetes.* FASEB J, 2002. **16**(14): p. 1853.
49. Zimmet, P., K.G. Alberti, and J. Shaw, *Global and societal implications of the diabetes epidemic.* Nature, 2001. **414**(6865): p. 782-7.
50. Donath, M.Y. and J.A. Ehses, *Type 1, type 1.5, and type 2 diabetes: NOD the diabetes we thought it was.* Proc Natl Acad Sci U S A, 2006. **103**(33): p. 12217-8.
51. Kolb, H. and T. Mandrup-Poulsen, *An immune origin of type 2 diabetes?* Diabetologia, 2005. **48**(6): p. 1038-50.

52. Foulis, A.K., et al., *The histopathology of the pancreas in type 1 (insulin-dependent) diabetes mellitus: a 25-year review of deaths in patients under 20 years of age in the United Kingdom.* Diabetologia, 1986. **29**(5): p. 267-74.
53. Imagawa, A., et al., *Immunological abnormalities in islets at diagnosis paralleled further deterioration of glycaemic control in patients with recent-onset Type I (insulin-dependent) diabetes mellitus.* Diabetologia, 1999. **42**(5): p. 574-8.
54. Foulis, A.K., *In type 1 diabetes, does a non-cytopathic viral infection of insulin-secreting B-cells initiate the disease process leading to their autoimmune destruction?* Diabet Med, 1989. **6**(8): p. 666-74.
55. Alberti, K.G. and P.Z. Zimmet, *Definition, diagnosis and classification of diabetes mellitus and its complications. Part 1: diagnosis and classification of diabetes mellitus provisional report of a WHO consultation.* Diabet Med, 1998. **15**(7): p. 539-53.
56. Atkinson, M.A. and G.S. Eisenbarth, *Type 1 diabetes: new perspectives on disease pathogenesis and treatment.* Lancet, 2001. **358**(9277): p. 221-9.
57. Kantarova, D. and M. Buc, *Genetic susceptibility to type 1 diabetes mellitus in humans.* Physiol Res, 2007. **56**(3): p. 255-66.
58. de Luca, C. and J.M. Olefsky, *Inflammation and insulin resistance.* FEBS Lett, 2008. **582**(1): p. 97-105.
59. Rhodes, C.J., *Type 2 diabetes-a matter of beta-cell life and death?* Science, 2005. **307**(5708): p. 380-4.
60. Schenk, S., M. Saberi, and J.M. Olefsky, *Insulin sensitivity: modulation by nutrients and inflammation.* J Clin Invest, 2008. **118**(9): p. 2992-3002.
61. Muoio, D.M. and C.B. Newgard, *Mechanisms of disease: molecular and metabolic mechanisms of insulin resistance and beta-cell failure in type 2 diabetes.* Nat Rev Mol Cell Biol, 2008. **9**(3): p. 193-205.
62. Bernal-Mizrachi, E., et al., *Islet beta cell expression of constitutively active Akt1/PKB alpha induces striking hypertrophy, hyperplasia, and hyperinsulinemia.* J Clin Invest, 2001. **108**(11): p. 1631-8.
63. Kim, Y.B., et al., *Normal insulin-dependent activation of Akt/protein kinase B, with diminished activation of phosphoinositide 3-kinase, in muscle in type 2 diabetes.* J Clin Invest, 1999. **104**(6): p. 733-41.
64. Bjornholm, M., et al., *Insulin receptor substrate-1 phosphorylation and phosphatidylinositol 3-kinase activity in skeletal muscle from NIDDM subjects after in vivo insulin stimulation.* Diabetes, 1997. **46**(3): p. 524-7.
65. Thies, R.S., et al., *Insulin-receptor autophosphorylation and endogenous substrate phosphorylation in human adipocytes from control, obese, and NIDDM subjects.* Diabetes, 1990. **39**(2): p. 250-9.
66. Capeau, J., *Insulin resistance and steatosis in humans.* Diabetes Metab, 2008. **34**(6 Pt 2): p. 649-57.
67. Prentki, M. and C.J. Nolan, *Islet beta cell failure in type 2 diabetes.* J Clin Invest, 2006. **116**(7): p. 1802-12.
68. Donath, M.Y., et al., *Mechanisms of beta-cell death in type 2 diabetes.* Diabetes, 2005. **54 Suppl 2**: p. S108-13.
69. Maedler, K., et al., *Glucose-induced beta cell production of IL-1beta contributes to glucotoxicity in human pancreatic islets.* J Clin Invest, 2002. **110**(6): p. 851-60.
70. Chang-Chen, K.J., R. Mullur, and E. Bernal-Mizrachi, *Beta-cell failure as a complication of diabetes.* Rev Endocr Metab Disord, 2008. **9**(4): p. 329-43.
71. Neels, J.G. and J.M. Olefsky, *Inflamed fat: what starts the fire?* J Clin Invest, 2006. **116**(1): p. 33-5.
72. Hotamisligil, G.S., N.S. Shargill, and B.M. Spiegelman, *Adipose expression of tumor necrosis factor-alpha: direct role in obesity-linked insulin resistance.* Science, 1993. **259**(5091): p. 87-91.
73. Ehses, J.A., et al., *Increased number of islet-associated macrophages in type 2 diabetes.* Diabetes, 2007. **56**(9): p. 2356-70.

74. Homo-Delarche, F., et al., *Islet inflammation and fibrosis in a spontaneous model of type 2 diabetes, the GK rat.* Diabetes, 2006. **55**(6): p. 1625-33.
75. Larsen, C.M., et al., *Interleukin-1-receptor antagonist in type 2 diabetes mellitus.* N Engl J Med, 2007. **356**(15): p. 1517-26.
76. Yuan, M., et al., *Reversal of obesity- and diet-induced insulin resistance with salicylates or targeted disruption of Ikkbeta.* Science, 2001. **293**(5535): p. 1673-7.
77. Owyang, A.M., et al., *XOMA 052, a potent, high-affinity monoclonal antibody for the treatment of IL-1beta-mediated diseases.* MAbs, 2011. **3**(1): p. 6-17.
78. Mogensen, T.H., *Pathogen recognition and inflammatory signaling in innate immune defenses.* Clin Microbiol Rev, 2009. **22**(2): p. 240-73, Table of Contents.
79. Aderem, A. and R.J. Ulevitch, *Toll-like receptors in the induction of the innate immune response.* Nature, 2000. **406**(6797): p. 782-7.
80. Akira, S., K. Takeda, and T. Kaisho, *Toll-like receptors: critical proteins linking innate and acquired immunity.* Nat Immunol, 2001. **2**(8): p. 675-80.
81. Medzhitov, R. and C.A. Janeway, Jr., *Innate immunity: the virtues of a nonclonal system of recognition.* Cell, 1997. **91**(3): p. 295-8.
82. Frantz, S., et al., *Toll4 (TLR4) expression in cardiac myocytes in normal and failing myocardium.* J Clin Invest, 1999. **104**(3): p. 271-80.
83. Seibl, R., et al., *Expression and regulation of Toll-like receptor 2 in rheumatoid arthritis synovium.* Am J Pathol, 2003. **162**(4): p. 1221-7.
84. Chen, Y.C., et al., *Sequence variants of Toll-like receptor 4 and susceptibility to prostate cancer.* Cancer Res, 2005. **65**(24): p. 11771-8.
85. Kiechl, S., et al., *Toll-like receptor 4 polymorphisms and atherogenesis.* N Engl J Med, 2002. **347**(3): p. 185-92.
86. Bjorkbacka, H., et al., *Reduced atherosclerosis in MyD88-null mice links elevated serum cholesterol levels to activation of innate immunity signaling pathways.* Nat Med, 2004. **10**(4): p. 416-21.
87. Michelsen, K.S., et al., *Lack of Toll-like receptor 4 or myeloid differentiation factor 88 reduces atherosclerosis and alters plaque phenotype in mice deficient in apolipoprotein E.* Proc Natl Acad Sci U S A, 2004. **101**(29): p. 10679-84.
88. Joosten, L.A., et al., *Toll-like receptor 2 pathway drives streptococcal cell wall-induced joint inflammation: critical role of myeloid differentiation factor 88.* J Immunol, 2003. **171**(11): p. 6145-53.
89. Lee, J.Y., et al., *Saturated fatty acid activates but polyunsaturated fatty acid inhibits Toll-like receptor 2 dimerized with Toll-like receptor 6 or 1.* J Biol Chem, 2004. **279**(17): p. 16971-9.
90. Shi, H., et al., *TLR4 links innate immunity and fatty acid-induced insulin resistance.* J Clin Invest, 2006. **116**(11): p. 3015-25.
91. Netea, M.G., et al., *Toll-like receptors and the host defense against microbial pathogens: bringing specificity to the innate-immune system.* J Leukoc Biol, 2004. **75**(5): p. 749-55.
92. Lin, Y., et al., *The lipopolysaccharide-activated toll-like receptor (TLR)-4 induces synthesis of the closely related receptor TLR-2 in adipocytes.* J Biol Chem, 2000. **275**(32): p. 24255-63.
93. Hacker, H., et al., *Immune cell activation by bacterial CpG-DNA through myeloid differentiation marker 88 and tumor necrosis factor receptor-associated factor (TRAF)6.* J Exp Med, 2000. **192**(4): p. 595-600.
94. Lee, J.Y., et al., *Saturated fatty acids, but not unsaturated fatty acids, induce the expression of cyclooxygenase-2 mediated through Toll-like receptor 4.* J Biol Chem, 2001. **276**(20): p. 16683-9.
95. Senn, J.J., *Toll-like receptor-2 is essential for the development of palmitate-induced insulin resistance in myotubes.* J Biol Chem, 2006. **281**(37): p. 26865-75.
96. Nguyen, M.T., et al., *A subpopulation of macrophages infiltrates hypertrophic adipose tissue and is activated by free fatty acids via Toll-like receptors 2 and 4 and JNK-dependent pathways.* J Biol Chem, 2007. **282**(48): p. 35279-92.
97. Shoelson, S.E. and A.B. Goldfine, *Getting away from glucose: fanning the flames of obesity-induced inflammation.* Nat Med, 2009. **15**(4): p. 373-4.

98. Donath, M.Y., et al., *Islet inflammation in type 2 diabetes: from metabolic stress to therapy.* Diabetes Care, 2008. **31 Suppl 2**: p. S161-4.
99. Wellen, K.E. and G.S. Hotamisligil, *Inflammation, stress, and diabetes.* J Clin Invest, 2005. **115**(5): p. 1111-9.
100. Hong, E.G., et al., *Interleukin-10 prevents diet-induced insulin resistance by attenuating macrophage and cytokine response in skeletal muscle.* Diabetes, 2009. **58**(11): p. 2525-35.
101. Chiang, S.H., et al., *The protein kinase IKKepsilon regulates energy balance in obese mice.* Cell, 2009. **138**(5): p. 961-75.
102. Ehses, J.A., et al., *IL-1 antagonism reduces hyperglycemia and tissue inflammation in the type 2 diabetic GK rat.* Proc Natl Acad Sci U S A, 2009. **106**(33): p. 13998-4003.
103. Patsouris, D., et al., *Ablation of CD11c-positive cells normalizes insulin sensitivity in obese insulin resistant animals.* Cell Metab, 2008. **8**(4): p. 301-9.
104. Hundal, R.S., et al., *Mechanism by which high-dose aspirin improves glucose metabolism in type 2 diabetes.* J Clin Invest, 2002. **109**(10): p. 1321-6.
105. Turnbaugh, P.J., et al., *An obesity-associated gut microbiome with increased capacity for energy harvest.* Nature, 2006. **444**(7122): p. 1027-31.
106. Himes, R.W. and C.W. Smith, *Tlr2 is critical for diet-induced metabolic syndrome in a murine model.* FASEB J, 2010. **24**(3): p. 731-9.
107. Poggi, M., et al., *C3H/HeJ mice carrying a toll-like receptor 4 mutation are protected against the development of insulin resistance in white adipose tissue in response to a high-fat diet.* Diabetologia, 2007. **50**(6): p. 1267-76.
108. Tsukumo, D.M., et al., *Loss-of-function mutation in Toll-like receptor 4 prevents diet-induced obesity and insulin resistance.* Diabetes, 2007. **56**(8): p. 1986-98.
109. Caricilli, A.M., et al., *Inhibition of toll-like receptor 2 expression improves insulin sensitivity and signaling in muscle and white adipose tissue of mice fed a high-fat diet.* Journal of Endocrinology, 2008. **199**(3): p. 399-406.
110. Weir, J.B., *New methods for calculating metabolic rate with special reference to protein metabolism.* J Physiol, 1949. **109**(1-2): p. 1-9.
111. Wueest, S., et al., *Deletion of Fas in adipocytes relieves adipose tissue inflammation and hepatic manifestations of obesity in mice.* J Clin Invest, 2010. **120**(1): p. 191-202.
112. Boni-Schnetzler, M., et al., *Free fatty acids induce a proinflammatory response in islets via the abundantly expressed interleukin-1 receptor I.* Endocrinology, 2009. **150**(12): p. 5218-29.
113. Takeda, K. and S. Akira, *TLR signaling pathways.* Semin Immunol, 2004. **16**(1): p. 3-9.
114. Triantafilou, M., et al., *Membrane sorting of toll-like receptor (TLR)-2/6 and TLR2/1 heterodimers at the cell surface determines heterotypic associations with CD36 and intracellular targeting.* J Biol Chem, 2006. **281**(41): p. 31002-11.
115. Boni-Schnetzler, M., et al., *Increased interleukin (IL)-1beta messenger ribonucleic acid expression in beta -cells of individuals with type 2 diabetes and regulation of IL-1beta in human islets by glucose and autostimulation.* J Clin Endocrinol Metab, 2008. **93**(10): p. 4065-74.
116. Hummel, K.P., M.M. Dickie, and D.L. Coleman, *Diabetes, a new mutation in the mouse.* Science, 1966. **153**(740): p. 1127-8.
117. Sharma, K., P. McCue, and S.R. Dunn, *Diabetic kidney disease in the db/db mouse.* Am J Physiol Renal Physiol, 2003. **284**(6): p. F1138-44.
118. (WHO), W.H.O., *Global Burden of Disease Study.* 2004.
119. U.S. Department of Health and Human Services, C.f.D.C.a.P., *Behavioral Risk Factor Surveillance System Survey Questionnaire.* 2009.
120. Seidell, J.C., *Obesity in Europe: scaling an epidemic.* Int J Obes Relat Metab Disord, 1995. **19 Suppl 3**: p. S1-4.
121. Rathmann, W. and G. Giani, *Global prevalence of diabetes: estimates for the year 2000 and projections for 2030.* Diabetes Care, 2004. **27**(10): p. 2568-9; author reply 2569.
122. Pickup, J.C., et al., *NIDDM as a disease of the innate immune system: association of acute-phase reactants and interleukin-6 with metabolic syndrome X.* Diabetologia, 1997. **40**(11): p. 1286-92.

123. Cani, P.D., et al., *Metabolic endotoxemia initiates obesity and insulin resistance.* Diabetes, 2007. **56**(7): p. 1761-72.
124. Lumeng, C.N., J.L. Bodzin, and A.R. Saltiel, *Obesity induces a phenotypic switch in adipose tissue macrophage polarization.* J Clin Invest, 2007. **117**(1): p. 175-84.
125. Surwit, R.S., et al., *Diet-induced type II diabetes in C57BL/6J mice.* Diabetes, 1988. **37**(9): p. 1163-7.
126. Considine, R.V., et al., *Serum immunoreactive-leptin concentrations in normal-weight and obese humans.* N Engl J Med, 1996. **334**(5): p. 292-5.
127. Farooqi, I.S., et al., *Beneficial effects of leptin on obesity, T cell hyporesponsiveness, and neuroendocrine/metabolic dysfunction of human congenital leptin deficiency.* J Clin Invest, 2002. **110**(8): p. 1093-103.
128. Farooqi, I.S. and S. O'Rahilly, *Monogenic obesity in humans.* Annu Rev Med, 2005. **56**: p. 443-58.
129. Heymsfield, S.B., et al., *Recombinant leptin for weight loss in obese and lean adults: a randomized, controlled, dose-escalation trial.* JAMA, 1999. **282**(16): p. 1568-75.
130. Ghanim, H., et al., *Increase in plasma endotoxin concentrations and the expression of Toll-like receptors and suppressor of cytokine signaling-3 in mononuclear cells after a high-fat, high-carbohydrate meal: implications for insulin resistance.* Diabetes Care, 2009. **32**(12): p. 2281-7.
131. Dasu, M.R., et al., *Increased toll-like receptor (TLR) activation and TLR ligands in recently diagnosed type 2 diabetic subjects.* Diabetes Care, 2010. **33**(4): p. 861-8.
132. Creely, S.J., et al., *Lipopolysaccharide activates an innate immune system response in human adipose tissue in obesity and type 2 diabetes.* Am J Physiol Endocrinol Metab, 2007. **292**(3): p. E740-7.
133. Rine, J., et al., *A suppressor of mating-type locus mutations in Saccharomyces cerevisiae: evidence for and identification of cryptic mating-type loci.* Genetics, 1979. **93**(4): p. 877-901.
134. Kennedy, B.K., et al., *Mutation in the silencing gene SIR4 can delay aging in S. cerevisiae.* Cell, 1995. **80**(3): p. 485-96.
135. Kaeberlein, M., M. McVey, and L. Guarente, *The SIR2/3/4 complex and SIR2 alone promote longevity in Saccharomyces cerevisiae by two different mechanisms.* Genes Dev, 1999. **13**(19): p. 2570-80.
136. Guarente, L. and F. Picard, *Calorie restriction--the SIR2 connection.* Cell, 2005. **120**(4): p. 473-82.
137. Rogina, B. and S.L. Helfand, *Sir2 mediates longevity in the fly through a pathway related to calorie restriction.* Proc Natl Acad Sci U S A, 2004. **101**(45): p. 15998-6003.
138. Boily, G., et al., *SirT1 regulates energy metabolism and response to caloric restriction in mice.* PLoS One, 2008. **3**(3): p. e1759.
139. Wang, R.H., et al., *Impaired DNA damage response, genome instability, and tumorigenesis in SIRT1 mutant mice.* Cancer Cell, 2008. **14**(4): p. 312-23.
140. Rodgers, J.T., et al., *Nutrient control of glucose homeostasis through a complex of PGC-1alpha and SIRT1.* Nature, 2005. **434**(7029): p. 113-8.
141. Westerheide, S.D., et al., *Stress-inducible regulation of heat shock factor 1 by the deacetylase SIRT1.* Science, 2009. **323**(5917): p. 1063-6.
142. Brunet, A., et al., *Stress-dependent regulation of FOXO transcription factors by the SIRT1 deacetylase.* Science, 2004. **303**(5666): p. 2011-5.
143. Asher, G., et al., *SIRT1 regulates circadian clock gene expression through PER2 deacetylation.* Cell, 2008. **134**(2): p. 317-28.
144. Moynihan, K.A., et al., *Increased dosage of mammalian Sir2 in pancreatic beta cells enhances glucose-stimulated insulin secretion in mice.* Cell Metab, 2005. **2**(2): p. 105-17.
145. Bordone, L., et al., *Sirt1 regulates insulin secretion by repressing UCP2 in pancreatic beta cells.* PLoS Biol, 2006. **4**(2): p. e31.
146. Feige, J.N., et al., *Specific SIRT1 activation mimics low energy levels and protects against diet-induced metabolic disorders by enhancing fat oxidation.* Cell Metab, 2008. **8**(5): p. 347-58.

147. Banks, A.S., et al., *SirT1 gain of function increases energy efficiency and prevents diabetes in mice.* Cell Metab, 2008. **8**(4): p. 333-41.
148. Pfluger, P.T., et al., *Sirt1 protects against high-fat diet-induced metabolic damage.* Proc Natl Acad Sci U S A, 2008. **105**(28): p. 9793-8.
149. Sun, C., et al., *SIRT1 improves insulin sensitivity under insulin-resistant conditions by repressing PTP1B.* Cell Metab, 2007. **6**(4): p. 307-19.
150. Alcendor, R.R., et al., *Sirt1 regulates aging and resistance to oxidative stress in the heart.* Circulation Research, 2007. **100**(10): p. 1512-21.
151. Potente, M., et al., *SIRT1 controls endothelial angiogenic functions during vascular growth.* Genes Dev, 2007. **21**(20): p. 2644-58.
152. Stein, S., et al., *SIRT1 reduces endothelial activation without affecting vascular function in ApoE-/- mice.* Aging (Albany NY), 2010. **2**(6): p. 353-60.
153. Saunders, L.R. and E. Verdin, *Sirtuins: critical regulators at the crossroads between cancer and aging.* Oncogene, 2007. **26**(37): p. 5489-504.
154. Kim, D., et al., *SIRT1 deacetylase protects against neurodegeneration in models for Alzheimer's disease and amyotrophic lateral sclerosis.* EMBO J, 2007. **26**(13): p. 3169-79.
155. Li, X., et al., *SIRT1 deacetylates and positively regulates the nuclear receptor LXR.* Mol Cell, 2007. **28**(1): p. 91-106.
156. Zhang, J., et al., *The type III histone deacetylase Sirt1 is essential for maintenance of T cell tolerance in mice.* J Clin Invest, 2009. **119**(10): p. 3048-58.
157. Kang, S.M., et al., *Transactivation by AP-1 is a molecular target of T cell clonal anergy.* Science, 1992. **257**(5073): p. 1134-8.
158. Gao, X., et al., *Immunomodulatory activity of resveratrol: suppression of lymphocyte proliferation, development of cell-mediated cytotoxicity, and cytokine production.* Biochem Pharmacol, 2001. **62**(9): p. 1299-308.
159. Cheng, H.L., et al., *Developmental defects and p53 hyperacetylation in Sir2 homolog (SIRT1)-deficient mice.* Proc Natl Acad Sci U S A, 2003. **100**(19): p. 10794-9.
160. Yeung, F., et al., *Modulation of NF-kappaB-dependent transcription and cell survival by the SIRT1 deacetylase.* EMBO J, 2004. **23**(12): p. 2369-80.
161. Lee, J.H., et al., *Overexpression of SIRT1 protects pancreatic beta-cells against cytokine toxicity by suppressing the nuclear factor-kappaB signaling pathway.* Diabetes, 2009. **58**(2): p. 344-51.
162. Milne, J.C., et al., *Small molecule activators of SIRT1 as therapeutics for the treatment of type 2 diabetes.* Nature, 2007. **450**(7170): p. 712-6.
163. Milne, J.C. and J.M. Denu, *The Sirtuin family: therapeutic targets to treat diseases of aging.* Curr Opin Chem Biol, 2008. **12**(1): p. 11-7.
164. Greenbaum, C.J., *Insulin resistance in type 1 diabetes.* Diabetes Metab Res Rev, 2002. **18**(3): p. 192-200.
165. Sequeira, J., et al., *sirt1-null mice develop an autoimmune-like condition.* Exp Cell Res, 2008. **314**(16): p. 3069-74.
166. McBurney, M.W., et al., *The mammalian SIR2alpha protein has a role in embryogenesis and gametogenesis.* Mol Cell Biol, 2003. **23**(1): p. 38-54.
167. Lee, I.H., et al., *A role for the NAD-dependent deacetylase Sirt1 in the regulation of autophagy.* Proc Natl Acad Sci U S A, 2008. **105**(9): p. 3374-9.
168. Boitard, C., et al., *T cell-mediated inhibition of the transfer of autoimmune diabetes in NOD mice.* J Exp Med, 1989. **169**(5): p. 1669-80.
169. Pacholec, M., et al., *SRT1720, SRT2183, SRT1460, and resveratrol are not direct activators of SIRT1.* J Biol Chem, 2010. **285**(11): p. 8340-51.
170. Dai, H., et al., *SIRT1 activation by small molecules: kinetic and biophysical evidence for direct interaction of enzyme and activator.* J Biol Chem, 2010. **285**(43): p. 32695-703.
171. Lee, S.M., et al., *Prevention and treatment of diabetes with resveratrol in a non-obese mouse model of type 1 diabetes.* Diabetologia, 2011.
172. Bordone, L., et al., *SIRT1 transgenic mice show phenotypes resembling calorie restriction.* Aging Cell, 2007. **6**(6): p. 759-67.

5 AMENDMENT

5.1 Contributions

It is rather difficult to state exactly which experiments were performed by which person, since most experiments were repeated several times by different researchers. In addition, we had essential help by our technicians Marcela Borsigova and Kirsten Rappold, who do not wish to be listed as authors in our publications.

Person	Technique	Experiments
D. T. Meier	RNA profiling, GTT, ITT, harvesting organs, glucose uptake fat, adipose tissue size distribution, rtPCR (Taqman), liver lipid measurement, GSIS, BMDM/BMDC isolation/differentiation, db/db backcrossing, genotyping, antibody injections, western blotting, glycogen content in muscle, writing manuscript, planning parts of TLR2 project and whole SIRT1 project, NOD breeding, testing glucosuria and glycaemia, staining and scoring insulitis, gavage, establishing MLD-STZ, organizing/breeding/genotyping *Sirt1* $^{+/-}$	2.3.1, 2.3.2, 2.3.3, 2.3.4, 2.3.5, 2.3.6, 2.4.1, 2.4.2, 2.4.3, 2.4.5, 2.4.6, 2.4.8, 3.3.1, 3.3.2, 3.3.3, 3.3.4, 3.3.5
J. A. Ehses	GTT, ITT, harvesting organs, GSIS, BMDM/BMDC isolation/differentiation, luminex, teaching techniques, writing manuscript, planning and supervising TLR2 project	2.3.1, 2.3.2, 2.3.3, 2.3.4, 2.3.5, 2.4.1, 2.4.2, 2.4.4, 2.4.8, 2.4.9
M. Böni-Schnetzler	Teaching techniques, supervising SIRT1 project, giving input on all projects, correcting thesis	
Marc Y. Donath	Organizing funds, supervising SIRT1 project, giving input on all projects, correcting thesis	
M. Borsigova	RNA profiling, GTT, ITT, harvesting organs, glucose uptake fat, adipose tissue size distribution, rtPCR	2.3.1, 2.3.2, 2.3.3, 2.3.4, 2.3.5, 2.4.1,

	(Taqman), liver lipid measurement, Immunohistochemistry, GSIS, BMDM/BMDC isolation/differentiation	2.4.2, 2.4.4, 2.4.8, 2.4.9, 3.3.2
K. Rappold	Animal handling, weaning, cutting biopsies, gavage, measuring glucosuria and glycaemia	3.3.1, 3.3.2, 3.3.3, 3.3.4
C. Boitard	Input (NOD experiments)	
S. Wueest	clamping	2.3.3, 2.4.7
J. Rytka	clamping	2.3.3, 2.4.7
P. Y. Wielinga	Indirect colorimetry, activity determination	2.3.2
H. Esterbauer	congenics	Discussion
O. Tschopp	Muscle triacylglycerols	2.4.6
S. M. Schultze	Muscle triacylglycerols	2.4.6
U. Malipiero	Taught how to isolate/differentiate BMDM/BMDC	2.3.5
H. Ellingsgaard	support splenocyte preparation for adoptive transfer	3.3.3
F. C. Schuit	gene array	2.3.1
D. Konrad	input and suggestions	

5.2 Acknowledgements

Many people merit gratitude for their input during my time as a PhD student. I would like to mention the most important and apologize to the ones that are not cited.

I would like to thank…

… Marianne, Jan and Marc for opening the door to the exciting world of science, for their encouraging and patient way of leading, and for being excellent teachers

… my co-workers Helga, Nadine, Desirée and Sabine for valuable input and support

… Marcela for her assistance, endless GTT hours and discussions about life

… Kirsten for her devotional and highly reliable animal work, also on weekends, danke vielmals!

… our master students Anja, Rahel, Noëmi,Yuliya and Irina for fun times

… our technicians Iris, Greta and Richi for their help

… my lab mate Julia for her companionship and for making C Lab 22 an even more enjoyable place

… Francesca, Simone and Linhua for making lab life amusing

… members of the c-floor for support, fruitful discussions, lab events and aperos

… Jyrki Eloranta and his team for excellent teaching and input

… Walter Ettlin, Andreas Rettich and the whole BZL staff for professional animal work

... ZIHP, EASD, SGED, SNF for financial support

… François Verrey and Philippe Halban for taking the time to be on my thesis committee

... my familiy and friends for always being there

… and you for your interest in this thesis.

May the journey continue!

5.3 Curriculum vitae

PERSONAL INFORMATION

Name	Daniel Thomas Meier
Address	Seetalstrasse 44
	5503 Schafisheim
	Switzerland
Date of birth	February 28th 1981
E-mail Address	daniel.meier@postmail.ch
Cell phone	+41 (0)78 872 2112

EDUCATION

2007-2011	PhD candidate, University Hospital Zurich, Switzerland, Prof. Dr. Marc Donath
2005-2007	Master in Human Movement Sciences (Exercise Physiology), ETH, Zurich, Switzerland
2003-2007	Master of Advanced Studies in Secondary and Higher Education, ETH Zurich, Switzerland (Teaching Certificate)
2002-2005	Bachelor in Biology / Human Movement Sciences, ETH Zurich, Switzerland
1999-2000	Senior year in Wolbach Public High School, Nebraska, USA
1998-2002	Matura, Alte Kantonsschule Aarau, Switzerland, Type C (Natural Sciences)

5.4 List of publications

1. Low- and high-density lipoproteins modulate function, apoptosis, and proliferation of primary human and murine pancreatic beta-cells

Rütti S, Ehses JA, Sibler RA, Prazak R, Rohrer L, Georgopoulos S, **Meier DT**, Niclauss N, Berney T, Donath MY, von Eckardstein A.

Endocrinology. 2009 Oct;150(10):4521-30.

2. Free fatty acids induce a proinflammatory response in islets via the abundantly expressed interleukin-1 receptor I

Böni-Schnetzler M, Boller S, Debray S, Bouzakri K, **Meier DT**, Prazak R, Kerr-Conte J, Pattou F, Ehses JA, Schuit FC, Donath MY.

Endocrinology. 2009 Dec;150(12):5218-29.

3. Toll-like receptor 2-deficient mice are protected from insulin resistance and beta cell dysfunction induced by a high-fat diet

Meier DT*, Ehses JA*, Wueest S, Rytka J, Boller S, Wielinga PY, Schraenen A, Lemaire K, Debray S, Van Lommel L, Pospisilik JA, Tschopp O, Schultze SM, Malipiero U, Esterbauer H, Ellingsgaard H, Rütti S, Schuit FC, Lutz TA, Böni-Schnetzler M, Konrad D, Donath MY.

* shared first authorship

Diabetologia. 2010 Aug;53(8):1795-806.